AD-A094 730 GENERAL ELECTRIC CO CINCINNATI OH AIRCRAFT ENGINE GROUP F/G 21/5
BACKUP CONTROL FOR A VARIABLE CYCLE ENGINE.(U)
JUL 80 H B KAST F33615-76-C-2086
UNCLASSIFIED R80AEG450 AFAPL-TR-79-2069 NL

1 OF 2
AD
A0 94 7 30

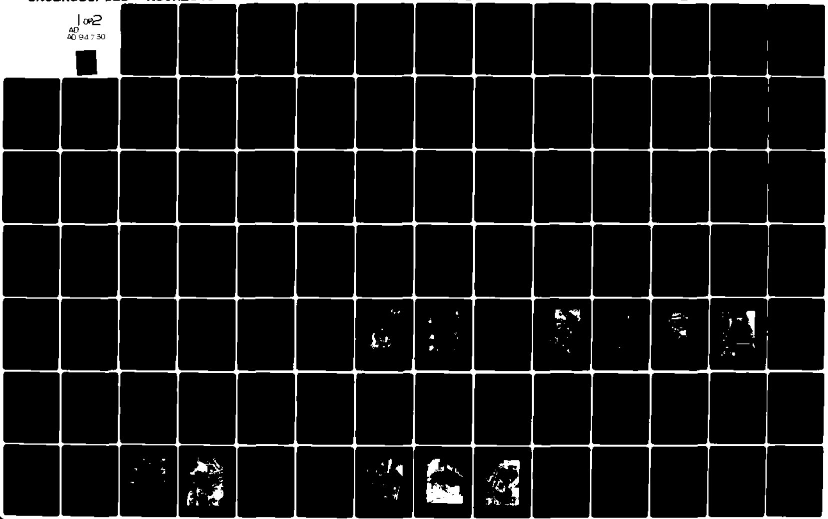

AFAPL-TR-79-2069

LEVEL II

2

BACKUP CONTROL FOR A VARIABLE CYCLE ENGINE

Phase II Final Report

AD A094730

Howard B. Kast
General Electric Company
Aircraft Engine Group
Cincinnati, Ohio 45215

JULY 1980

TECHNICAL REPORT AFAPL-TR-79-2069

Final Report For Period 1 September 1977 - 16 April 1979

Approved for Public Release; Distribution Unlimited

Aero Propulsion Laboratory
Air Force Wright Aeronautical Laboratories
Air Force Systems Command
Wright-Patterson Air Force Base, Ohio 45433

NOTICE

When Government drawings, specifications, or other data are used for any purpose other than in connection with a definitely related Government procurement operation, the United States Government thereby incurs no responsibility nor any obligation whatsoever; and the fact that the government may have formulated, furnished, or in any way supplied the said drawings, specifications, or other data, is not to be regarded by implication or otherwise as in any manner licensing the holder or any other person or corporation, or conveying any rights or permission to manufacture use, or sell any patented invention that may in any way be related thereto.

This report has been reviewed by the Office of Public Affairs (ASD/PA) and is releasable to the National Technical Information Service (NTIS). At NTIS, it will be available to the general public, including foreign nations.

This technical report has been reviewed and is approved for publication.

Lester L. Small

LESTER L. SMALL
Project Engineer

David H. Quick

DAVID H. QUICK, Lt Col, USAF
Chief, Components Branch

FOR THE COMMANDER

H I Bush

H. I. BUSH
Deputy Director
Turbine Engine Division

"If your address has changed, if you wish to be removed from our mailing list, or if the addressee is no longer employed by your organization please notify AFWAL/POTC, W-PAFB, OH 45433 to help us maintain a current mailing list".

Copies of this report should not be returned unless return is required by security considerations, contractual obligations, or notice on a specific document.

SECURITY CLASSIFICATION OF THIS PAGE (When Data Entered)

REPORT DOCUMENTATION PAGE

READ INSTRUCTIONS BEFORE COMPLETING FORM

1. REPORT NUMBER: AFAPL-TR-79-2069	2. GOVT ACCESSION NO.: AD-A094 730
3. RECIPIENT'S CATALOG NUMBER	
4. TITLE (and Subtitle): BACKUP CONTROL FOR A VARIABLE CYCLE ENGINE, PHASE II FINAL REPORT	5. TYPE OF REPORT & PERIOD COVERED: Final Technical Report, 1 Sep [redacted]77 – 16 Apr [redacted]79
	6. PERFORMING ORG. REPORT NUMBER: R80AEG450
7. AUTHOR(s): Howard B. Kast	8. CONTRACT OR GRANT NUMBER(s): F33615-76-C-2086
9. PERFORMING ORGANIZATION NAME AND ADDRESS: General Electric Company, Aircraft Engine Group, Cincinnati, Ohio 45215	10. PROGRAM ELEMENT, PROJECT, TASK AREA & WORK UNIT NUMBERS: Project 3066, Task 306603 W.U. 30660373
11. CONTROLLING OFFICE NAME AND ADDRESS: Air Force Aero Propulsion Laboratory (TBC), Wright-Patterson AFB, Ohio 45433	12. REPORT DATE: Jul[redacted]80
	13. NUMBER OF PAGES: 117
14. MONITORING AGENCY NAME & ADDRESS (if different from Controlling Office)	15. SECURITY CLASS. (of this report): Unclassified
	15a. DECLASSIFICATION/DOWNGRADING SCHEDULE: N/A

16. DISTRIBUTION STATEMENT (of this Report)

Approved for public release; distribution unlimited.

17. DISTRIBUTION STATEMENT (of the abstract entered in Block 20, if different from Report)

18. SUPPLEMENTARY NOTES

19. KEY WORDS (Continue on reverse side if necessary and identify by block number)

Backup Control
Emergency Control
Gas Turbine Engines
Control Reliability

20. ABSTRACT (Continue on reverse side if necessary and identify by block number)

The next generation of variable cycle aircraft engines (VCE) will have an increased complexity associated with the number of controlled engine variables, inherent cycle variability, and inlet-engine-exhaust control integration. This level of engine complexity and the expanding integration of aircraft/engine controls causes a commensurate increase in the control system complexity and capacity. Digital electronics has been identified as the only viable means for meeting these significantly more sophisticated

DD FORM 1 JAN 73 1473 EDITION OF 1 NOV 65 IS OBSOLETE

SECURITY CLASSIFICATION OF THIS PAGE (When Data Entered)

403467

requirements of the future VCE. Although recent digital electronic advances promise new levels of reliability, this improvement is offset by the increased circuitry of the more complex control. Especially in the case of the single-engine aircraft, it is recognized that such variable cycle engines should be equipped with a Backup Control for emergency use.

The results of Phase I, the trade studies, of the Backup Control for a Variable Cycle Engine program were reported earlier in AFAPL-TR-77-92. The trade studies were based on a single-engine aircraft, the JTDE-23 engine, and a full authority digital electronic primary control system. A minimum get-home capability was defined which included completing a takeoff, a minimum climb rate, deceleration from supersonic flight, windmill air start, minimum cruise range, wave-off, landing, and safe runway roll. Backup control requirements were determined using the YF-17 aircraft data for thrust, the JTDE-23 engine computer model for the variables to be controlled, and the F101 engine and control model for transient performance. Seven backup control approaches were selected for consideration from a list of 48 possibilities. These approaches included hydromechanical, electrical, fluidic, and a combination of electrical/hydromechanical technologies. Reliability estimates were made on six controls,and estimated performance, volume, weight, cost analyses and preliminary design studies were made in more detail on three of these approaches. A recommended approach was selected, namely the hydromechanical backup control using speed demand and fuel flow scheduling. This selection was based on the above analyses and studies, together with a comparison of the technologies, a comparison of parallel- versus series-type backup/primary control interface, and a tabulated evaluation of each backup control's advantages and disadvantages.

The recommended hydromechanical approach has been constructed, calibrated and evaluated in a test cell. These evaluations included transient operation and transfer from the primary control to the backup control and back to primary operation. Successful operation was achieved, providing test hardware which is intended for further validation through on-engine testing.

FOREWORD

This report describes a design effort conducted by the General Electric Company and sponsored by the Air Force Aero Propulsion Laboratory, Air Force Systems Command, Wright-Patterson AFB, Ohio, under Project 3066, Task 03 and Work Unit 73 with Lester L. Small, AFAPL/TBC, as Project Engineer.

The work reported herein was performed during the report period of September 1, 1977 to April 16, 1979. R. E. Anderson was the General Electric Program Manager; the technical work was performed under the direction of Howard B. Kast, Engineering Manager. The Engineering Manager was assisted by James E. Hurtle, Eugene T. Hill, and Robert P. Wanger.

This report covers Phase II of the Backup Control for a Variable Cycle Engine Program. Phase II involved the design, fabrication and bench testing of the selected backup control. Phase I was completed in August 1977 and covered the system trade studies and backup control selection. For the technical results of Phase 1, refer to report No. AFAPL-TR-77-92, "Backup Control for a Variable Cycle Engine, Phase I Interim Technical Report."

TABLE OF CONTENTS

TABLE OF CONTENTS (Concluded)

LIST OF ILLUSTRATIONS

LIST OF ILLUSTRATIONS (Continued)

LIST OF ILLUSTRATIONS (Continued)

LIST OF ILLUSTRATIONS (Concluded)

LIST OF TABLES

LIST OF SYMBOLS

B/U	-	Backup
BUC	-	Backup Control
F	-	Force
FADEC	-	Full Authority Digital Electronic Control
F/B	-	Feedback
JTDE	-	Joint Technology Demonstrator Engine
LVDT	-	Linear Variable Differential Transformer
LVPT	-	Linear Variable Phase Transformer
M	-	Magnitude
MFC	-	Main Fuel Control
N_1	-	Fan rpm
N_C	-	Control rpm
N_G (or N_2)	-	Gas Generator rpm
$\dot{N}_G$	-	Gas Generator rpm Rate
P_1	-	Pump Discharge Pressure
P_{C_1}	-	Metering Valve Servo Pressure, Closing
P_{C_2}	-	Metering Valve Servo Pressure, Opening
PLA	-	Power Lever Angle
P_B	-	Boost Pump Pressure
P_o	-	Case Pressure, Control
P_S	-	Servo Pressure
P_{S3} or CDP	-	Compressor Discharge Pressure, Static
P'_{S3}	-	Compressor Discharge Pressure, Static, Downstream of the Ratio Selector
P_{T2}	-	Inlet Pressure, Total
P_x	-	Throttling Valve Servo Pressure, Opening
P_y	-	Throttling Valve Servo Pressure, Closing
Q	-	Torque
S/V	-	Servovalve
$T_{2.5}$	-	Compressor Inlet Temperature
VCE	-	Variable Cycle Engine

LIST OF SYMBOLS (Concluded)

W_f	-	Fuel Flow
$\dot{W}_f$	-	Fuel Flow Rate
X or X_{MV}	-	Metering Valve Stroke
W_{fm}	-	Fuel Flow, Main
β_c	-	Core Stator Angle
β_F	-	Fan Stator Angle
ΔP	-	Metering Head
$\theta_{2.5}$	-	$T_{2.5}/518.7^\circ$ R
ρ	-	Specific Gravity
ϕ	-	Phase

SECTION I

INTRODUCTION

Today's military aircraft developments are addressing mission scenarios and application needs which place a wide range of different operating conditions on the propulsion system. The propulsion system requirements result in conflicting demands for optimizing the engine cycle selected for the aircraft gas turbine. To meet this need, aircraft engine designers are moving toward the use of gas turbines having an increased number of parameters that are variable in flight. Ultimately this leads to the variable cycle engine (VCE).

This program covered the design, fabrication, and testing of a Backup Control for a Variable Cycle Engine. This development effort is in support of the evolving full-authority digital electronic control technology. The backup control will provide the aircraft with an emergency get-home capability in the event that the primary electronic control system is inoperative due to a failure or loss of electrical power.

Minimum get-home capability was defined as those functions which the aircraft/engine system should be capable of performing while transferring to, and while operating on, backup control. This capability included completing a takeoff, a minimum climb rate, deceleration from supersonic flight, windmill air start, minimum cruise range, wave-off, landing, and safe runway roll. Operational constraints were determined; these included pilot action to (1) adjust for tolerable but undesirable overspeed or overtemperature, (2) decelerate from supersonic speeds, and (3) execute windmill air starting. There will be no PLA restrictions at subsonic conditions. The control environmental requirements are those of an aircraft engine for Mach number 2.5 operation.

The need for the electronic engine control arises from the increased complexity - i.e., increased number of controlled engine variables, inherent cycle variability, inlet-engine-exhaust control integration - of the next generation of sophisticated variable cycle engines. This increased engine complexity, together with the expanding need for more complete aircraft/engine control integration, demands a commensurate increase in the complexity of the control system, whose capabilities must expand if it is to provide stable, responsive, safe, and, precise engine control.

Digital electronics represents the only viable means of meeting the significantly more sophisticated requirements of the variable cycle engine of the future. With its inherent ability to time-share in the computational section of the control, increasing requirement complexity yields a much smaller increase in hardware compared to present control system mechanizations. Digital electronics also lends itself to "hardening" to the aircraft engine environment through hybrid construction, packaging, and environmental conditioning techniques.

As good as digital electronics are today, significant improvements are being developed for application to gas turbine engine controls in order to achieve the higher levels of control reliability desired in 1985-1990. It is recognized that the full-authority digital electronic control for VCE is yet to be evaluated under field conditions and compared to the reliability record demonstrated by hydromechanical computer/controllers. This program was pursued in consideration of the significantly increased complexity of a VCE control system, and the current development status of the digital electronic approach. Since VCE propulsion systems are rapidly becoming a reality, conducting this program to develop VCE backup control technology was most timely.

The program consisted of two primary phases. The Phase I objectives were to conduct comprehensive reliability, cost and performance evaluations on a variety of hydromechanical, electronic and fluidic backup control approaches for variable cycle engines having a primary electronic control system and then to select a single approach for subsequent design, fabrication and testing. The objectives of Phase II were to conduct the detailed design of the selected backup control, fabricate the control, and conduct bench testing in conjunction with a specifically designed backup control test console.

Based on the results of the above analyses and comparisons, the parallel hydromechanical backup control, which demands N_G and schedules W_f, was recommended for design fabrication and test in Phase II of this program. This selection was made because it has the reduced unscheduled shutdown associated with parallel systems and because the analyses showed this to be a lightweight economical approach. It has the further advantage of representing a construction technology inherently different from the primary electronic control, thus assuring a reduction in common-mode, single-cause failures.

The hydromechanical backup control, which is of the parallel or standby type, demands N_G and schedules W_f for the transient limit. The W_f and β_c schedules are computed based on N_G, $T_{2.5}$, and compressor discharge pressure (P_{S3}). This computer is very similar to those used on many prior hydromechanical main fuel controls. A transfer valve is used to switch W_f and β_c servo pressures from the primary servovalves to those of the backup servovalves.

This report covers Phase II of the Backup Control development for a Variable Cycle Engine. The material which follows includes hardware design and design drawings, a fabrication summary, the test plans and the test results, followed by conclusions and recommendations.

SECTION II

HARDWARE DESIGN

1. APPROACH

The backup control approach recommended for design, fabrication, and testing is shown by a functional block diagram in Figure 1 and schematically by Figure 2. This N_G - demanding and W_f - scheduling hydromechanical backup control was recommended based on the trade study conducted during Phase I of this program.

The computation section and $T_{2.5}$ sensor are based on the equivalent portion of the J85-GE-21 Main Fuel Control. In the backup mode, N_G is the demanded parameter and closed-loop speed control is maintained by the hydromechanical governor. Accel/decel W_f limits are computed based on N_G, $T_{2.5}$, and P_{S3}. The β_c schedule is computed based on N_G and $T_{2.5}$.

In the primary mode the backup control fuel valve and β_c servo flows are blocked by a transfer valve. This approach minimizes interference and the possible resulting backup control failures which could cause power loss. The backup control is continuously computing the W_f and β_c limits, thus tracking the engine. This is necessary to prevent stall, which could be caused by a jump in W_f during transfer.

Transfer can be initiated (1) by pilot action, (2) by loss of primary control power, (3) by loss of primary control "good health" signal, or (4) by an overspeed condition as sensed by the backup control speed sensor. Transfer is accomplished by a current signal to the latching solenoid valve, which ports servo pressure to the piston driving the transfer valve spool. The latching solenoid was selected because it is compatible with (1) aircraft electrical power and its possible interruptions, (2) the types of electrical signals preferred for pilot action, (3) loss of primary control power, and (4) loss of the primary control "good health." Direct-acting hydromechanical overspeed protection is provided to guard against a stuck-open metering valve. In the backup mode, the primary metering valve and β_c servo flows are blocked and the backup control has sole authority to control these variables.

The fuel valve is based on the design used for the Light Weight Fuel Delivery System program conducted by GE for the U.S. Navy. This valve was designed to operate on fuel contaminated per Mil-E-5007C. The flow-dividing function for the vortex valves is also provided.

Some modifications to the above components were required to provide the added functions needed by the backup control. A switch was added to the computer to initiate transfer to backup upon N_G overspeed as sensed by the hydromechanical control. An overspeed valve was also added. This valve

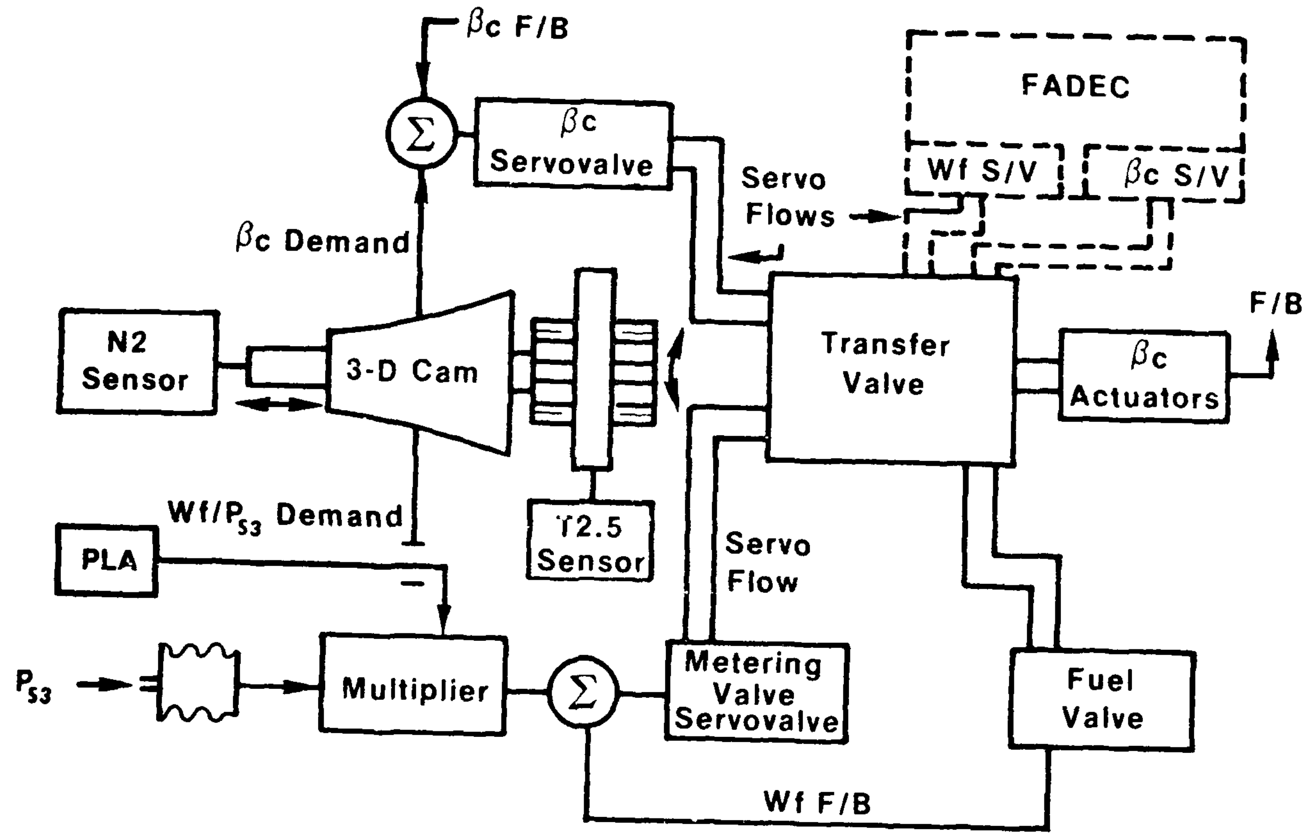

Figure 1. Functional Block Diagram of the Backup Control.

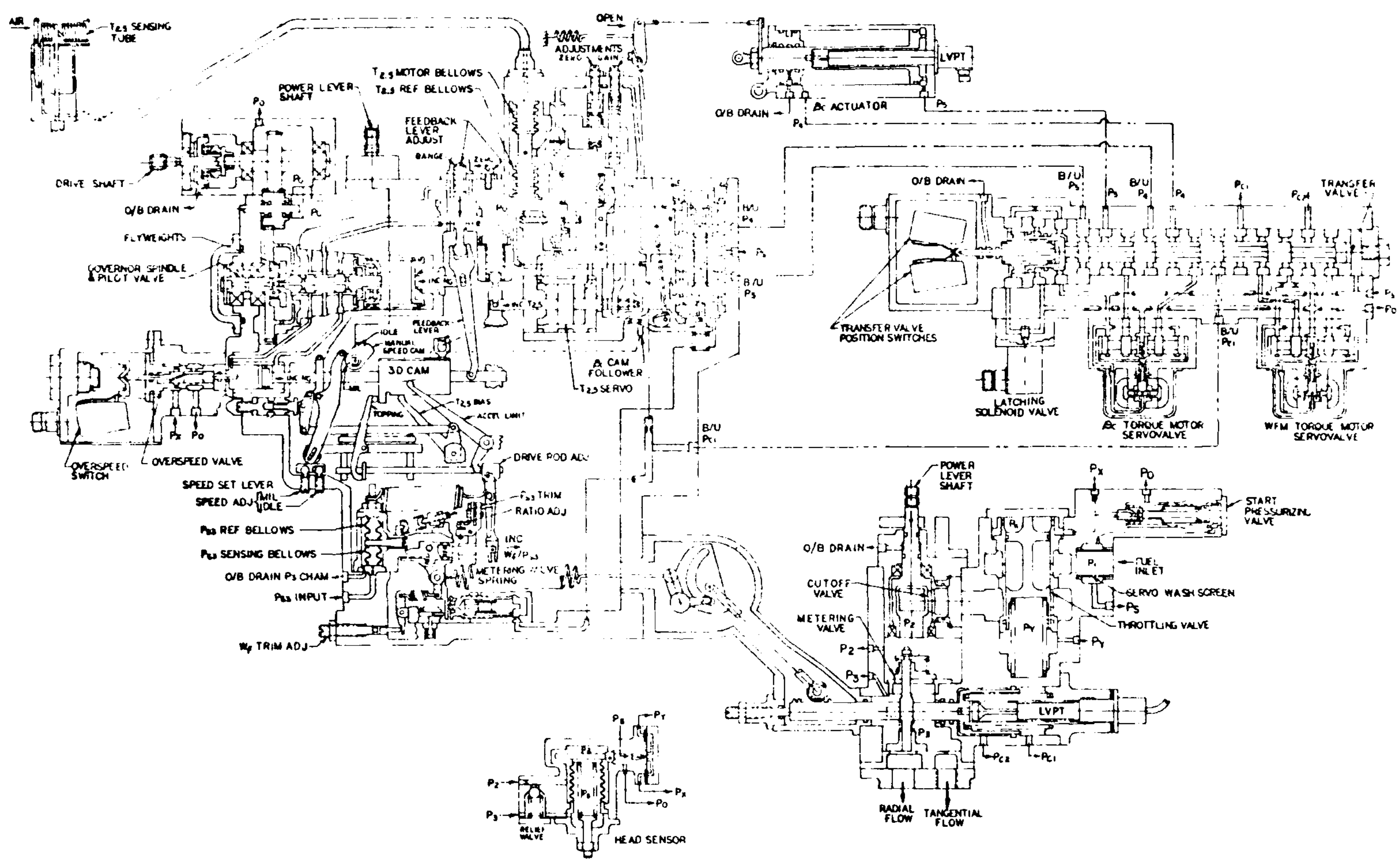

Figure 2. Hydromechanical Backup Control Schematic.

modulates the throttling valve in case the metering valve sticks open.

The transfer valve was designed specifically for this program. As indicated above, this valve determines whether the primary or backup servo pressures control the metering valve and β_c actuators. The transfer valve has two switches. The first provides feedback to the primary control, notifying it that the transfer valve spool is in the backup position; the second turns on the cockpit indicator light.

An off-engine electrical unit and a test console were also designed. The off-engine electrical unit includes a four-way switch to simulate the pilot's switch(es). The test console simulated the primary control during bench testing of the backup control.

The various subassemblies involved are discussed in detail in the paragraphs that follow.

2. HYDROMECHANICAL BACKUP CONTROL COMPUTER

The backup control computer is shown schematically by Figure 3. In the backup mode, this control computes a metering valve position for each engine operating condition. Steady-state conditions are maintained in conjunction with limiting and biasing functions, such as core maximum RPM, accel/decel limits, minimum W_f and $T_{2.5}$ bias, which are integrated so that a single output signal representing demand is generated.

Motion of the W_f lever occurs whenever an unbalance exists in the moments of force acting on it. The position of the rollers represents the proper value of W_f/P_{S3}, as determined by the integration of three engine operating parameters: N_G, PLA, and $T_{2.5}$. A multiplying force acts on the rollers through a lever and is a function of P_{S3} absolute. The lever system is arranged as a multiplier such that the load, P_{S3}, times the point of load application, W_f/P_{S3}, equals fuel flow. In equation form, it is:

$$P_{S3} \times W_f/P_{S3} = W_f$$

P_{S3} is sensed by a bellows. The pressure times the bellows area produces a force. The multiplying force is transmitted to the rollers by a lever attached to the sensing bellows. An evacuated bellows of equal effective area is mounted opposite the sensing bellows to serve as a reference. This second bellows also provides compensation for undesired sensing bellows movement that results from changes of temperature and pressure in the bellows chamber. The bellows chamber is sealed off from the control casing and vented to the atmosphere through a small orifice. A ruptured sensing bellows would fill the chamber with compressor discharge air, the seal and orifice maintaining a level of P_{S3}. P_{S3} acting on the outside of the reference bellows generates a force on the P_{S3} lever to prevent complete loss of the P_{S3} signal if the sensing bellows fails.

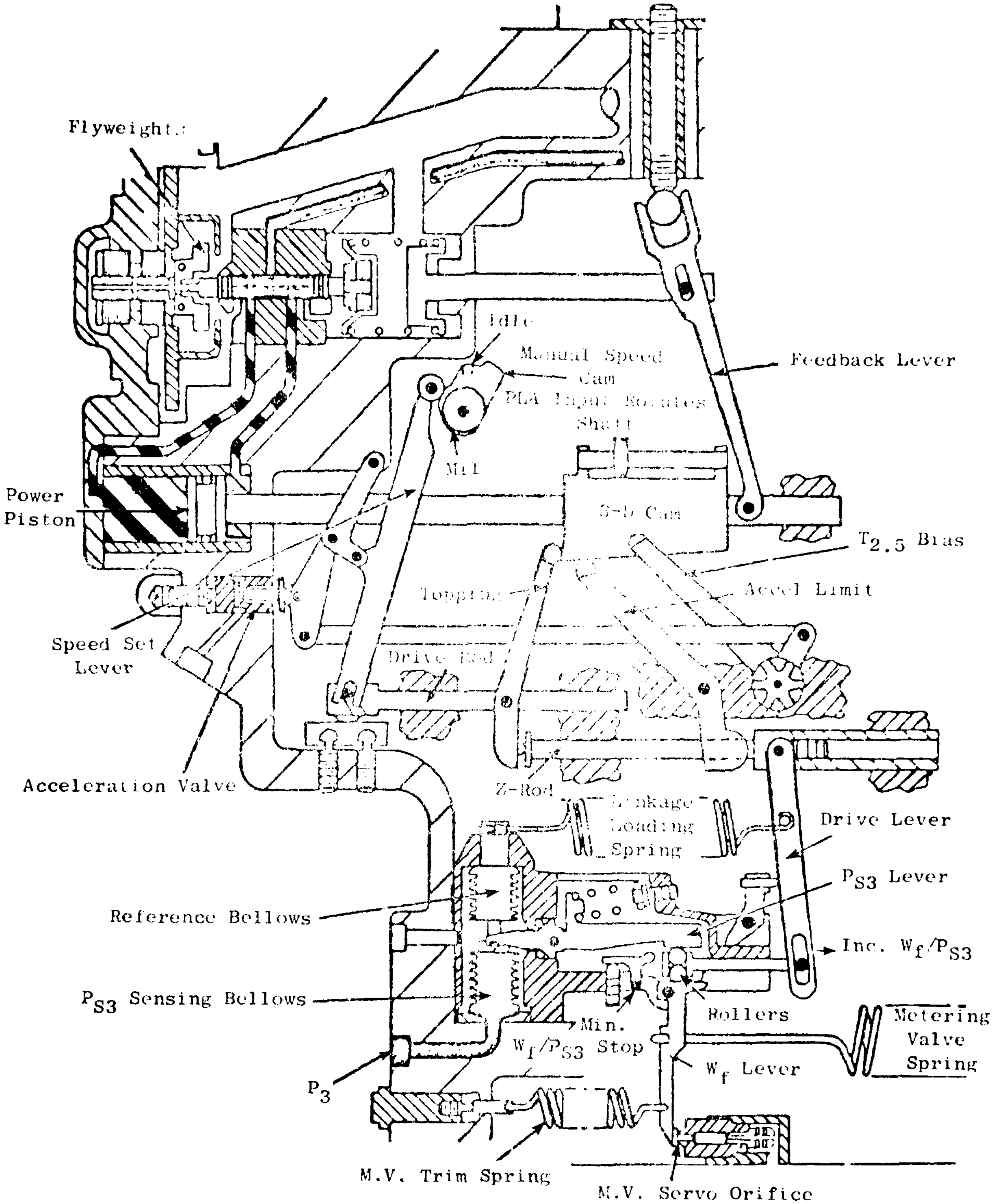

Figure 3. Backup Control Computer Schematic.

The speed sensing system is composed of an engine-driven flyweight governor, pilot valve, feedback spring and lever, 3-D cam, and power piston (See Figures 3 and 4). During engine steady state operation, governor flyweight centrifugal force is balanced by feedback spring force. Under these conditions, the pilot valve is held in null position. Assume an increase in fuel flow in response to a control lever advance. Additional fuel flow produces increased engine speed in response to which the governor flyweights move outward, displacing the pilot valve to the right. High-pressure fuel, ported to the right end of the power piston, moves it to the left. By virtue of its mechanical connection, the 3-D cam follows this motion. Movement of the power piston to the left rotates the feedback lever clockwise and around its pivot point. This action compresses the spring until the spring force overcomes the centrifugal force of the flyweights. The pilot valve moves back toward the null position and the flyweights move toward their steady state position. When spring force is balanced by flyweight centrifugal force, the pilot valve is in a null position. The speed sensing system responds to changes in engine speed and schedules fuel flow to the engine in accordance with prescribed limiting functions to provide safe engine operation.

The incorporation of a 3-D cam minimizes control size and weight by employing a single cam to perform a number of functions. Translation of the cam, a function of engine speed, is provided by the speed sensing system. Rotation of the cam, a function of compressor inlet temperature, is provided by the $T_{2.5}$ servo system discussed in the Section II-3 below. During steady-state operation, governor flyweight force is balanced against feedback spring force. For each steady state operating point, the 3-D cam has a corresponding equilibrium position.

The contoured surface of the 3-D cam provides for signals to initiate the limiting and scheduling functions of the control. Four contours are used. The topping contour provides a top speed setting as well as a constant idle speed regardless of $T_{2.5}$ droop operation. To protect against stall and over-temperature, the acceleration contour provides a W_f/P_{S3} versus N_2 schedule. To ensure optimum engine performance, the $T_{2.5}$ bias and topping contour provides for resetting engine speed at high RPM and low $T_{2.5}$'s. The variable geometry contour provides for scheduling the position of the variable stator vanes as a function of compressor inlet temperature and engine rotor speed.

The metering valve positioning servo is the link between the computing section and the metering valve. Hydraulic force on the metering valve piston, shown earlier in Figure 2 as part of the fuel valve, provides the motion necessary for changing the flow area. The magnitude and direction of the force are provided by a hydraulic servo which consists of the metering valve piston, a fixed supply orifice, a flapper valve with a pressure balancing piston, a metering valve feedback spring, and the W_f lever. Servo supply pressure (P_S), essentially pump discharge, is taken from the back side of a wash screen in the fuel valve. In the backup mode, one side of the servo piston sees a fraction of servo pressure, while the spring side sees

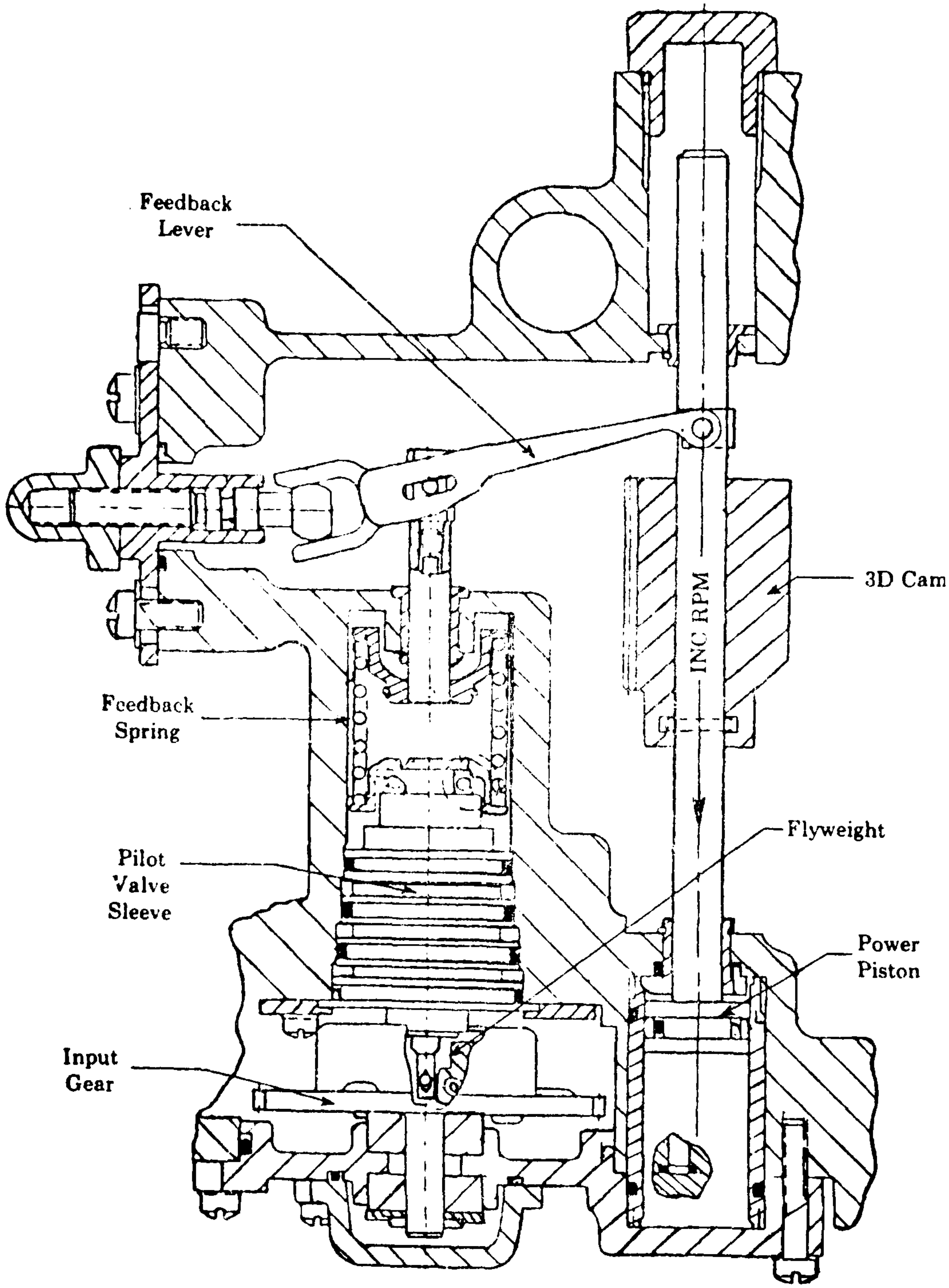

Figure 4. Partial Section Showing the Speed Sensor.

the variable [illegible] the flapper valve. During steady state [illegible] metering valve servo piston are balanced and [illegible]. If a signal to the W_f lever "requests" [illegible] increases, causing the pressure on the spring [illegible] decrease, and the metering valve moves [illegible] valve, which is considered part of the [illegible] Figure 2 to clarify the interface with the [illegible] some of the metering valve servo components.

Operation of [illegible], is scheduled as a function of engine [illegible] the 3-D cam. A hydraulic force amplifier [illegible] the variable geometry actuators. High pressure servo fuel [illegible] the β_c servo entering the servo piston from the side. After filling the passages in the piston, the fuel passes through [illegible] on the underside of the piston. The fuel discharges [illegible] orifice into the fuel control casing. The rate of flow is controlled [illegible] a gap between the servo discharge orifice [illegible] steady-state conditions, the gap size, as determined by [illegible] position, is such that hydraulic forces on both sides of the servo piston are balanced. Assume that the right end of the beam moves downward in [illegible] 3-D cam movement. The gap increases, allowing more fuel to be discharged [illegible] the case. Pressure on the underside of the piston decreases, upsetting the force balance, and the piston moves downward. The piston land [illegible] the [illegible], allowing high pressure fuel to flow to one side [illegible] to open the stator vanes. Fuel from the other side [illegible] through the upper port and exits [illegible]. Movement of the β_c actuators is fed back to the feedback [illegible], presenting a shorter radius to the beam, so that the [illegible] moves upward. The gap decreases, allowing [illegible] underside of the piston, moving it upward. Motion st[illegible] the scheduled position and the steady-state [illegible] provid[illegible] balanced hydraulic forces on the piston.

A discussion of the operation of the backup control during a backup mode acceleration follows. The most severe change in throttle setting is a rapid advance from IDLE to MILITARY, involving, of course, an engine acceleration of considerable magnitude. The following discussion will be primarily concerned with an acceleration of this type but will also cover variations in control operation where they [illegible] less severe throttle angle changes.

Rotation of the control power lever causes rotation of the manual speed cam inside the control because the two are mechanically connected. When the manual speed cam is rotated from IDLE to MILITARY, it presents a shorter radius to the top end of the speed set lever. The speed set lever rotates clockwise about its pivot point, moving the pivot rod to the left. Since the topping lever is [illegible] pivot rod and therefore pivots about this point, it will also move to the [illegible] with the pivot rod leaving both the 3-D cam and the [illegible]. The [illegible] spring [illegible] constantly exerting a force

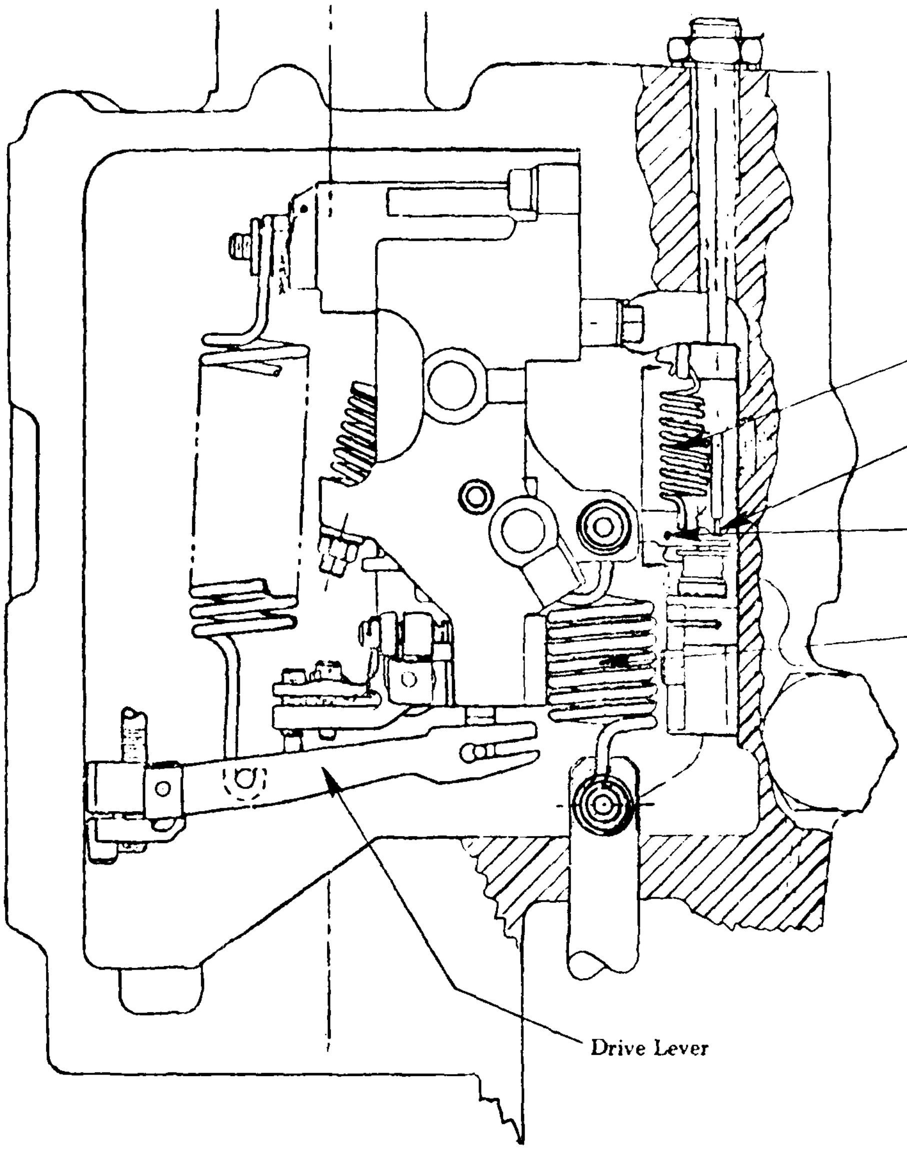

Figure 5. Partial Section Showing the Metering Valve Servo.

on the Z-rod [illegible] to the left, the Z-rod will [illegible] pivots counter-clockwise, moving [illegible] the moment arm on top of the W_f lever [illegible] rotating the W_f lever clockwise. [illegible] lever and the metering valve [illegible] orifice [illegible] decay in pressure behind the metering valve. [illegible] metering valve piston is upset and the piston [illegible] wider, causing an increase in fuel flow to the engine. [illegible] was considerable, the resultant movement of the [illegible]. The Z-rod movement to the left towards [illegible] continues until the Z-rod contacts the acceleration [illegible]. The acceleration limit lever pivots clockwise until its [illegible] the 3-D cam, at which point movement of the Z-rod [illegible] roller movement ceases and further increase [illegible] until the 3-D cam moves. The fuel flow now [illegible] exceeds the engine steady state requirements, causing an [illegible] engine speed. The centrifugal force of the governor flyweights [illegible] force and the fly-weights extend outward moving the [illegible] to the right. High pressure servo fuel, flowing [illegible] the power piston, moves the piston and the 3-D cam to the left. [illegible] acceleration limit lever further rotates clockwise in response [illegible] acceleration schedule cut on the cam. This allows the Z-rod [illegible] the left and the rollers to the right scheduling [illegible] by the acceleration schedule on the 3-D cam. Meanwhile, as engine [illegible] as a result of increased fuel flow, compressor discharge pressure [illegible]. This expands the P_{S3} sensing bellows, [illegible] P_{S3} lever clockwise and increasing the force [illegible] cumulative effect of increased engine rpm and P_{S3} [illegible] on the fuel flow scheduled by the cam and P_{S3}.

During the acceleration [illegible] Z-rod are moving toward the topping lever, which [illegible] the 3-D cam and the Z-rod. This results in a [illegible] the topping lever is not in tension between the 3-D cam and the Z-rod. [illegible] speed during this type of acceleration is, therefore, [illegible] the topping schedule on the end of the 3-D cam [illegible] the side of the cam. Eventually, the 3-D cam [illegible] topping lever and rotates it counterclockwise until [illegible] the Z-rod. At this point, the acceleration [illegible] acceleration schedule on the cam because of the movement [illegible] the right. Continued movement of the 3-D cam [illegible] lever to push the Z-rod to the right and [illegible] fuel flow. It should be noted that for each [illegible] inlet temperature there is a different acceleration [illegible] line. The schedule is changed when the [illegible] the 3-D cam presenting a different contour to the [illegible] which is controlling fuel flow at the time. The engine accelerates with the maximum fuel flow possible without encountering [illegible] excessive turbine discharge temperature, or rich [illegible] i.e., rapid

throttle movements of considerable magnitude, will follow the same pattern. These may be initiated at any point along the steady state line and, if great enough, will involve the employment of the acceleration schedule on the 3-D cam.

A power lever movement of only a few degrees does not follow the above pattern. This slight movement rotates the manual speed cam slightly, presenting a shorter radius to the speed set lever. The speed set lever pivots clockwise and moves the drive rod and, therefore, the topping lever, to the left. The linkage loading spring causes the Z-rod to follow the lower end of the topping lever to the left and the rollers to move to the right, thus increasing fuel flow. However, in contrast with an acceleration of considerable magnitude, the Z-rod does not travel far enough to contact the acceleration limit lever before it catches up with the topping lever. The increase in fuel flow causes an increase in engine speed which is sensed in the governor. The centrifugal force of the flyweights overcomes the spring force balancing the pilot valve and the pilot valve moves to the right. High pressure fuel moves the power piston and the 3-D cam to the left rotating the topping lever counterclockwise. Since the Z-rod is in contact with the topping lever, it will move to the right and the rollers to the left, decreasing fuel flow. Movement of the 3-D cam pivots the feedback lever clockwise sufficiently to increase the spring force against the pilot valve. The pilot valve moves towards the governor flyweights until the forces on the spring and flyweights are again in balance. The engine is now operating at a steady-state point, the operating condition selected by the power lever. (See Figure 6.)

3. COMPRESSOR INLET TEMPERATURE SENSOR

The compressor inlet temperature sensor ($T_{2.5}$) is shown schematically by Figure 7. The servoed $T_{2.5}$ sensor output rotates the 3-D cam.

The $T_{2.5}$ sensing tube is filled with nitrogen. The spiral tubes in the inlet are shrouded for protection. The gas is very sensitive to minute changes in temperature. This sensitivity causes a motor bellows located within the control to expand or contract with changes in compressor inlet temperature. A reference bellows, also filled with gas but at a lower pressure, is located opposite the motor bellows. The reference bellows compensates for changes in fuel temperature within the control. The $T_{2.5}$ servo nozzle, connected to the bellows assembly, pivots with expansion and contraction of the bellows, thereby directing servo fuel to the right or left side of the servo piston which moves axially within the chamber. The piston is mounted on a shaft with one end of the shaft attached to a gear sector which in turn mates with a similar gear sector on the 3-D cam. The other end of the shaft is attached to a control arm which, along with a feedback spring, works to establish a force-balance system within the servo. In a null or steady-state position, a force balance positions the servo nozzle, so that servo fuel discharging through the nozzle impinges upon a spike at the entrance to the servo piston, dividing the flow to create equal or balanced pressure on both sides of the piston. Assume that an increase in $T_{2.5}$ causes the bellows to expand. The servo nozzle, attached

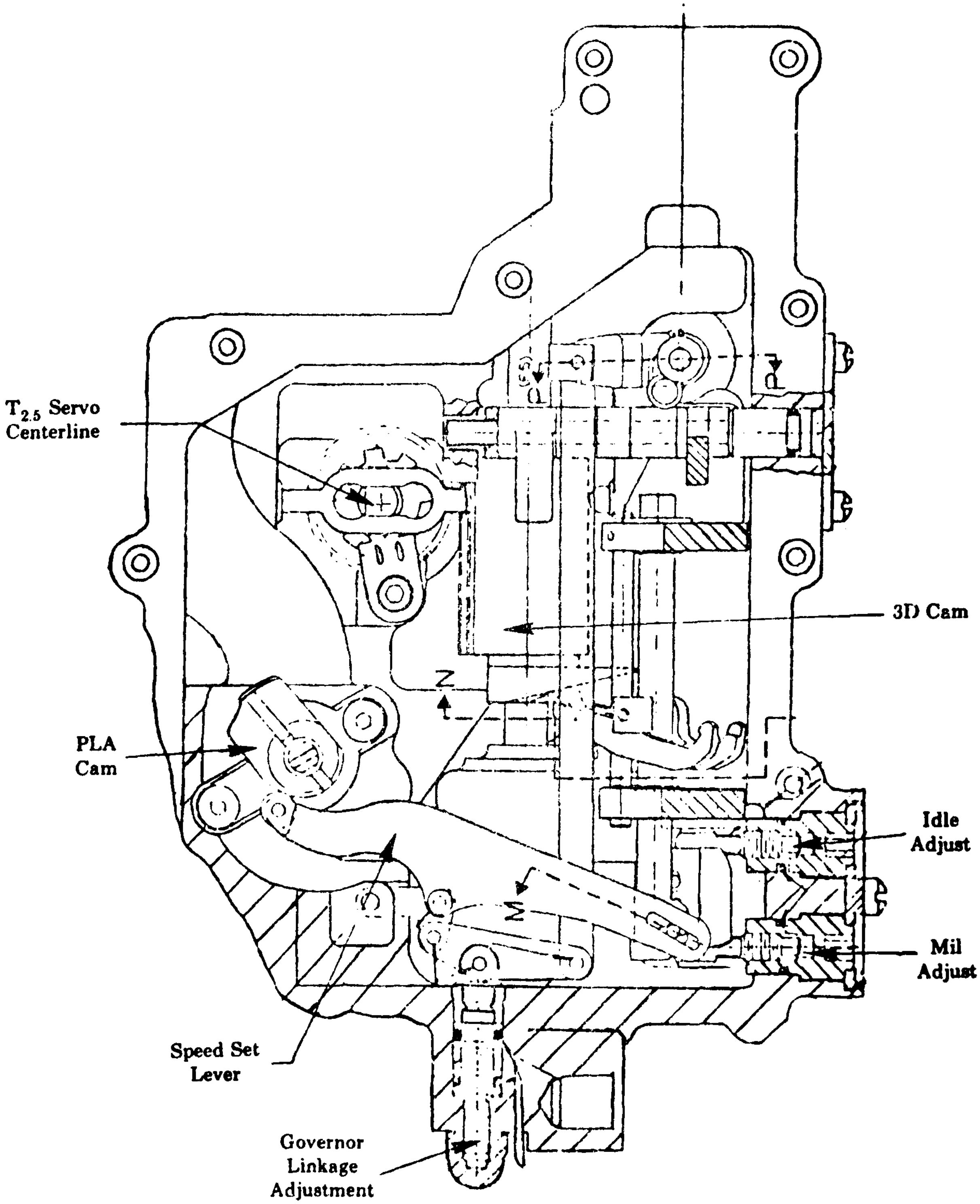

Figure 6. Partial Section Showing the PLA Cam and Several Levers.

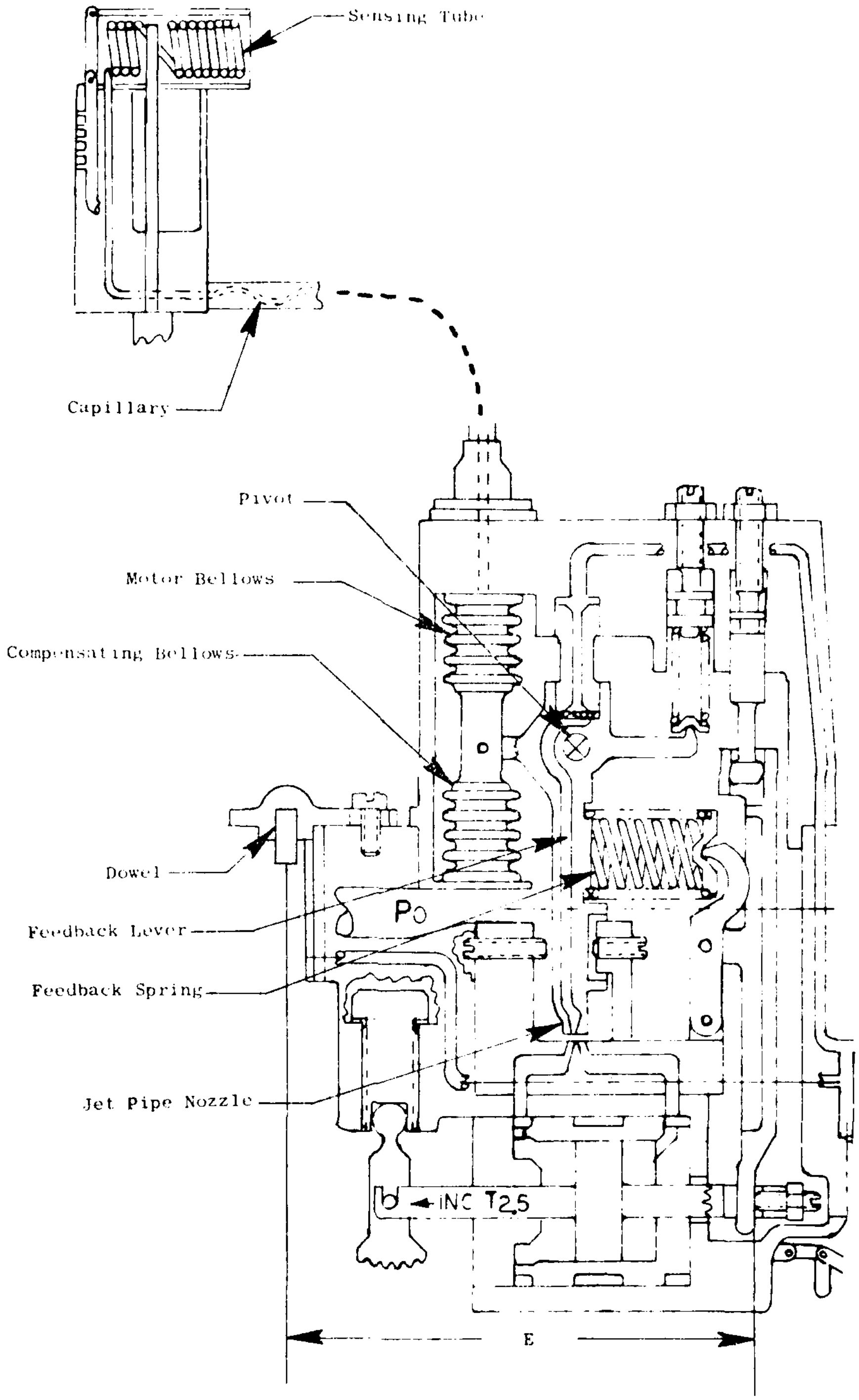

Figure 7. $T_{2.5}$ Sensor.

to the bellows, will pivot in a counterclockwise direction, directing high pressure servo fuel to the right side of the spike and to the right side of the servo piston. Because the greater portion of servo fuel is directed to the right side of the servo piston, a pressure differential now exists, creating a force unbalance across the piston. With this force unbalance, the servo piston now moves to the left, rotating the 3-D cam counterclockwise. In moving to the left, the servo piston moves the feedback arm in a counterclockwise direction, compressing the servo nozzle spring. As the spring force increases, with the piston moving to the left, it moves the nozzle servo counterclockwise, gradually directing more flow to the left side of the servo piston. A steady-state or null position is reached; i.e., forces generated by the expanding of the bellows are balanced by counteracting spring force. At this point, the servo nozzle is located such that servo fuel flow is directed equally to the right- and left-hand sides of the servo piston, maintaining equal pressure on both sides of the servo piston.

Figure 8 is a partial section showing some of the components of the $T_{2.5}$ servo. It is integrated with the hydromechanical computer as shown in Figure 2.

The charge pressures and the feedback spring rate and preload were the variables that could be adjusted to allow the use of the J85 $T_{2.5}$ sensor for the backup control. Further, the expected test temperature range is 20° F to 400° F while the present sensor range is -65° F to 275° F. For this backup control, the pressure was adjusted so that 20° F corresponded with the present -65° F cam position. Calibration allows obtaining the best accuracy at a given $T_{2.5}$ and fuel temperature. The temperatures selected for this were a $T_{2.5}$ of 224° F and a fuel temperature of 100° F. These are nominal temperatures for engine testing.

4. FUEL VALVE

a. General

The fuel valve used with the hydromechanical backup control is based on the one designed, fabricated and tested for the Light Weight Fuel Delivery System program under U.S. Navy Contract No. 0140-75-C-0040.

The mechanization of the main fuel components employs shear-type valves and a jet-pipe hydraulic amplifier to provide maximum contamination resistance. The main fuel metering package provides for (1) main fuel metering, including a throttling valve for holding a constant head, (2) main fuel cutoff, (3) positional readout of the metering valve for electrical computation use, and (4) splitting of the flow for the vortex valve distribution system. These functions, appearing as they are required for the backup control, are shown schematically in Figure 9.

The main fuel valve package contains the following elements:

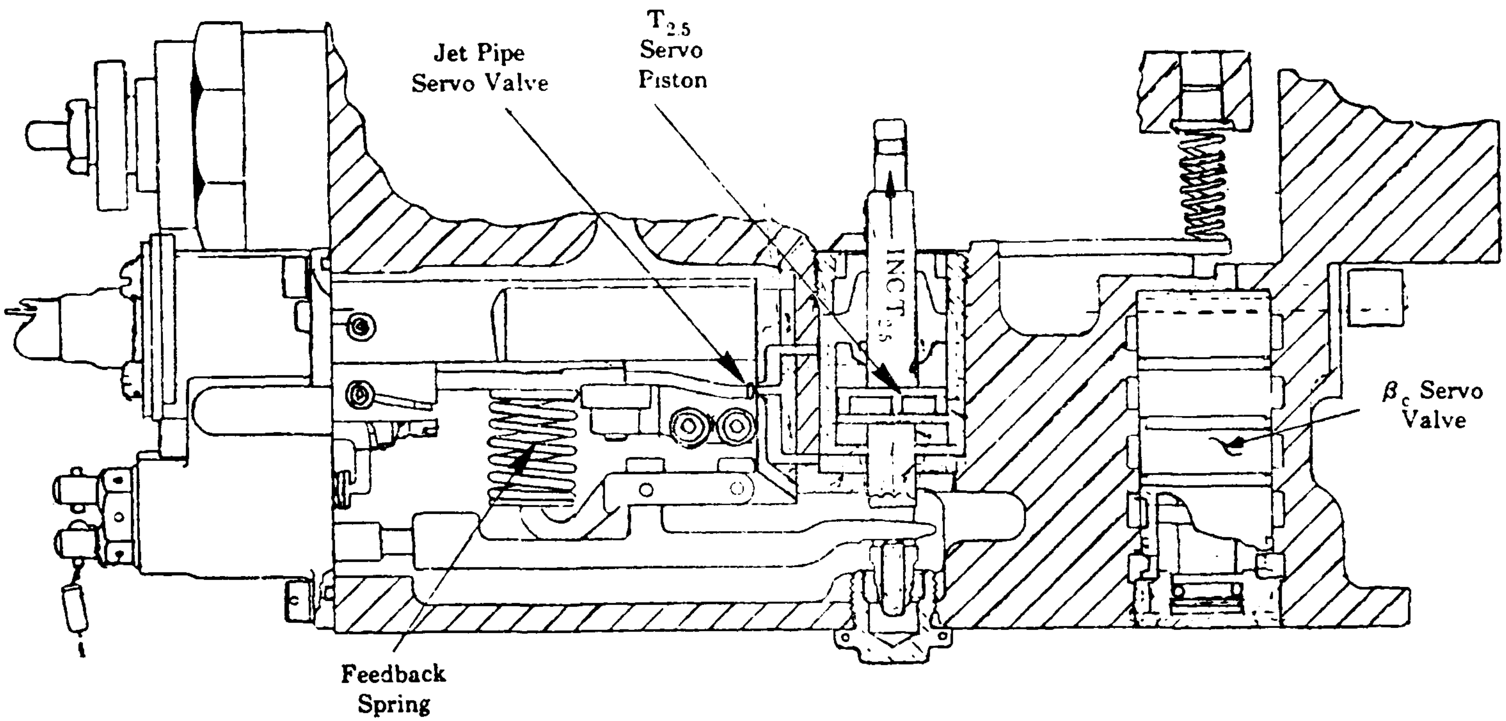

Figure 8. Partial Section Showing the $T_{2.5}$ Servo.

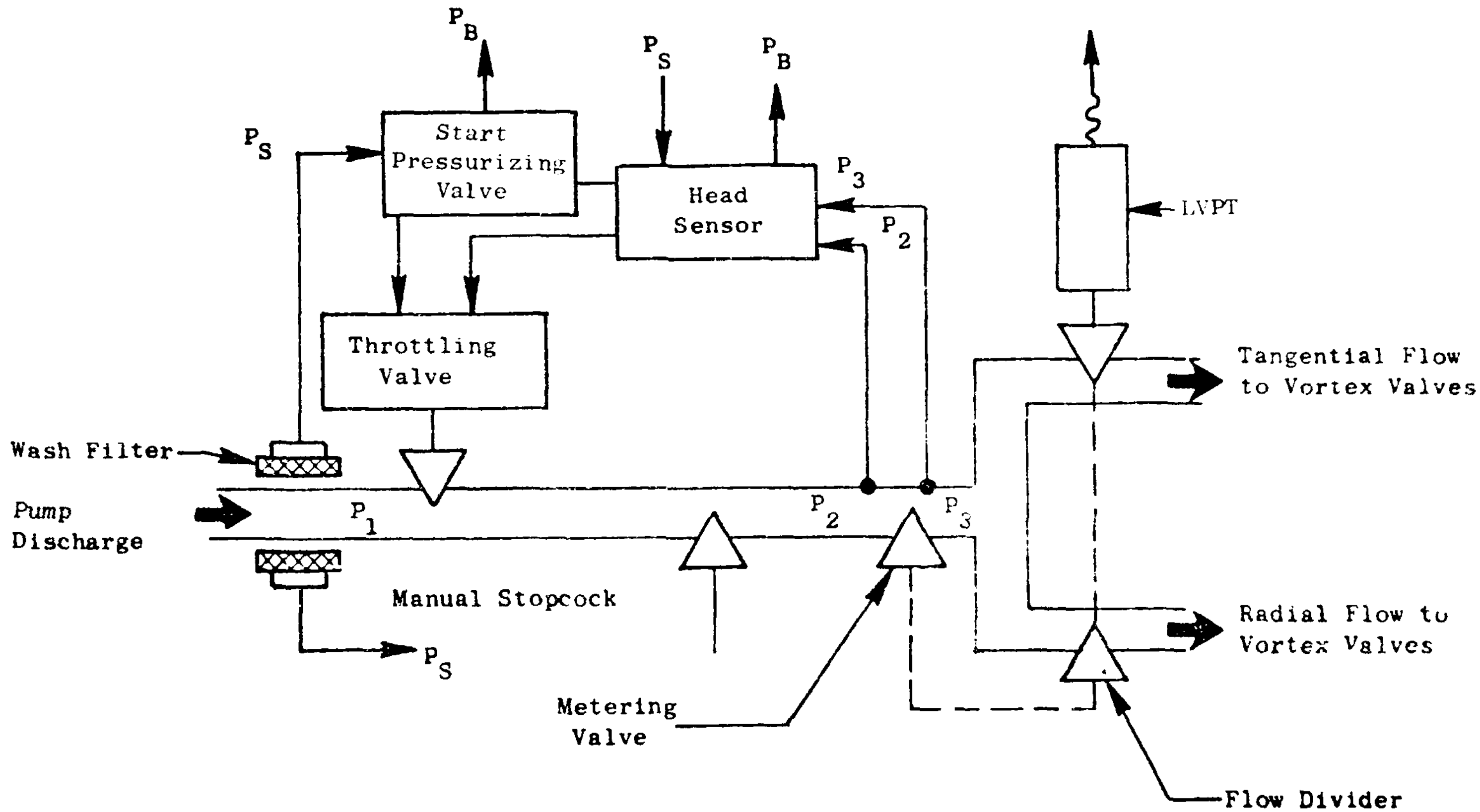

Figure 9. Fuel Valve Functional Block Diagram.

- main fuel metering valve
- flow divider valve
- cutoff valve
- throttling valve
- head sensor
- servo wash screen
- start pressurizing valve

Figure 10 is a cross section showing the functional relationship of the valves and some of their details. The major components of the fuel valve are discussed in detail in the following paragraphs.

b. Main Metering Valve

The metering valve is a shear-type valve lapped to zero clearance to avoid silting and leakage. The shoe is driven by an actuation piston which is controlled by either the primary or backup control servovalve.

Fuel flow feedback is provided by the LVPT, which is discussed later. The pressure drop across the metering valve is kept constant at approximately 53 psid by the head sensor and throttling valve.

The shoe of the metering valve is loaded by the 53 psi differential pressure but is balanced by pressure grooves machined into the plate to minimize friction. The shoe is also loaded by a light spring (5 lb) to maintain contact during non-operation. The valve port is triangular.

The valve nominal dimensions are as follows:

Maximum flow (at 53 psid)	16,670 pph
Valve stroke	0.6 in.
Piston area	1.0 sq. in.
Port gain	0.5473 X^2 sq. in./in. (X is stroke)

An adjustable minimum flow stop is provided that will set a minimum fuel flow below that which is normally scheduled by the primary or backup controls.

The dynamic seals on the metering valve piston and rod are Viton™ O-rings with Teflon™ cap seals. A rod scraper is used to protect the rod and seal from contamination carried through the metering valve cavity. The shoe and valve plate are of Type 440 stainless steel with a Dicronite™ (dry film lubricant) coating. The housing bores have a hard anodic coating.

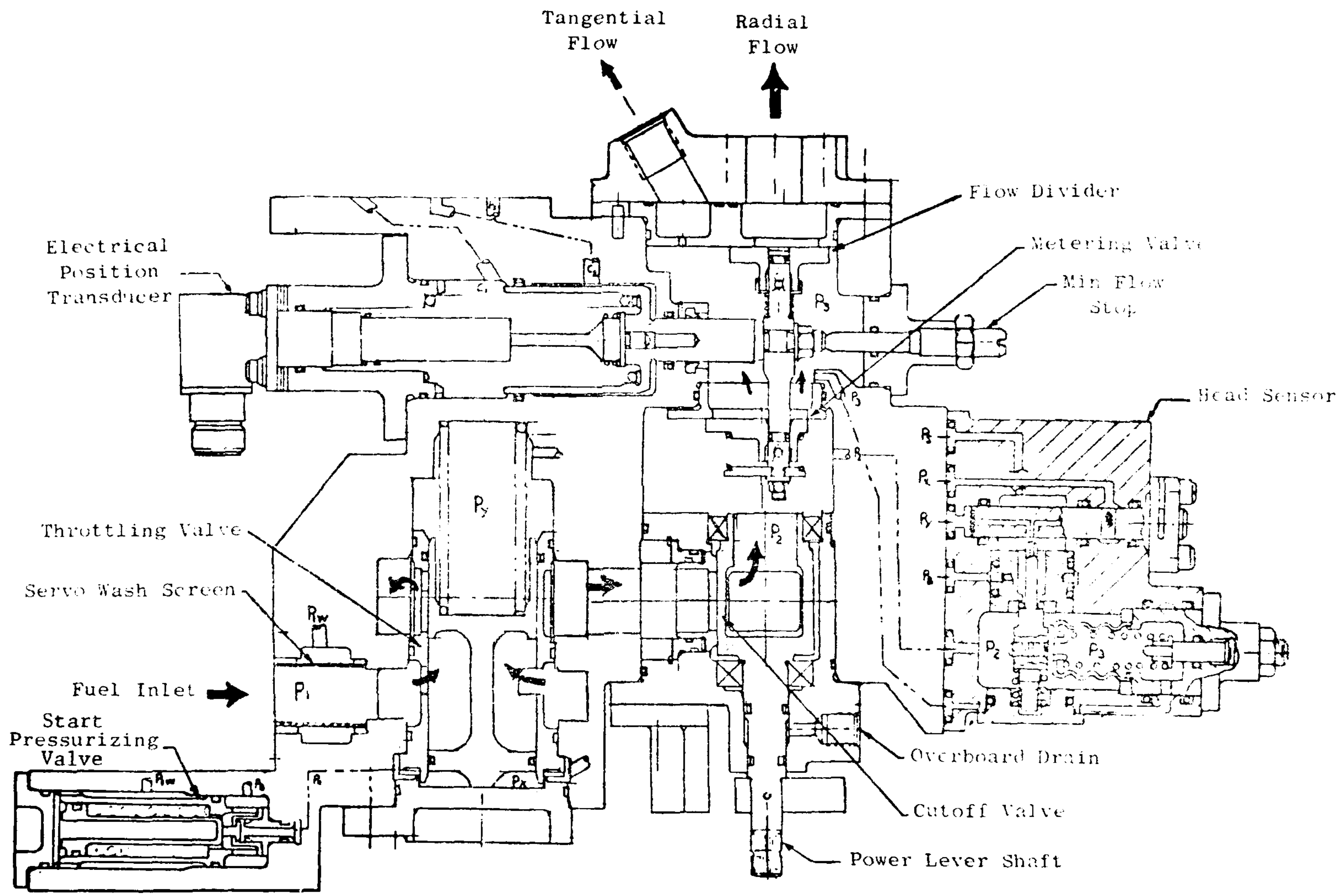

Figure 10. Main Fuel Valve Schematic.

c. Flow Divider Valve

The flow divider is a shear valve similar to the metering valve and is driven by the same servo piston. Its shoe loading and balancing are similar to those of the metering valve. The shoe and plate use the same material and coating as were used for the metering valve's shoe and plate.

c. Cutoff Valve

The cutoff valve is a rotary shear valve driven by the power lever. The plug and spool are lapped at assembly for near-zero leakage. The plug O-ring diameter and plug contact area have been defined to provide a limited pressure load to maintain sealing. To maintain contact at low pressure drop conditions, a spring preload of about 10 lb is used on the plug.

The plug material is hardened 440C stainless steel. The spool/shaft is a braze fabrication of 440C and 410 stainless steel.

To eliminate bearing internal clearance, the bearings are preloaded with a wave spring. The outboard bearing has been sized to carry the shaft thrust load at maximum pressures. A double rotary seal with an overboard drain in-between is used to maintain zero external leakage.

e. Throttling Valve

The throttling valve pictured in Figure 10 is an unmodified, F101 augmentor fuel control throttling valve based on an existing design. This valve was selected because of its success in passing F101 design-assurance contamination testing with no degradation. The augmentor fuel control was exposed to MIL-E-5007C contaminant filtered to 74 micron absolute. The test duration was 15 hours.

f. Head Sensor

The head sensor pictured in Figure 10 is an F101 augmentor fuel control head sensor utilizing a jet pipe driven by a bellows. The assembly uses the existing design with no changes. Past response testing of augmentor controls and the fuel valve has shown that the head sensor gain is adequate to meet the system requirements.

g. Servo Wash Screen

The servo wash screen provides clean servo flow to the primary W_f and P_c electrohydraulic servovalves, the head sensor/throttling valve servo and the hydromechanical backup control computer and servos. The filtration level is 40 micron absolute (25 micron nominal) and is based on the clean fuel requirements of the metering valve servovalve and the stator servovalve. The screen construction uses a square-weave Type 347 stainless steel wire wash surface mesh backed by coarse Rigimesh™ support.

The wash screen will be capable of supplying a maximum transient servo flow of 5000 pph at 100% speed.

h. Start Pressurizing Valve

To ensure that there would always be sufficient pressure for servo operation during start, a start pressurizing valve was added to the system in case (1) engine motoring would be initiated with the power lever at the idle (or above) position or (2) the metering valve would inadvertently be in a large-area position. Without the start pressurizing valve, system impedance would not be adequate to pressurize the servos and "hot" starts could occur. The start pressurizing valve senses inlet pressure and ports the throttling valve opening pressure to boost in order to keep the valve closed. At inlet pressure of 150 psi above boost, control of the throttling valve is returned to the head sensor for normal head regulation. Thus, sufficient servo pressure will be available during engine start regardless of the initial positions of the metering valve and cutoff valve.

i. Metering Valve Position Transducer

The primary electronic control (FADEC) is digital, and there are significant advantages to using digitally compatible sensors. A major advantage is that analog-to-digital converters are not necessary. FADEC will use linear variable phase transformers (LVPT's) for all position transducers including metering valve position.

The linear variable phase transformer is an electromechanical device that senses mechanical position and outputs an electrical signal that is directly convertible to digital form.(See Figure 11.) Its construction is very similar to a linear variable differential transformer (LVDT) having three coils (two primary and one secondary) arranged in line on a bobbin through which an iron core is moved. The two primary coils are excited by a constant-amplitude alternating current with specific phase separation that also is kept constant. The primary currents induce an alternating magnetic flux in the core. This flux is equal to the vector sum of the fluxes that would be induced in the core by the primary windings separately. The secondary coil has an induced potential of constant magnitude which is used to detect the phase of the core flux. The phase of the secondary current is a function of the core position. If the core is centered in the coils such that the number of turns engaged in each primary winding is the same, the secondary winding phase will be midway between the phase angles of the primary windings. As the core is moved away from the midposition and engages unequal numbers of primary turns of each type, the secondary coil phase angle changes to be more closely aligned with the phase of the higher-coupled primary winding. With linear-wound primary coils, the theoretical phase output of the secondary coil is an arctangent function of core position. If the primary coils are wound in a special pattern, such as exponential, the output signal becomes a nearly linear function of core position.

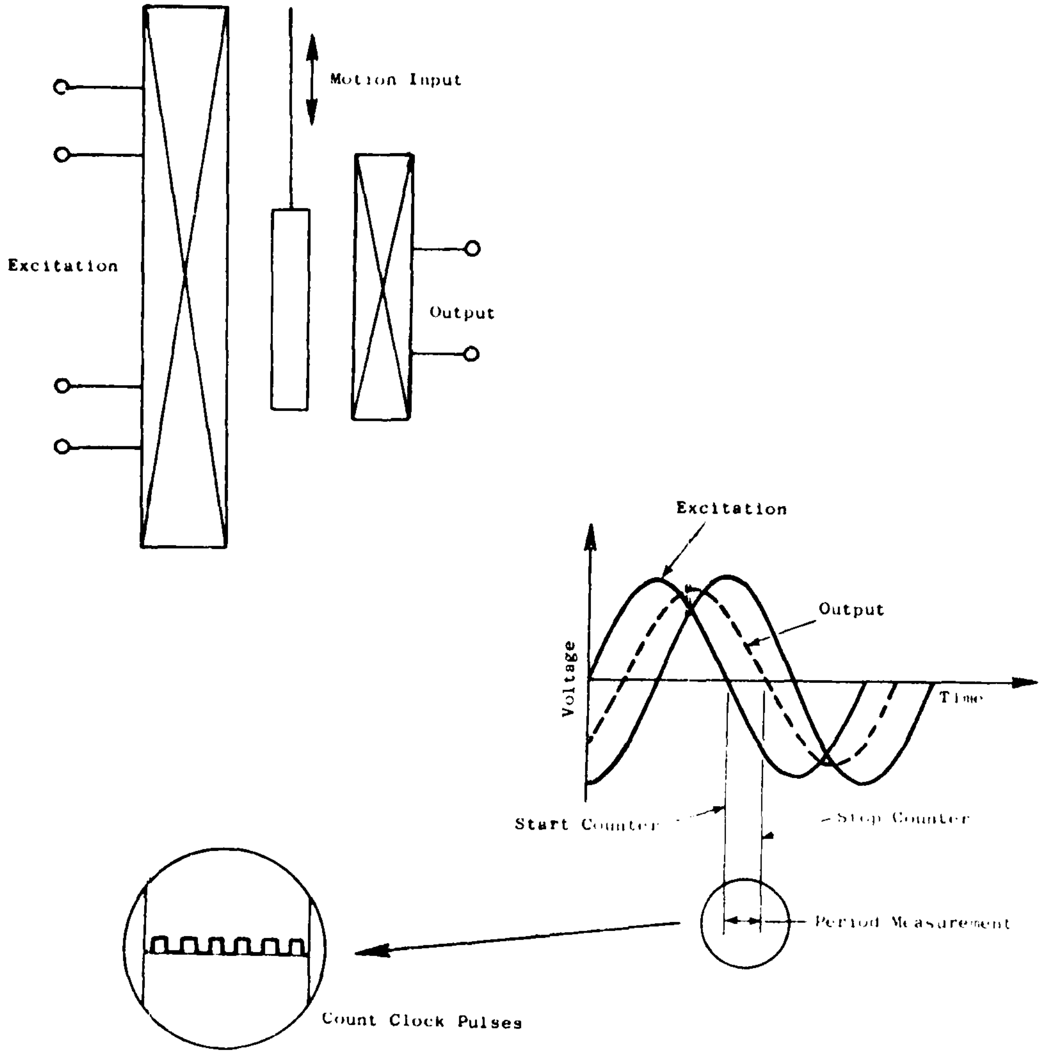

Figure 11. LVPT Position Transducer Schematic.

With suitable digital electronic elements, the output phase angle shift from a null reference position is detected and converted to a binary word that can be used directly in a digital closed-loop system.

Physically, the LVPT is similar to the LVDT in size, shape, construction and materials. Therefore, it has similar very high levels of reliability and identical mounting requirements.

j. Summary

The fuel valve discussed above was recognized to be a low risk item because except for the LVPT, this valve has been thoroughly tested as a component and as an element in systems tests. This fuel valve design was also used successfully on five GE23 engine tests.

5. METERING VALVE MECHANICAL POSITION FEEDBACK

The metering valve previously used for the J85-21 Main Fuel Control (MFC) did not have sufficient capacity for the JTDE engine. In addition, this control used a bypass valve while a throttling valve is needed with the intended centrifugal main fuel pump. Therefore, the fuel valve discussed previously was mounted adjacent to the computer on the same mounting adapter.

Metering valve mechanical position feedback is needed to stabilize the fuel metering loop. Figure 12 shows the mechanism at the fuel valve. A guided rod is threaded to the metering valve servo piston rod. A rod seal is used to separate the metered fuel from the cavity containing the rack and pinion. This cavity is at boost pump pressure (P_B). The rack is mounted to a second member, which in turn is threaded to the guided rod. Shims and a backup roller are used in eliminating the backlash between the rack and pinion. The pinion is attached to a rod which transmits the rotation to the computer portion of the backup control. The adjustable minimum fuel flow stop is also shown.

The feedback mechanism at the computer is shown by Figures 13 and 14. A rotary shaft is used to transmit the metering valve position from the fuel valve to the computer. This shaft (Figure 13) rotates a slot-type cam. A bellcrank, with a roller at one end and a low-friction pivot by the other, is used to transmit the cam rise to the feedback spring (Figure 14).

The feedback cam rise versus degrees rotation was defined. The following design information was used:

Pinion Pitch Diameter	0.50 in.
Pinion Diametral Pitch	32 teeth/in.
Maximum Metering Valve Travel (X)	0.60 in.
Maximum Feedback Spring Stroke	0.575 in.
Maximum Fuel Flow (at 0.60 in.)	16,670 lb/hr
Metering Valve Gain	46,100 lb/hr/in.^{2}
Follower Roller Radius	0.156 in.

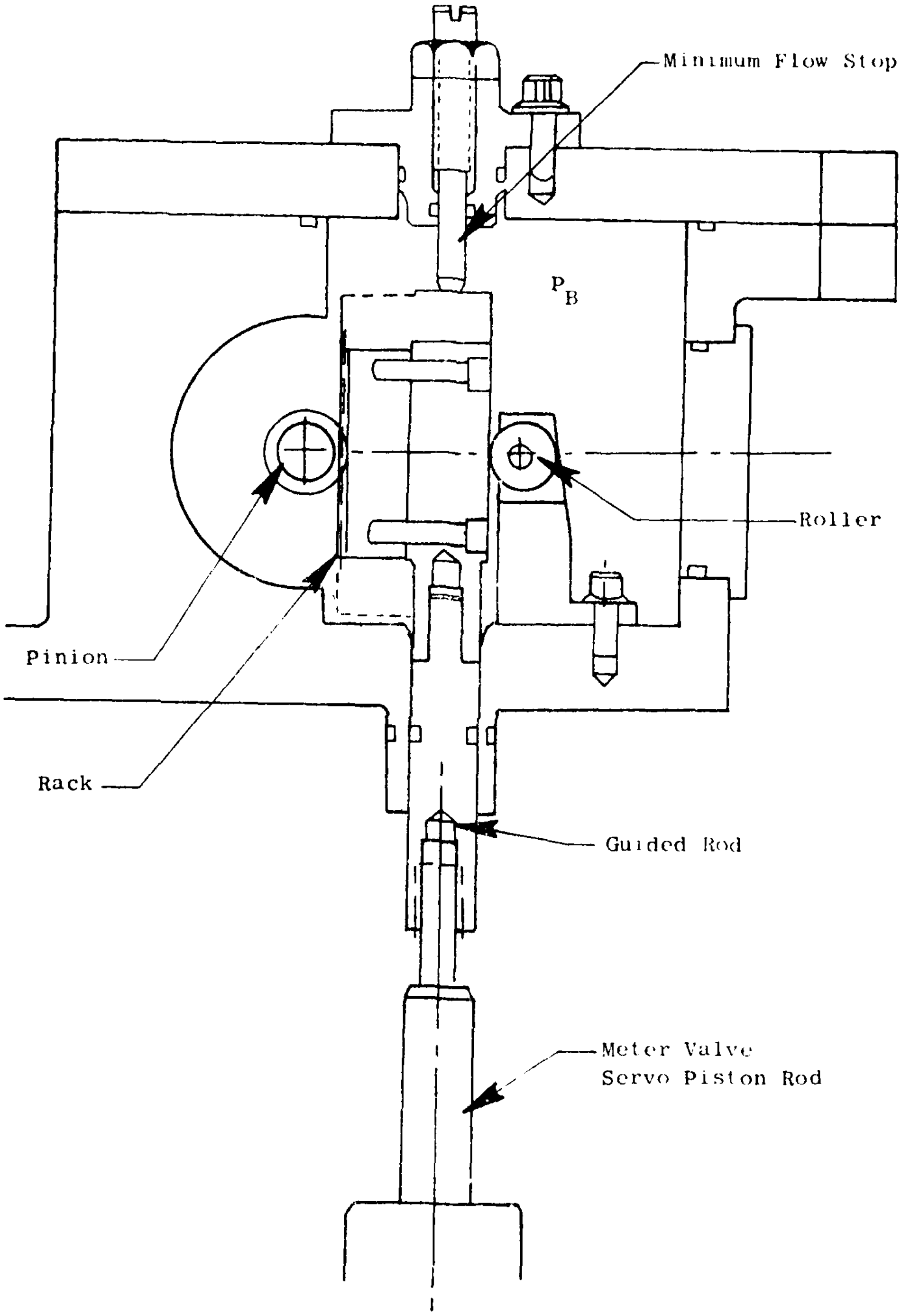

Figure 12. Metering Valve Position Feedback Mechanism at the Fuel Valve.

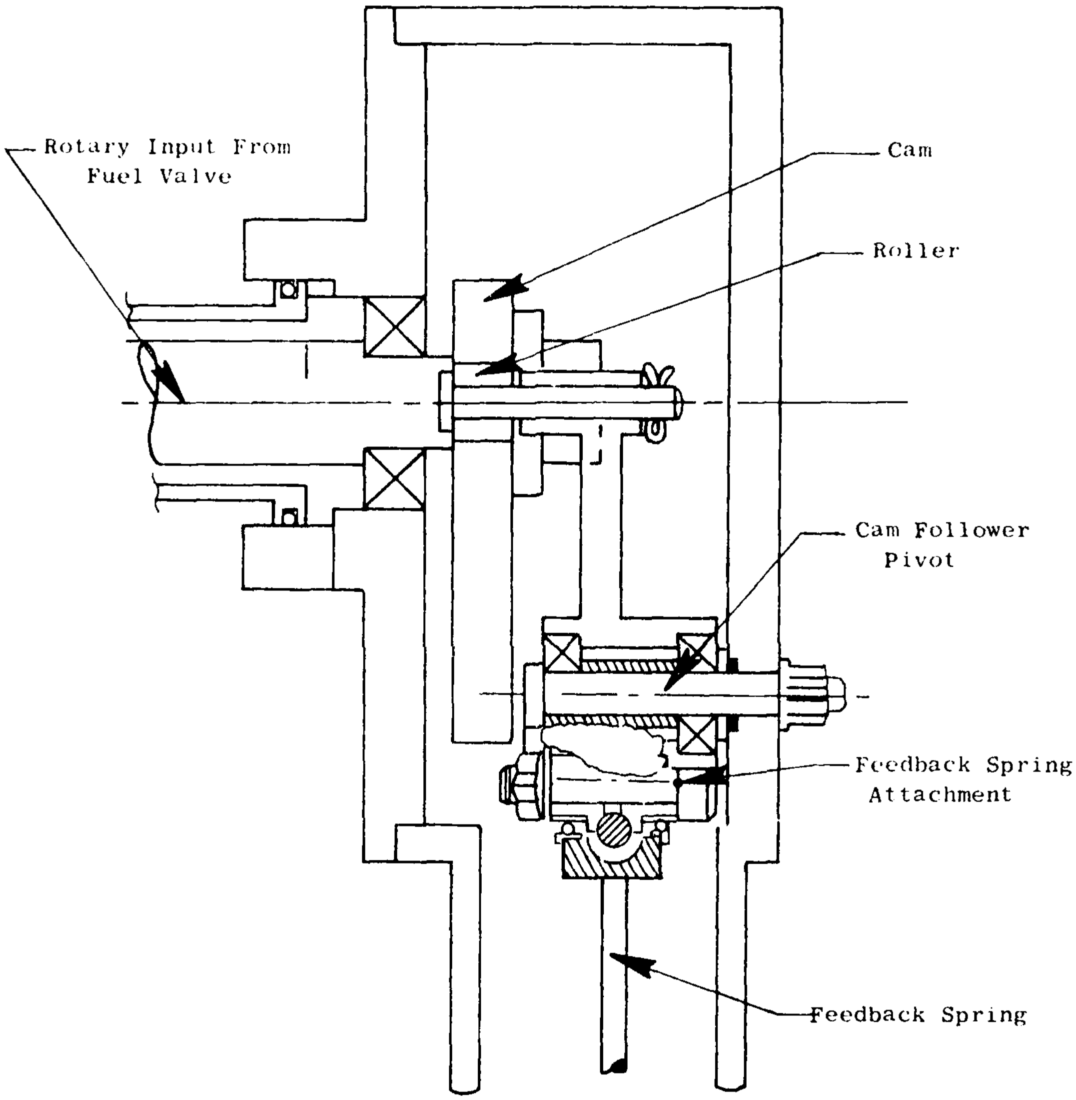

Figure 13. Metering Valve Position Feedback Mechanism at the Computer.

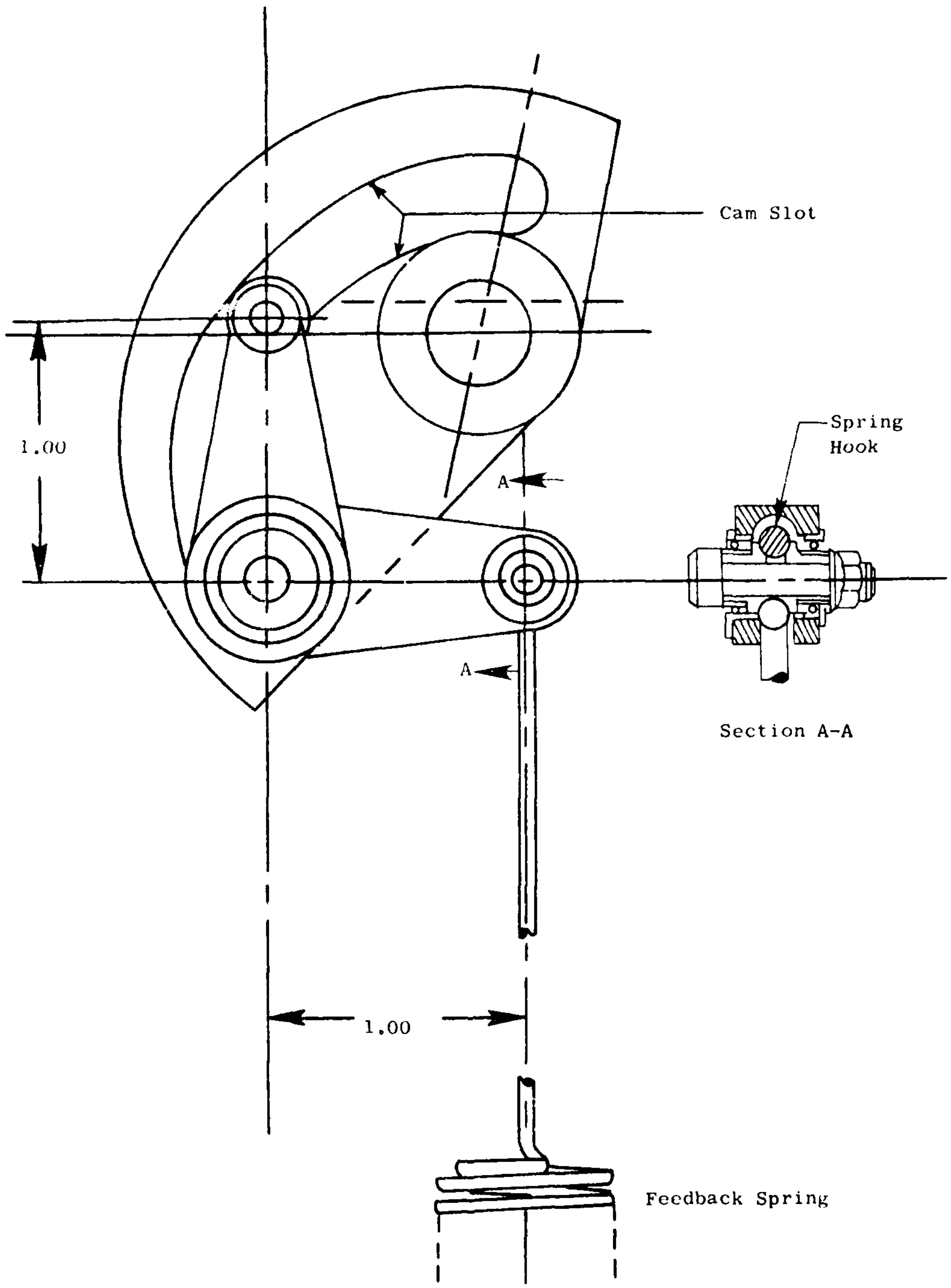

Figure 14. Feedback Cam and Follower.

Other calculations pertaining to the metering valve position feedback mechanisms were made. Some of the pertinent results are:

Maximum Spring Force	14.8 lb
Resulting Cam Torque, maximum	9.7 in.-lb
Cam Contact Stress	55,245 psi
Pinion Gear Tooth Load, maximum	38.8 lb
Pinion Gear Tooth Stress, maximum	19,968 psi
Feedback Spring Stress, maximum	69,210 psi
Feedback Spring Hook Stress	64,000 psi

The stresses given in the above list are considered to be conservative.

6. TRANSFER LOGIC

The following transfer criteria were used in the design of the backup control.

- Core overspeed as detected by the hydromechanical backup control computer
- Pilot demand
- Lack of electrical power to the primary control
- Lack of a "good health" signal as determined by the self-test feature of the primary control

The selected transfer logic and its implementation are shown by Figure 15. The various means of initiating and completing transfer are discussed below.

When overspeed is detected, the speed sensor in the hydromechanical backup control closes the normally open overspeed switch. This connects 28 volts (aircraft power) to the backup solenoid no matter what the mode is for the four-position switch in the off-engine unit. The speed sensor also opens a normally closed switch in the primary solenoid circuit. When overspeed occurs, the opening of this switch prevents applying 28 volts to both solenoids when the four-position switch is in the PRIMARY mode. The desirability of the normally closed switch was identified late in the design phase. Instead of redesigning, this action was demonstrated by using the HOLD position. The backup solenoid actuates a valve that ports pressures in a manner that causes the valve spool to translate to the backup position. When the backup position is reached, two switches are closed. The first sends a signal to the primary control indicating that transfer of W_f and β_c control is complete; the primary control then turns off all current going to the remaining servovalves. This causes the remaining servos to drift toward their desired stops. The second switch turns on the indicator light in the off-engine unit.

The pilot can demand backup control operation by selecting the BACKUP position of the four-position switch. This connects 28 volts to only the backup solenoid. The action thereafter is the same as was discussed above for the case that occurs when overspeed is detected.

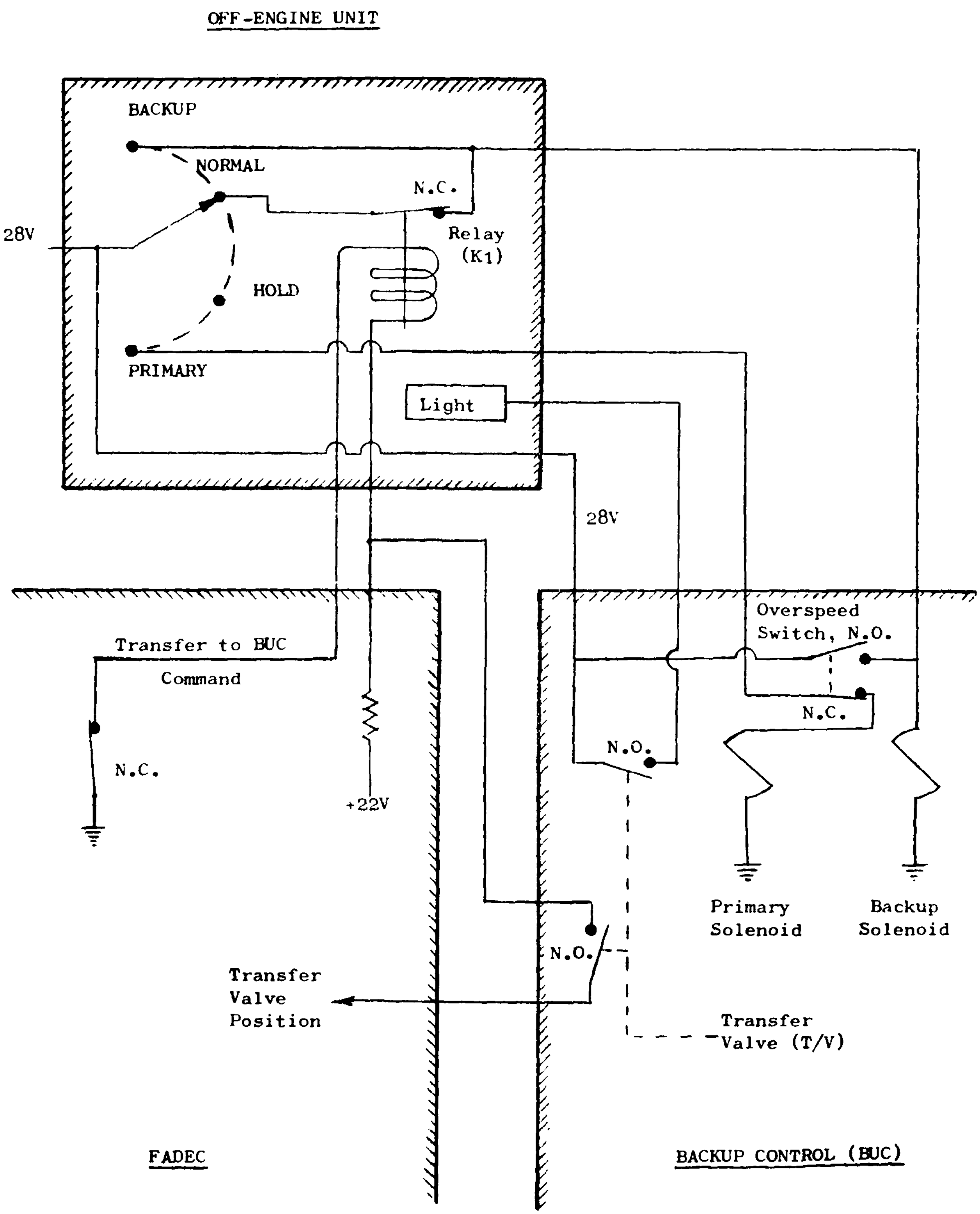

Figure 15. Primary/Backup Control Electrical Interface Block Diagram.

In Figure 15, the relay (K1) in the off-engine unit is held open by the 22-volt signal from the primary control. Assuming the four-position switch is in the NORMAL position, loss of primary control electrical power causes a loss of the 22-volt signal. This causes the relay (K1) to close, connecting 28 volts to the backup solenoid. The action thereafter is the same as for the case when overspeed is detected. The pilot can block this automatic transfer to backup control by having the four-position switch in the HOLD or PRIMARY position.

The primary electronic control has a self-test feature which continuously monitors performance. If a lack of "good health" is detected, the 22-volt signal to the relay (K1) is interrupted. The action thereafter is the same as for the loss of primary control electrical power.

The solenoids are of the latching type so that the 28-volt aircraft-supplied power need not be continuous. The four-position switch shown for the off-engine unit is not intended to represent aircraft cockpit switch design. Momentary contact switches could also be used.

7. TRANSFER VALVE

The transfer valve (Figure 16) is shown in the primary mode position. The solenoid valve is blocking the orifice flow back to the control case (P_O) so the pressure in the spring chamber is servo supply pressure (P_S). Since the larger piston area is at P_S and the spring force is to the right, the net force is to the right. The solenoid valve (Figure 17) is of the magnetic latching type. When the solenoid valve is opened, the transfer valve spool strokes to the left stop (backup mode). In this position, the transfer valve allows only backup W_f and β_C servo flows to the metering valve piston and core stator actuators.

The spool and sleeve are of 440C stainless steel (AMS 5630). These parts are heat treated at 1850° F to 1900° F for 50 to 70 minutes in a neutral atmosphere and then quenched. After quenching, the parts are stabilized at -110° F to -120° F for three hours minimum, tempered at 650° F to 700° F for one hour, stabilized at -110° F to -120° F for three hours minimum, and finally tempered at 650° F to 700° F for one hour minimum. The expected hardness is Rockwell 15N 87 minimum. The spool and sleeve are matched with a diametral clearance of 0.0003 to 0.0006 inch.

The backup control transfer sequence involves two switches which are normally open and are closed when the transfer valve spool is at or near the backup position. The switches and actuation means are shown in Figure 18. The switches are made by Texas Instruments, Inc. (Part Number MS 24456-3 or Vendor Part Number KX5-1-1). This type of switch is used on the F404 engine.

8. OVERSPEED SWITCH AND VALVE

As discussed in a previous section, a switch is used to initiate transfer to the backup mode when N_G overspeed is detected by the hydro-

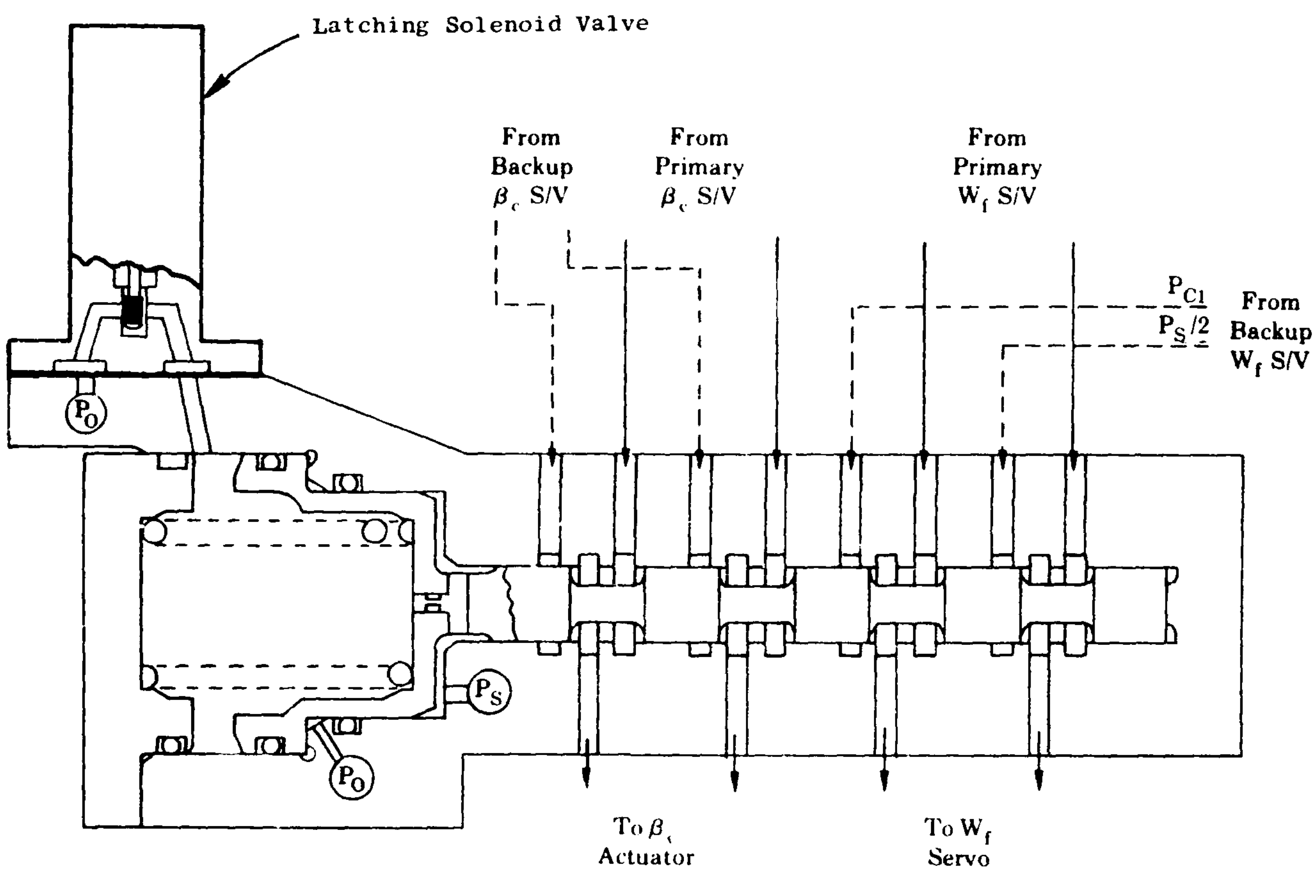

Scale $\approx$2:1

Figure 16. Transfer Valve Schematic.

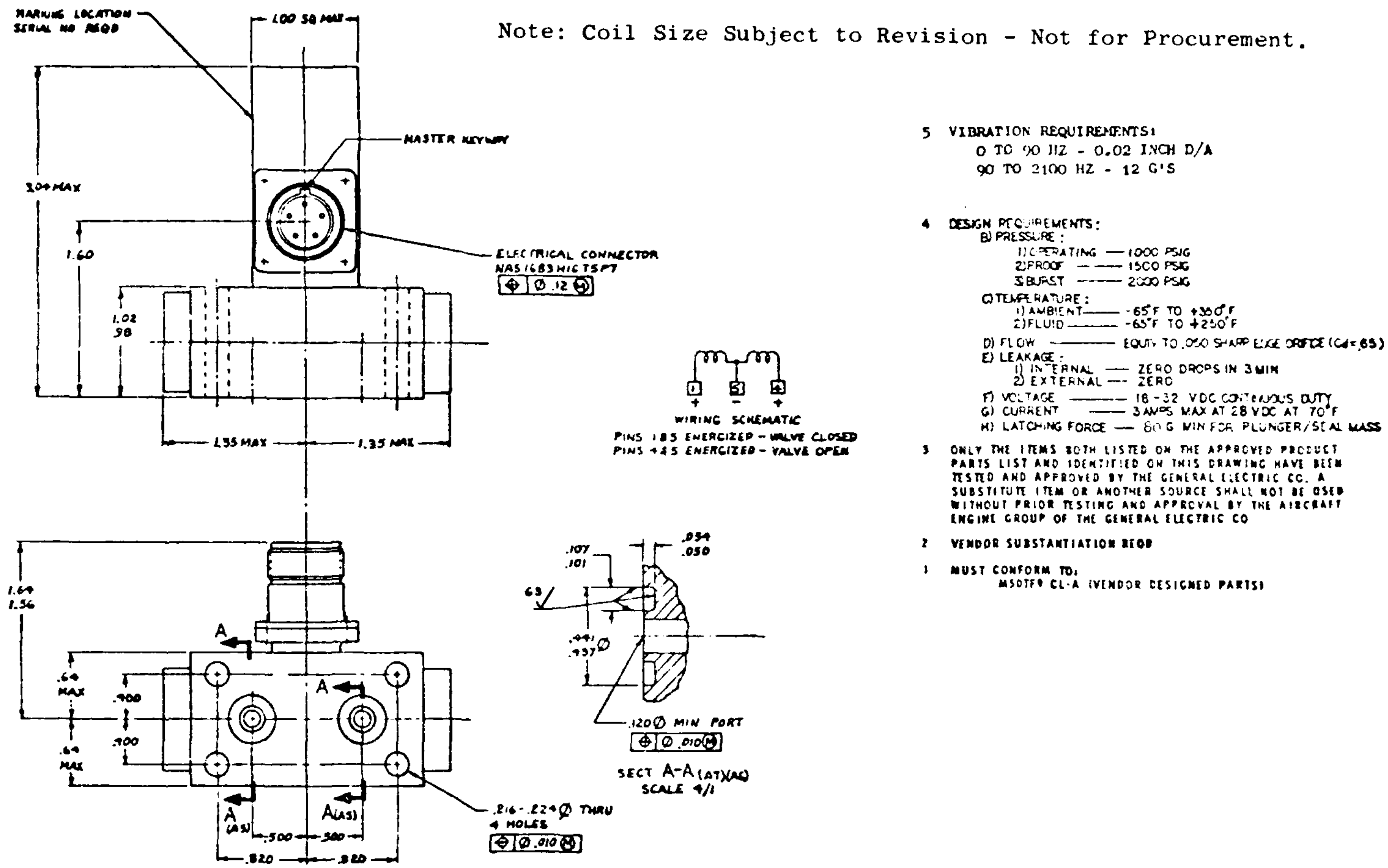

Figure 17. Latching Solenoid Valve Drawing.

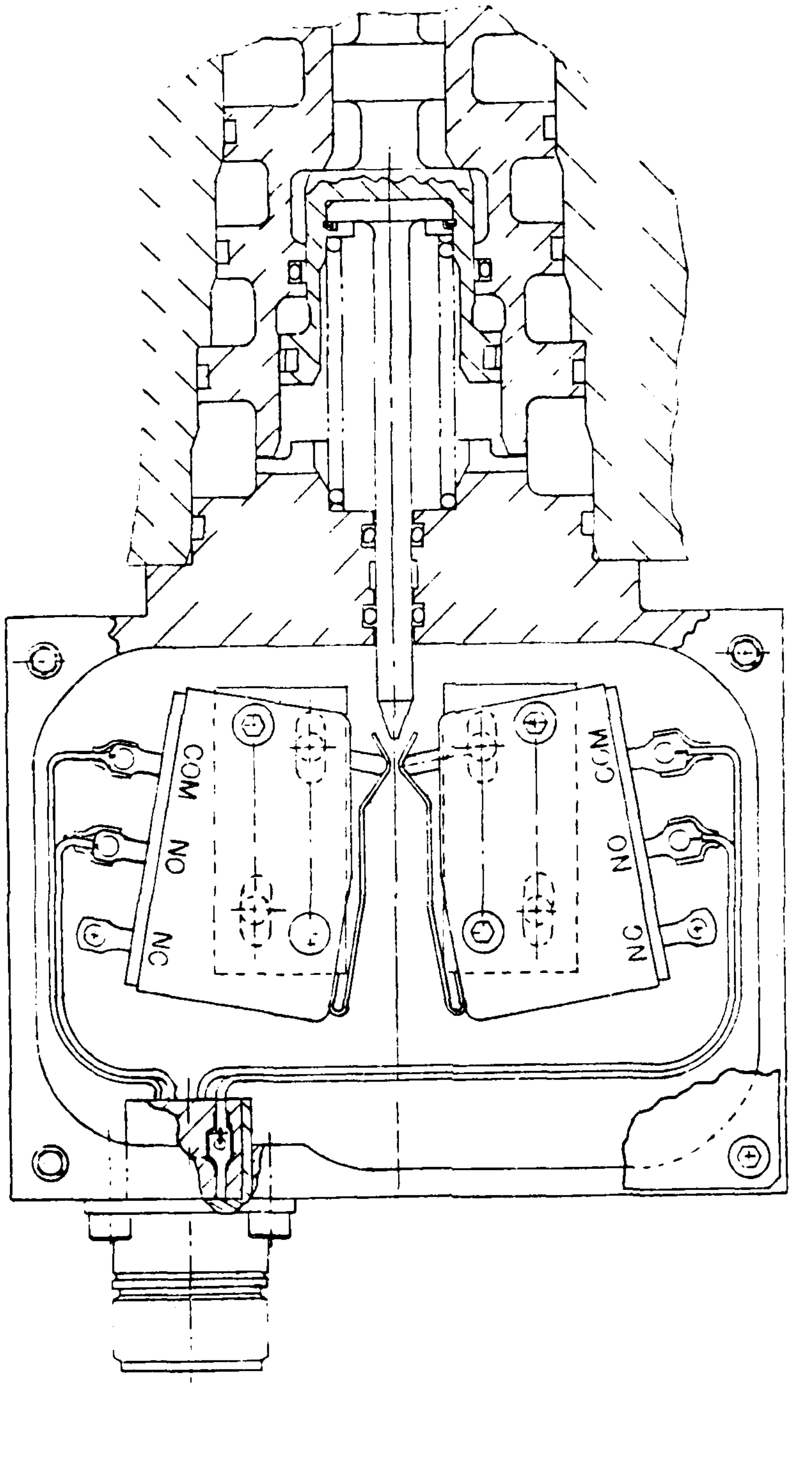

Figure 18. Section of Transfer Valve Showing Switches.

mechanical backup control speed sensor. The switch and the actuation means are shown in Figure 19. The switch (Texas Instruments Part Number MS 24456-3) is the same as those used on the transfer valve. Upon closing, the switch conducts 28-volt aircraft power to the backup solenoid. (See Figure 15.)

The speed sensor piston position is proportional to the square of core RPM (N_G^2). When overspeed is encountered, the piston moves the valve spool and spring seat to the left, camming the switch closed.

Referring to Figures 2 and 19, the spool valve modulates the throttling valve opening pressure (P_x). This action provides N_G limiting at a level higher than that required to close the overspeed switch. A possible failure mode which makes this additional protection desirable is a stuck-open metering valve.

Both the overspeed switch and the overspeed valve are adjustable. The switch can be moved on its mounts; and the sleeve for the valve can be shimmed. The nominal RPM settings and range are:

Switch	104% $\pm$ 5%
Valve	107% $+$ 3%, -7%

9. DRIVE AND MOUNTING ADAPTER

The drive and mounting adapter are shown by Figures 20 through 22. This adapter mounts the fuel valve, the backup control computer, and the transfer valve. The drive end of the adapter is designed to mount to the JTDE gearbox.

The drive shaft (Figure 20) input is 6690 rpm at 100% rated JTDE core speed (N_G). The drive gear at the computer interface has 45 teeth of 32 diametral pitch. The gear in the computer has 74 teeth so the speed sensor input is 4015 rpm. There is an idler gear between the two gears.

A carbon face seal (Sealol Part Number B-56910) rubbing on 440C stainless steel is used to seal fuel from the drive spline area. This seal is used on an aircraft boost pump at approximately the same RPM. The spline at the engine gearbox is oil lubricated and sealed by an O-ring. An overboard drain is provided between the fuel and oil seals.

To allow for possible misalignment, a separate quill shaft is used between the gearbox shaft and the backup control drive shaft. The bearings on the drive shaft are Marlin-Rockwell Corporation Part Number 104 KS or the equivalent. The outer races of the bearings are clamped by a lock nut. This clamping method is used in engine gearboxes. The second bearing inner race floats to allow for thermal expansion. The expansion was calculated to be 0.016 inch for a temperature change of 300° F. Bearing loads are modest: 67 lb thrust from a maximum case pressure of 150 psi. The thrust rating for this bearing at 5000 rpm is 500 lb. The calculated radial load is 6 lb.

The drive shaft and quill shaft are of Nitralloy™. The gear and

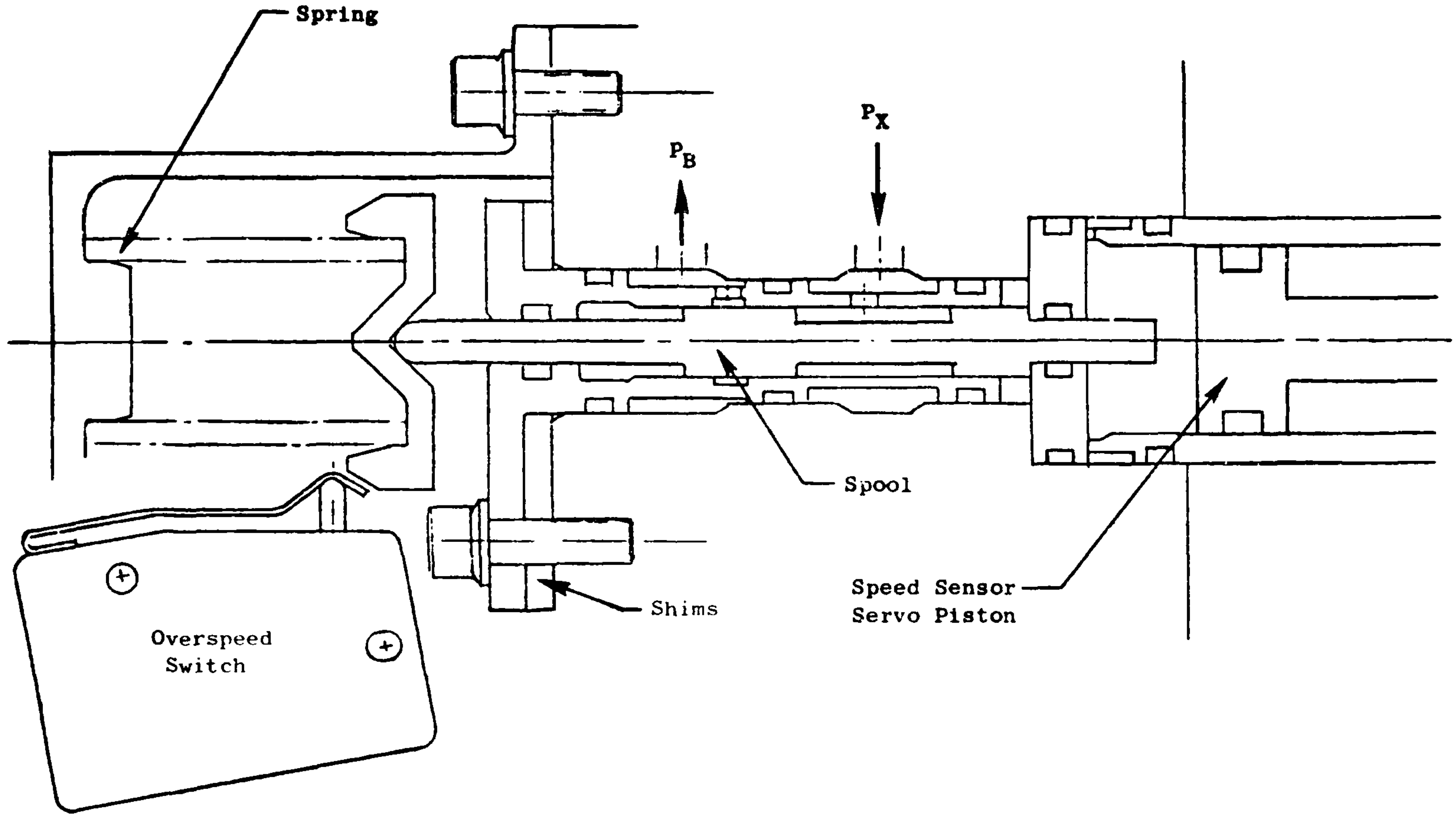

Figure 19. Overspeed Switch and Valve.

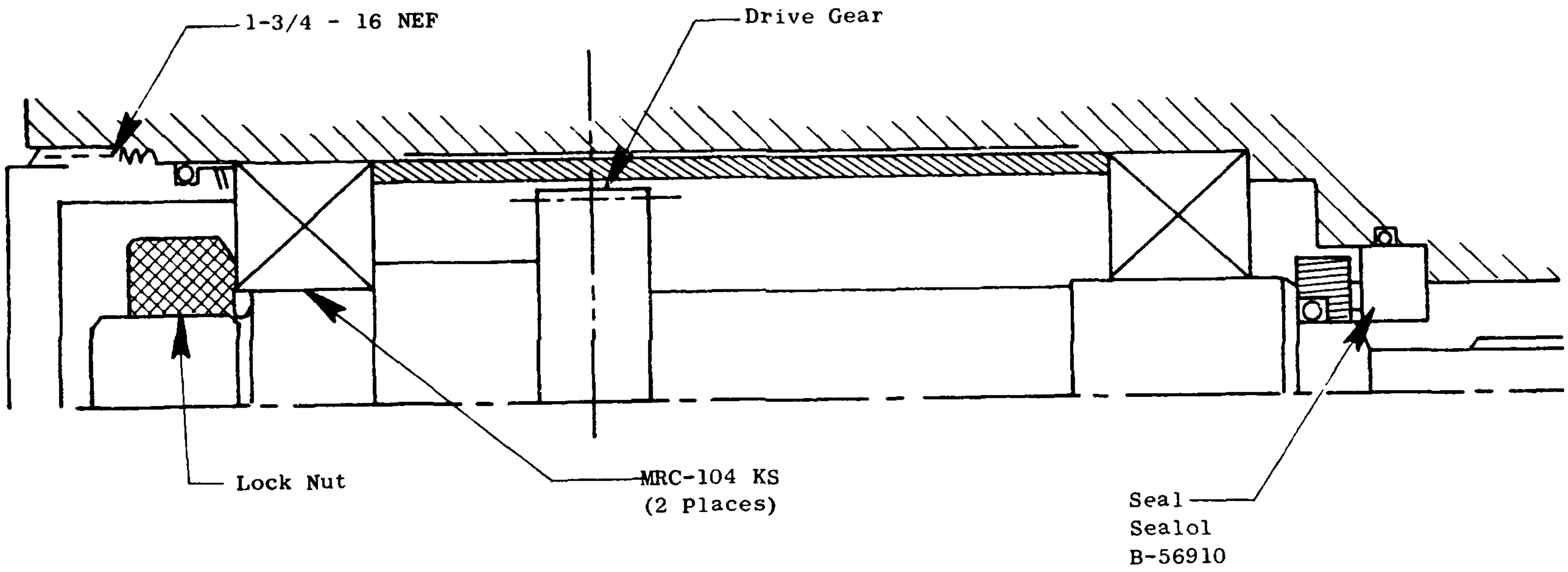

Figure 20. Partial Section - Backup Control Drive.

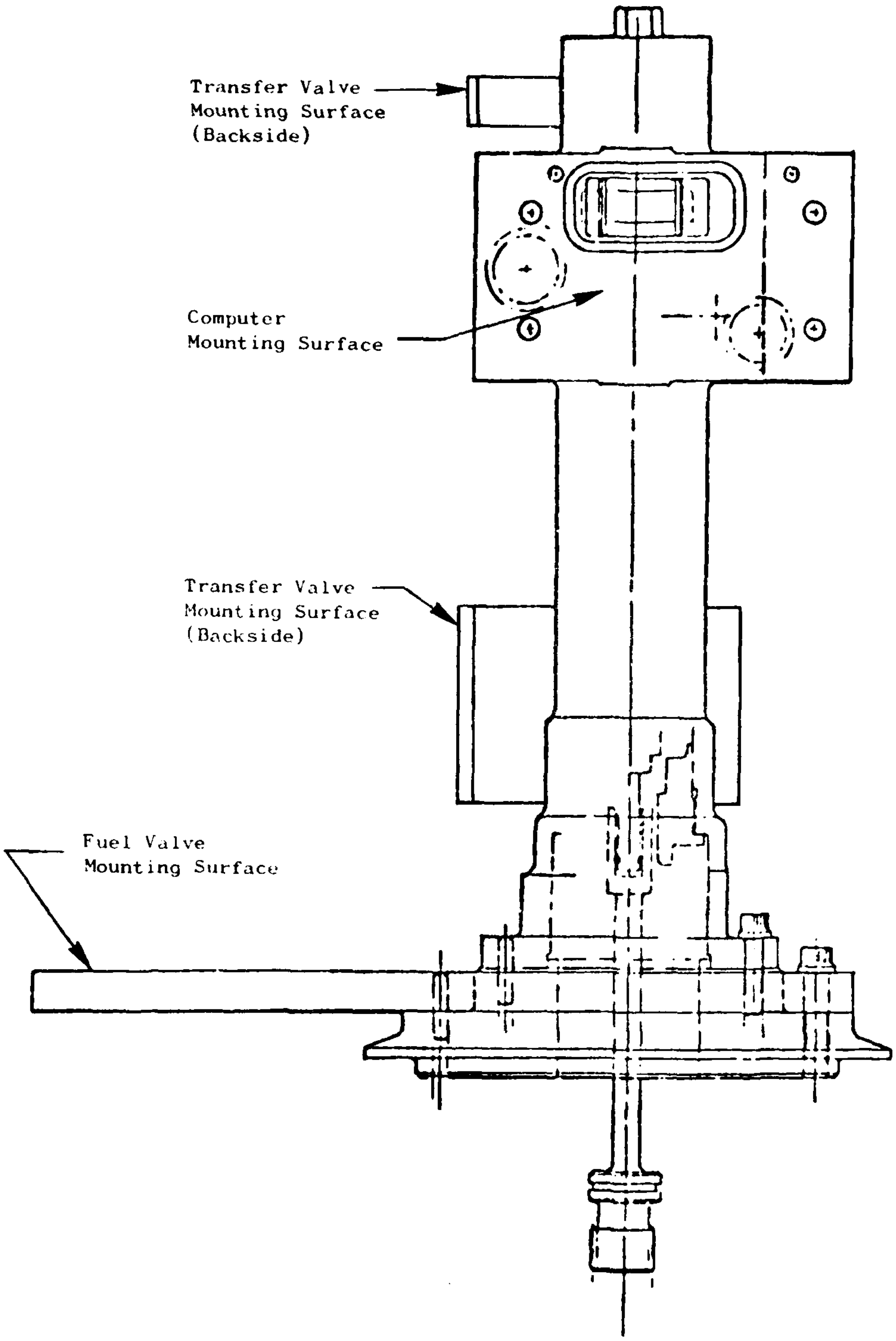

Figure 21. Sketch Showing Drive and Mounting Adapter.

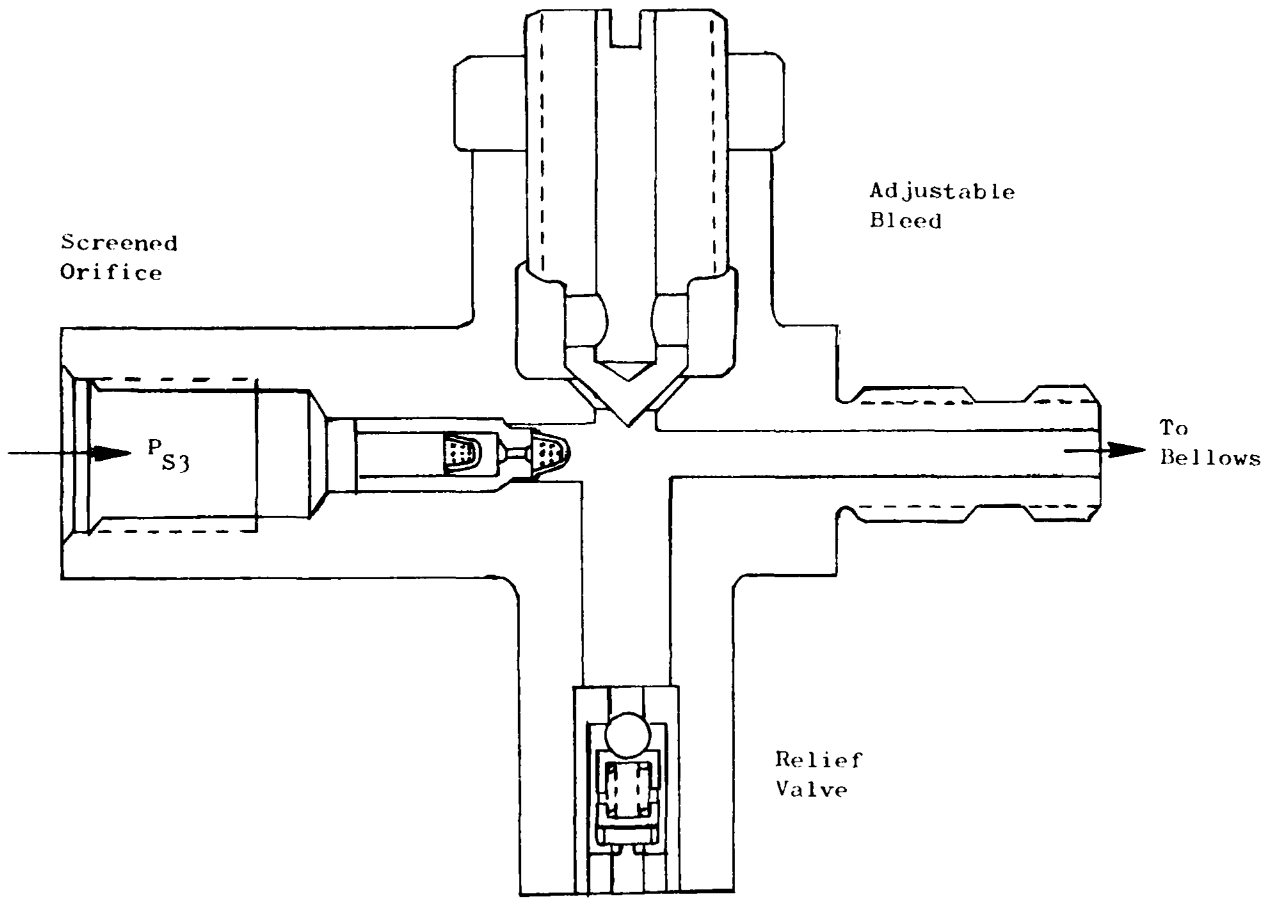

Figure 22. P_{S3} Pressure Divider.

spline are case hardened (nitrided). The housing is of aluminum alloy AMS 4117 (6061-T6).

Figure 21 shows the adapter. The mounting surfaces for the fuel valve and computer are indicated. The mounting surface for the transfer valve is on the back side of the indicated pad.

10. PRESSURE DIVIDER

The P_{S3} bellows in J85-21 MFC has a 200 psia rated pressure capability. A device consisting of two orifices in series was designed (Figure 22). Air from the compressor enters at the left and flows through a screened fixed-area orifice. Air leaves the device through an adjustable bleed which allows calibration. The fitting at the right connects the device to the P_{S3} transducer in the computer. A relief valve is provided to protect the bellows in case an overpressure is encountered during test. Both the screened orifice and the relief valve are made by The Lee Company. The pressure divider is adjustable so that the pressure level at the P_{S3} bellows is 200 psia or less.

A computer program was defined which predicted W_f/P_{S3} acceleration schedules using the P_{S3} pressure divider and the recalibrated $T_{2.5}$ sensor. Figure 23 shows the predicted schedules for various levels of $T_{2.5}$ with an existing J85-21 MFC cam (Cam 2108).

11. OFF-ENGINE UNIT

The backup control off-engine unit is shown schematically by Figure 24. This unit simulates the expected pilot's switches normally located in the cockpit. It also contains a relay which allows demonstrating a failure of the primary control. The role this unit plays in regard to backup control transfer logic is discussed in Section II-6.

Centralab makes the four-position switch (Type PA-2043). Struthers Dunn, Incorporated makes the relay (Part Number FCM-410-109).

12. TEST CONSOLE

A test console was designed to substitute for the primary control during bench testing. Figure 25 is the test console block diagram. This unit operated the primary W_f and β_c servo loops. The operator can demand a steady-state N_G or an N_G ramp just before transfer is initiated. The test console metering valve circuit schematic is shown by Figure 26; the stator circuit schematic, by Figure 27.

13. PRODUCTION HARDWARE DESIGN

The production design of the backup control would have several significant differences. Among these would be:

- The fuel valve, hydromechanical computer, drive, T2.5 sensor, and overspeed valve would all be integrated and housed in one or more machined aluminum castings.

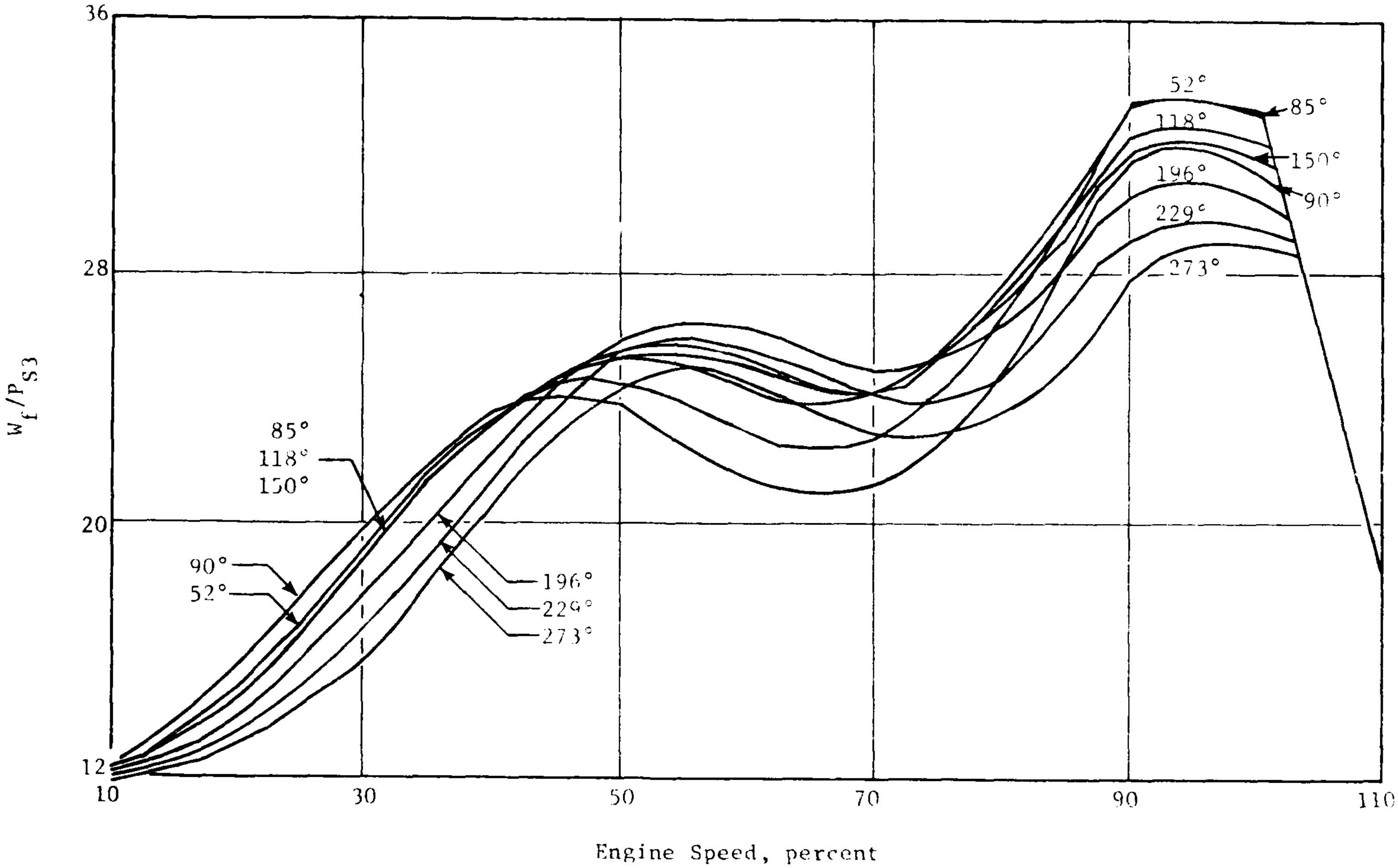

Figure 23. W_f/P_{S3} Vs. % N_g at Various Levels of $T_{2.5}$ (Cam 2108).

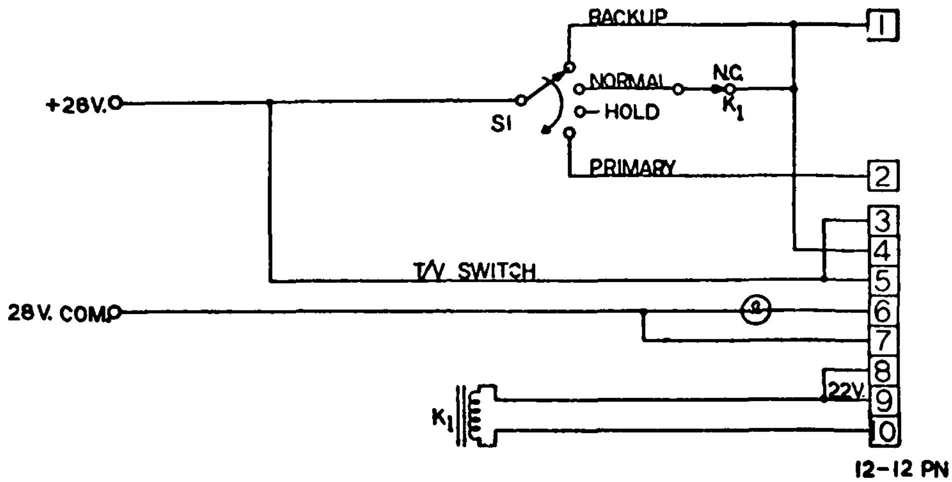

Figure 24. Schematic of the Backup Control Off-Engine Unit.

- The transfer valve assembly would be mounted directly to the housing for the above components and there would be few, if any, external lines. The body would be of cast aluminum.

- The overspeed switch would be mounted to the computer housing in a manner similar to that shown for this version of the backup control.

- The off-engine unit would be replaced by equivalent parts in the cockpit and in the primary control.

The anticipated external appearance of the backup control would be similar to that of a conventional hydromechanical main fuel control with a transfer valve assembly mounted to one side.

The cost, weight, and size of the production version of the backup control were estimated during Phase I of this program. The results were:

Cost (1977 dollars)	\$11,800
Weight	20.2 lb
Size	259 $in.^3$

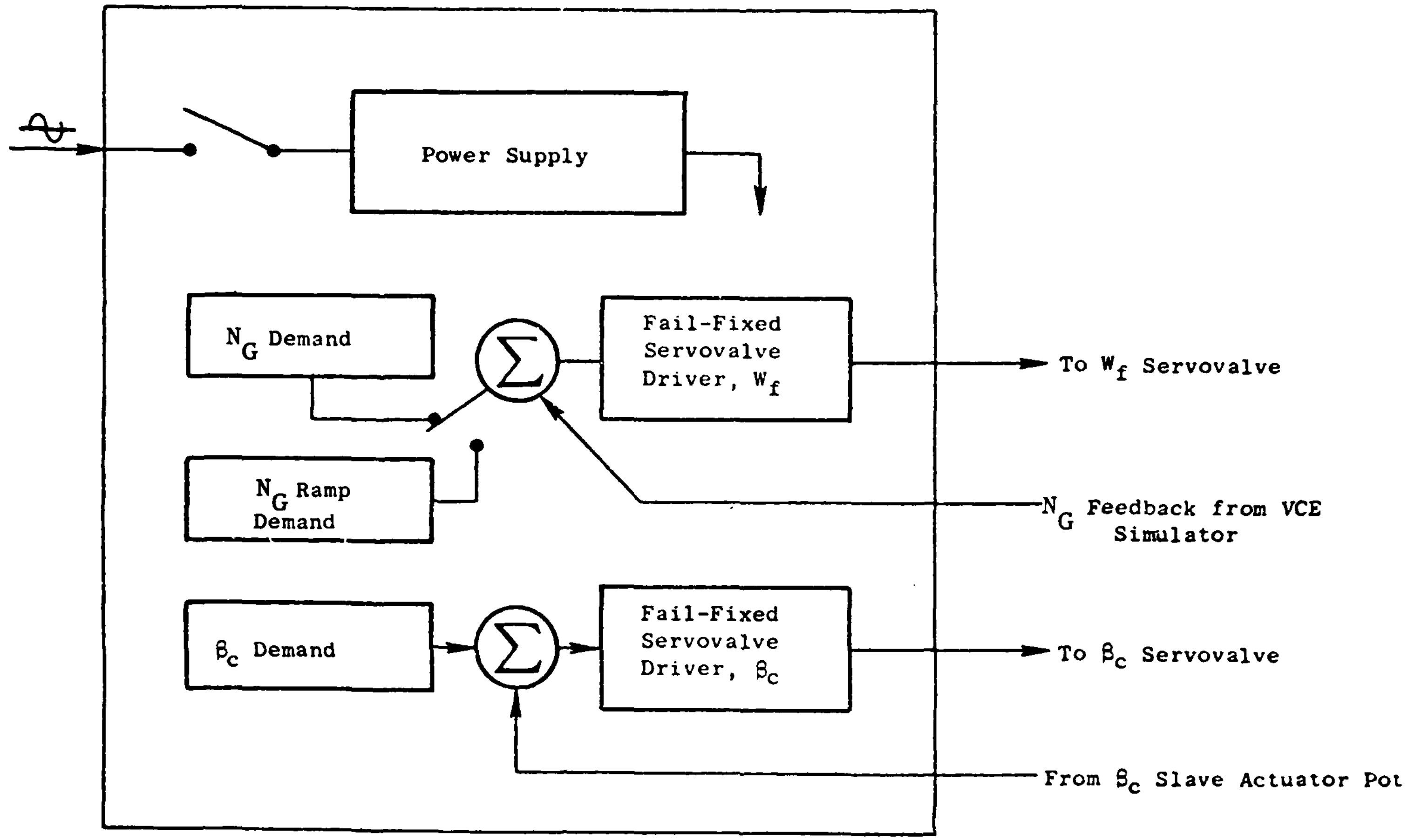

Figure 25. Test Console Block Diagram.

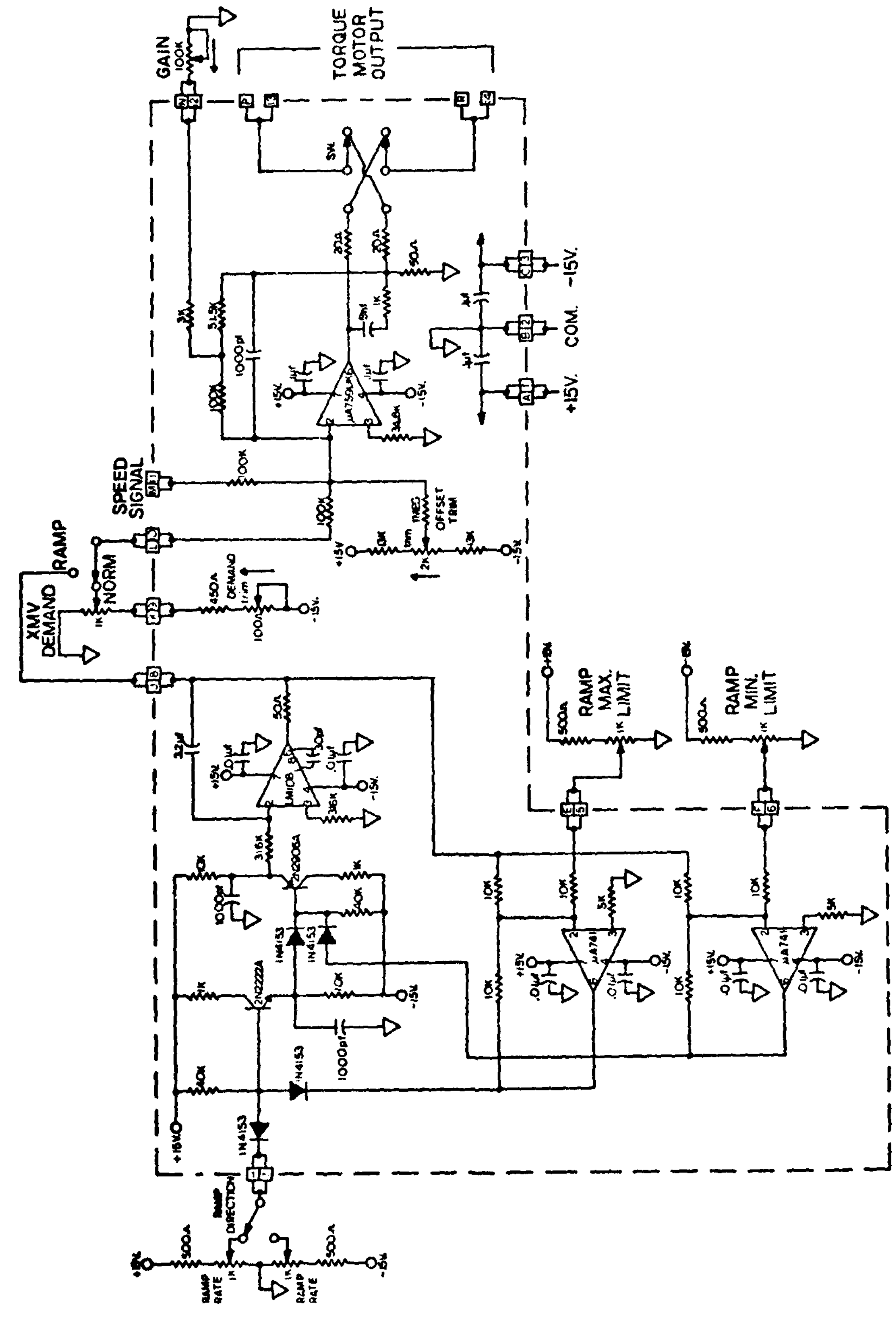

Figure 26. Test Control Metering Valve Circuit.

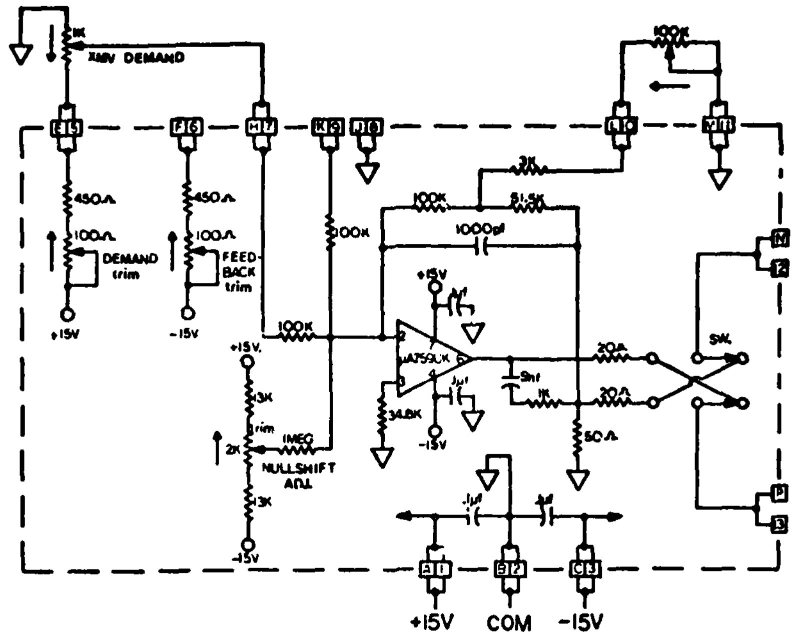

Figure 27. Test Console Stator Circuit.

SECTION III

FABRICATION OF HARDWARE

1. HYDROMECHANICAL COMPUTER AND COMPRESSOR INLET TEMPERATURE SENSOR

The hydromechanical computer and compressor inlet temperature sensor $T_{2.5}$ for the backup control are the equivalent portion of the J85-GE21 Main Fuel Control. These components are production items at General Electric's AEG, Lynn, Massachusetts, facility. The housings for both assemblies are of cast aluminum.

Figure 28 shows the computer and sensor.

2. FUEL VALVE ASSEMBLY

The fuel valve was designed at the General Electric AEG, Evendale, Ohio, facility. Most of the detail parts are the same as those used for the fuel valve designed, fabricated, and tested for the Light Weight Fuel Delivery System Program conducted by General Electric for the U.S. Navy.

The detail parts were manufactured by various independent machine shops. The body was machined from 6061-T6 aluminum. The other parts are prototype flight-type design. Figure 29 shows the fuel valve parts.

The fuel valve was assembled at the General Electric Company facility in Evendale, Ohio.

3. TRANSFER VALVE ASSEMBLY

The transfer valve assembly was specifically designed for the backup control. The detail drawings were prepared at General Electric's Evendale, Ohio facility.

The detail parts were manufactured by outside machine shops. The housing was machined from aluminum plate stock. The valve spool and sleeve are of AMS 5630 stainless steel, heat treated to a minimum hardness of Rockwell 15N-87.

The transfer valve assembly also involves some major purchased components. These include:

- The fuel metering servovalve, which is of the jet-pipe fail-safe type, was purchased from the Aerospace Division of the Abex Corporation (Vendor Part Number 72144).
- The β_c servovalve, also of the jet-pipe fail-safe type, was purchased from Aerospace Division, Abex Corporation (Vendor Part Number 72137).
- The latching solenoid valve, which is a shear type, was purchased from the Valcor Engineering Corporation (GE Part Number 4013145-337).

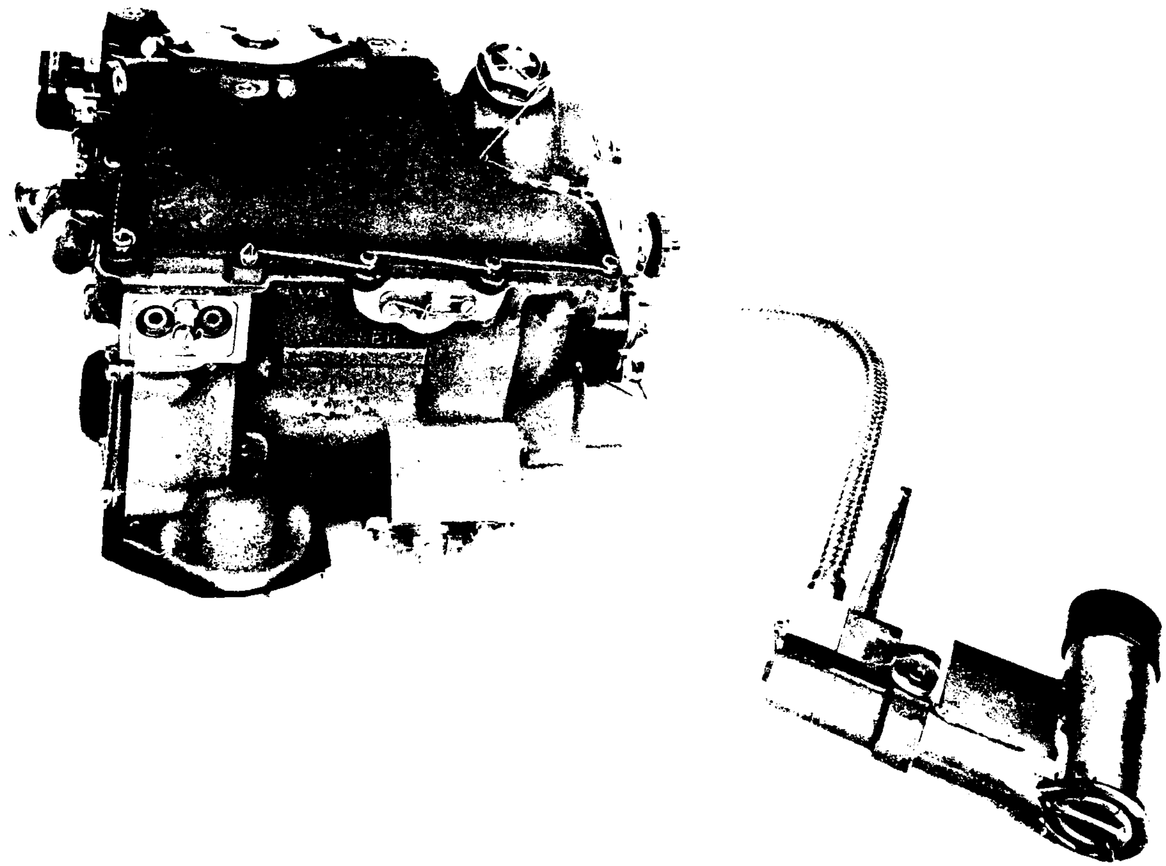

Figure 28. Control Computer and $T_{2.5}$ Sensor Assembly.

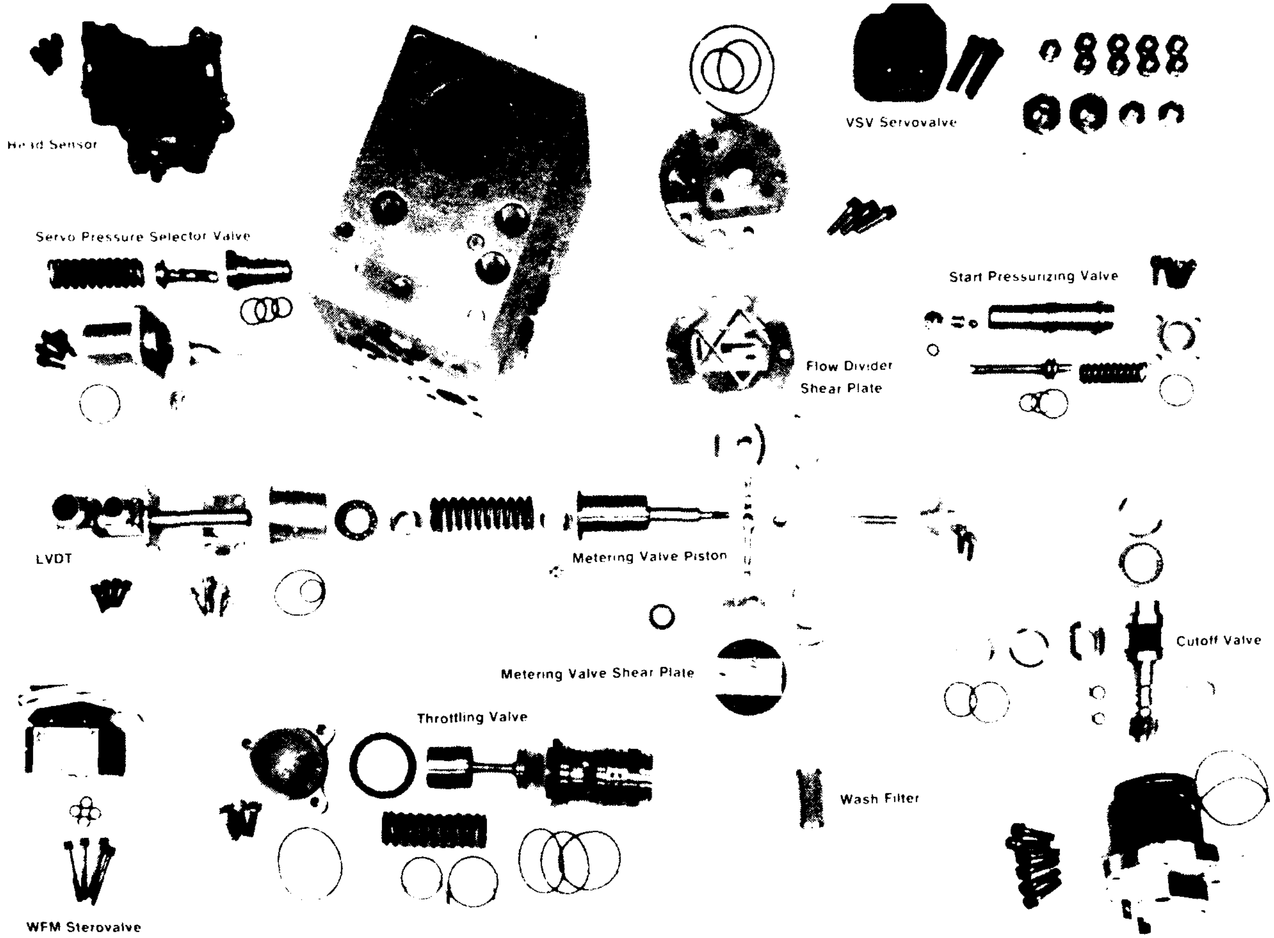

Figure 29. Detail Parts of the Fuel Valve.

The overall transfer valve assembly is shown (photographed) in Figure 30.

4. DRIVE ADAPTER, MECHANICAL POSITION FEEDBACK, AND OVERSPEED ASSEMBLIES

The drive adapter, mechanical position feedback and overspeed assemblies were designed specifically for the backup control. The detail drawings were prepared at the General Electric Company, Lynn, Massachusetts, facility.

The detail parts were manufactured by outside machine shops. All housings were machined from aluminum bar or plate. The parts were assembled internally at General Electric's Lynn, Massachusetts, facility. Where rework was necessary, this was also done at the Lynn facility.

Figure 31 shows the drive adapter, mechanical position feedback mechanism and overspeed switch detail parts. Figure 32 shows the hydromechanical portion of the backup control.

5. OFF-ENGINE UNIT AND BACKUP CONTROL TEST CONSOLE

The off-engine unit and the test conscle are electrical assemblies that were designed within the Advanced Controls and Accessories Electrical Engineering Unit of General Electric's AEG located at Evendale, Ohio. The piece parts were purchased. Assembly was done by the same people who designed the two units.

Figure 33 shows the resulting hardware.

Figure 30. Transfer Valve Assembly.

Figure 31. Mechanical Position Feedback Mechanism and Overspeed Switch Detail Parts.

Figure 32. Hydromechanical Portion of the Backup Control.

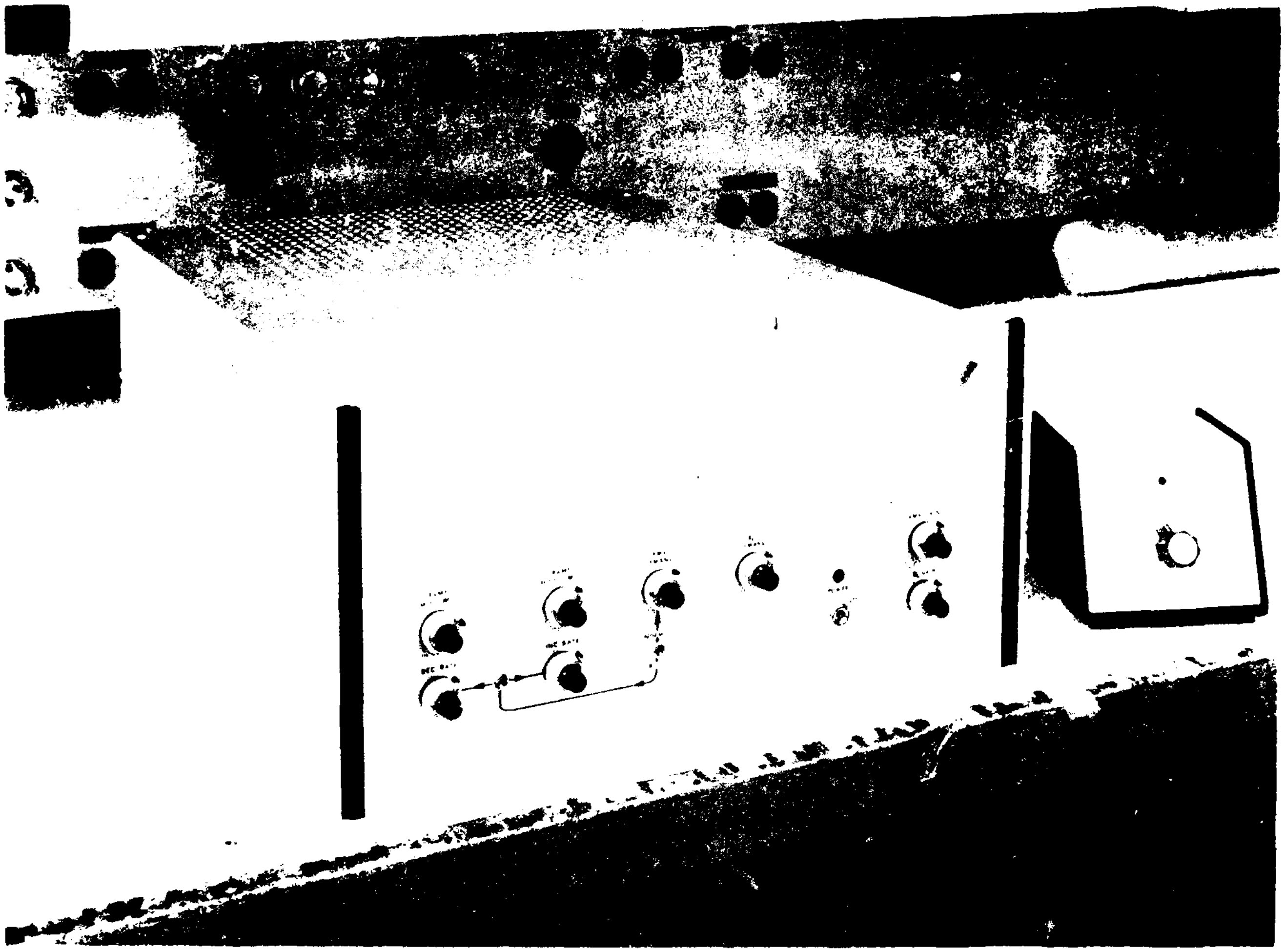

Figure 33. Backup Control Test Console and Off-Engine Unit.

SECTION IV

TEST PLANNING

1. ACCELERATION SCHEDULE

The GE23/J1A3 engine acceleration schedule was selected as the goal for calibrating the backup control. The plan was to use the J85-21 Main Fuel Control 3-D cam (2108) and make modifications so that the GE23/J1A3 acceleration schedule at the nominal $T_{2.5}$ and P_{T2} test condition ($T_{2.5}$ = 224° F and P_{T2} = 20 psia) could be approximated.

The modifications to the computer and $T_{2.5}$ sensor were:

- A pressure divider (see Paragraph II-10) was added between the P_{S3} source and the control, reducing the pressure at the bellows to 63% of the actual P_{S3}.
- The $T_{2.5}$ sensor (see Paragraph II-3) was recalibrated so that its range was 20° F to 360° F instead of the J85 range of -65° F to 275° F.
- A bias force equivalent to -5.0 psia P_{S3} was applied by means of an available adjustment.

The predicted analytical results are shown in Figure 34. The GE23/J1A3 acceleration schedule was for the digital electronic engine control. The two schedules are quite similar. The approximation was considered very satisfactory for the planned bench tests of the backup control. These data were used to determine the acceleration schedule limits for the calibration log sheets.

2. ENGINE MODEL

The GE23/J1A3 engine model was selected for the closed-loop testing of the backup control. The model is shown by Figures 35 through 37. This core engine is very similar to the core engine for the JTDE. The rated engine rotational speed at the control drive pad is 6739 rpm versus 6690 rpm for the JTDE - a close match.

3. EXPECTED TRANSIENT RESPONSE

Fuel flow response in both transfer and backup operation is dictated by the characteristics of the metering valve servo system, which includes the nutcracker and metering valve piston. Referencing Figure 38, the basic equations describing this portion of the control are derived as follows:

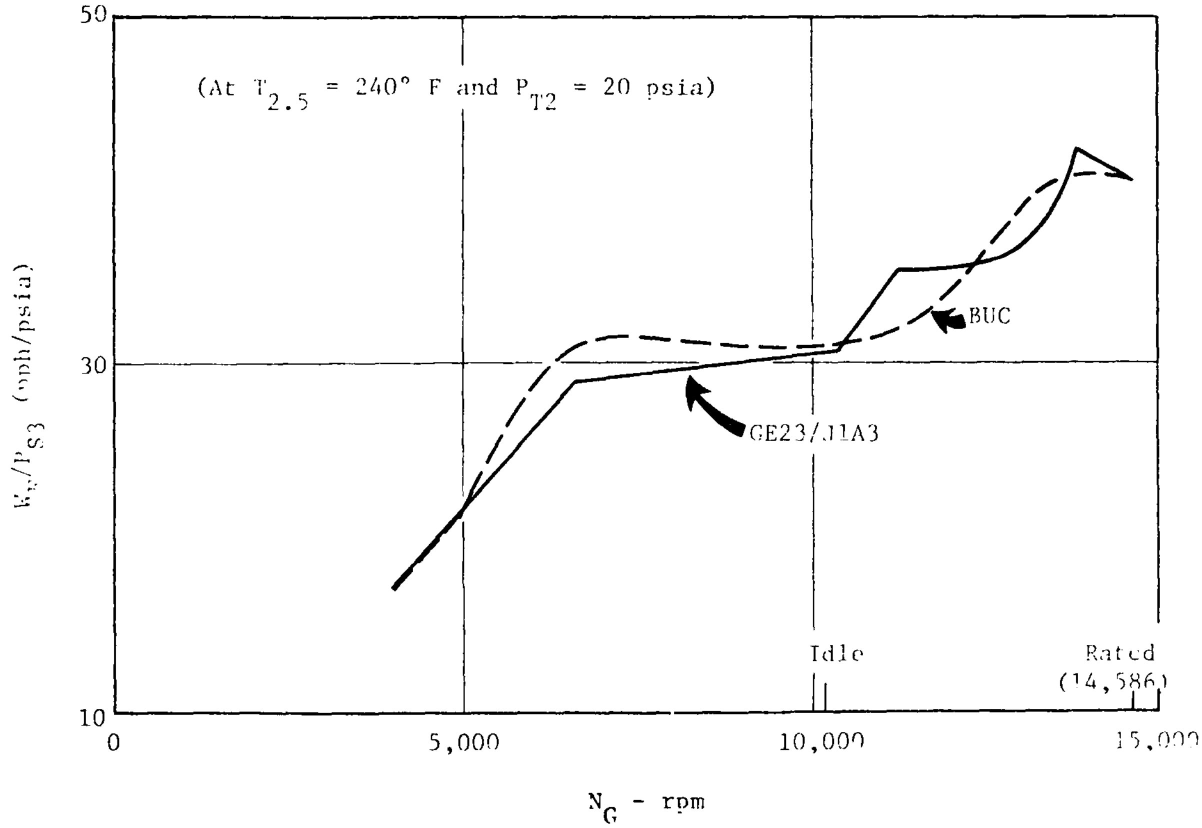

Figure 34. Comparison of Accel Schedules.

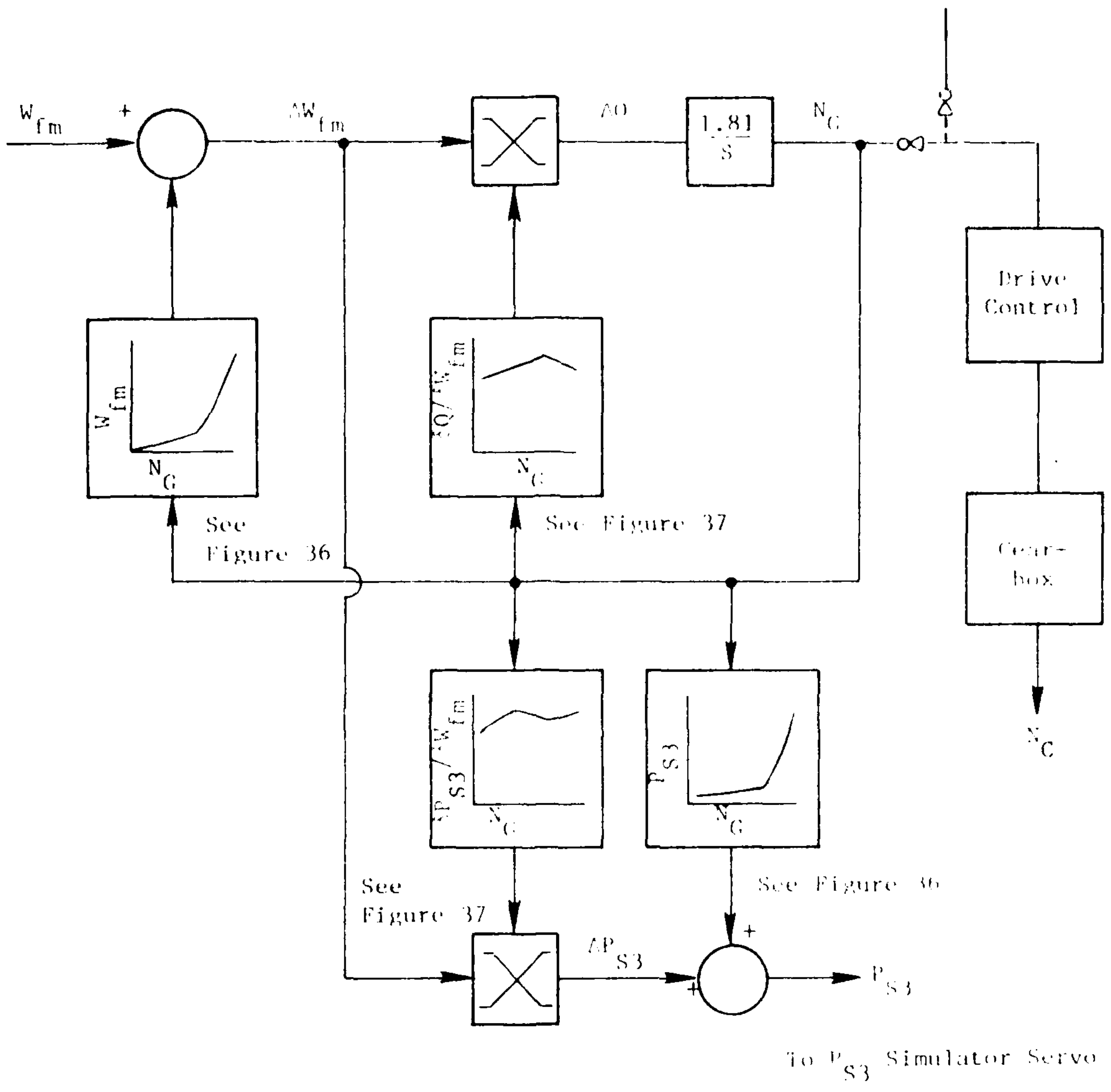

100% N_G = 14,586 rpm

100% N_C = 6,739 rpm

Figure 35. GE23/J1A3 Engine Model.

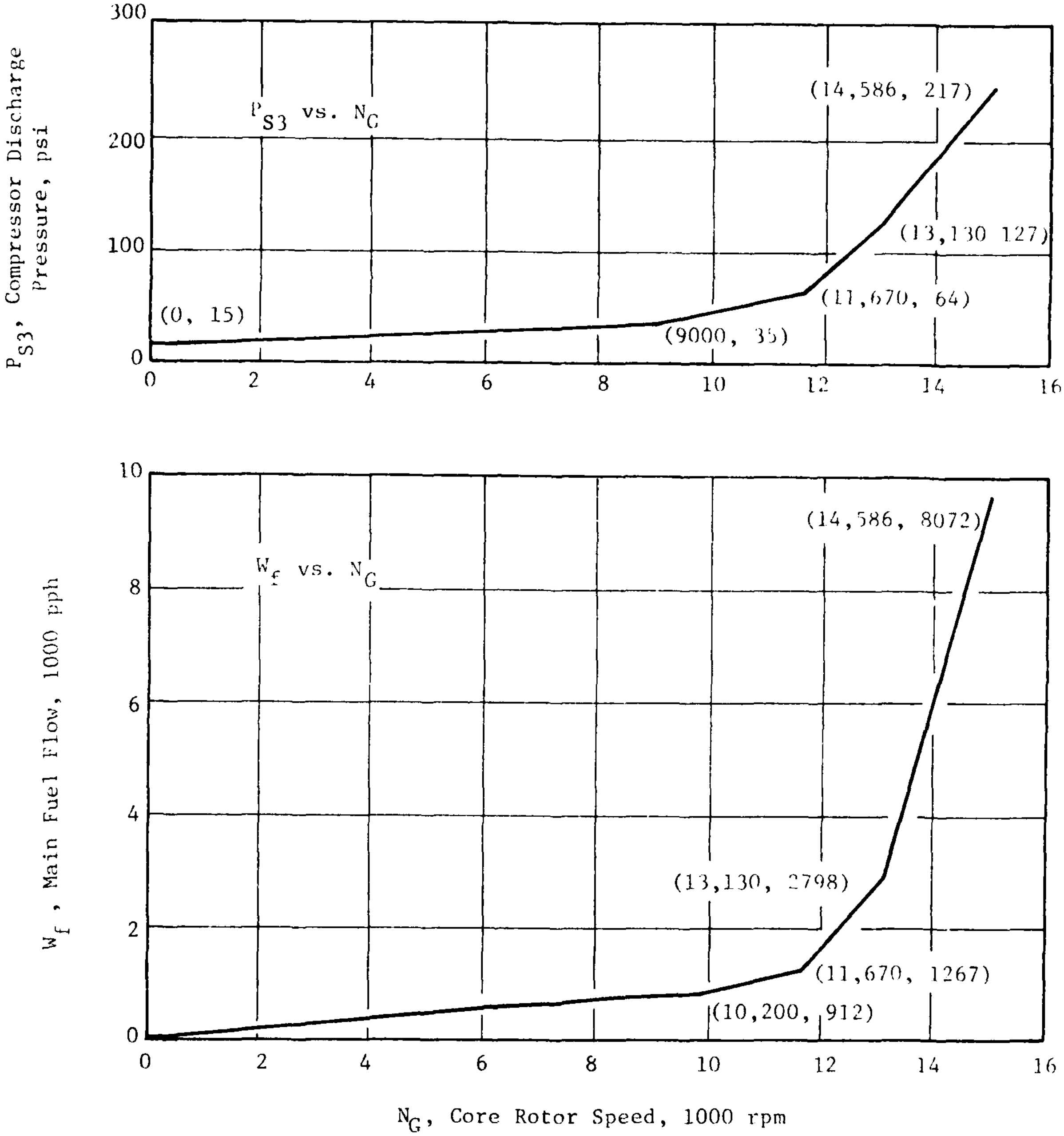

Figure 36. GE23/J1A3 Loop Closure Functions.

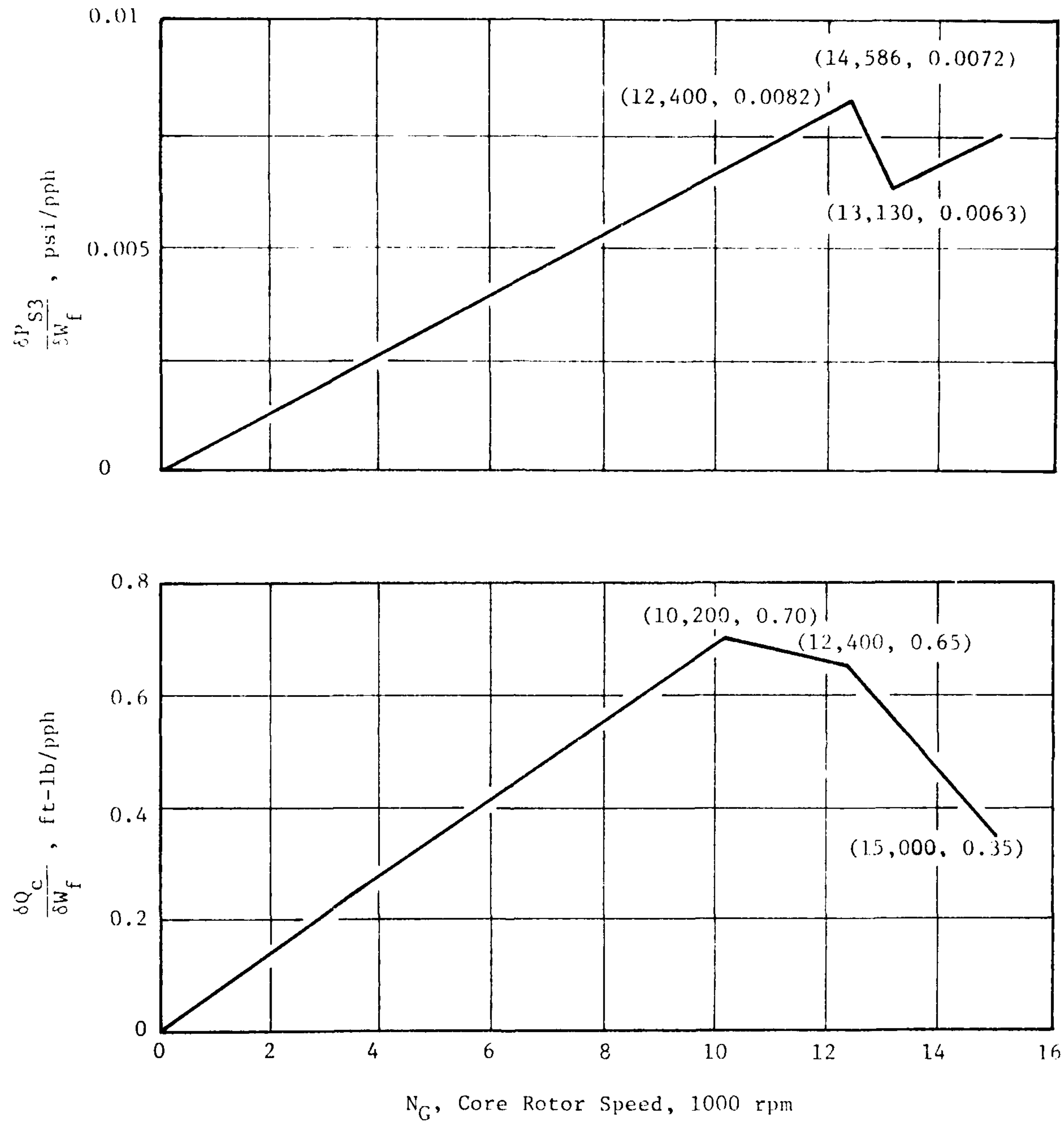

Figure 37. GE23/J1A3 Loop Closure Partials.

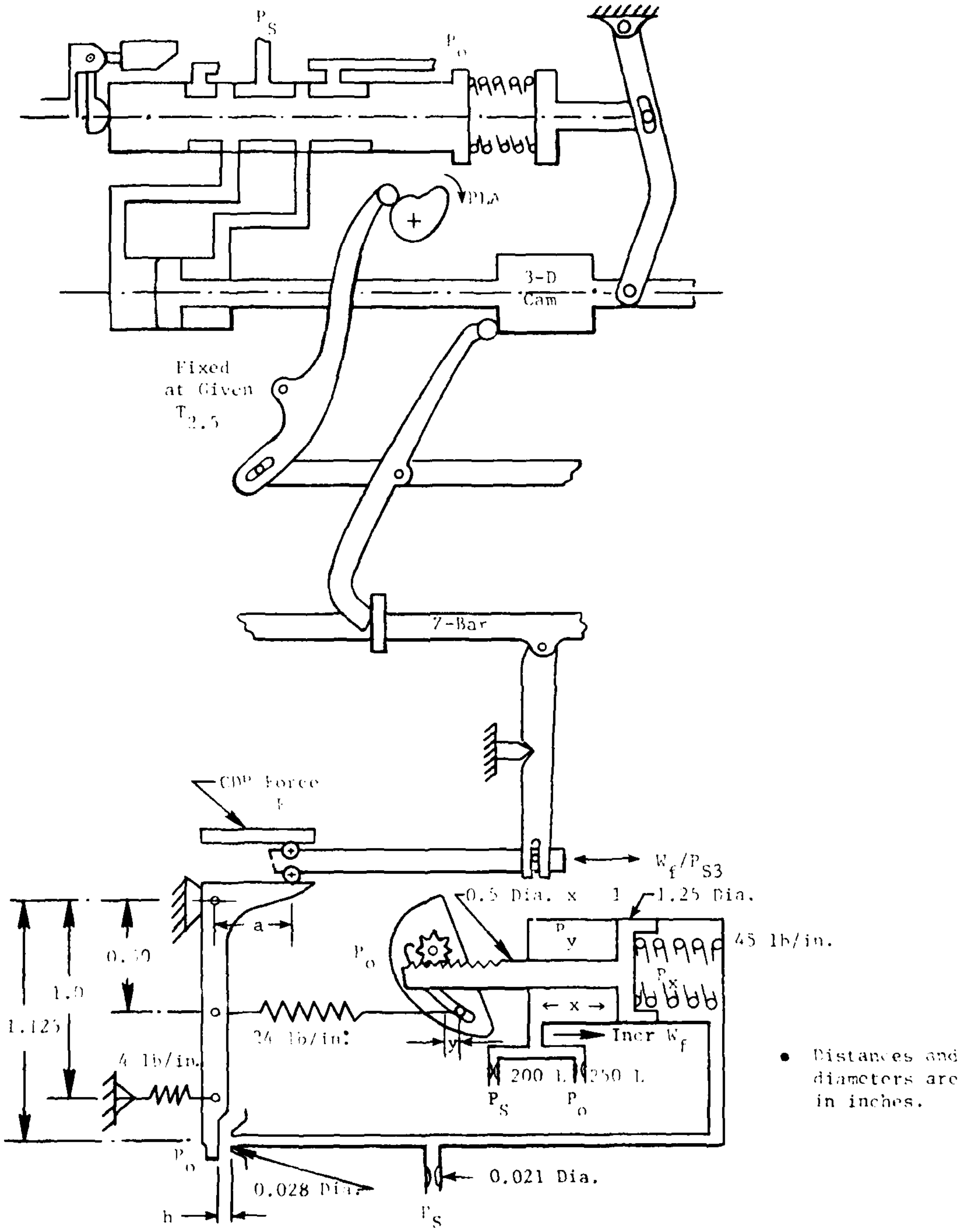

Figure 38. Backup Control Governor, Nutcracker, and Metering Valve Servo Mechanization.

The input, "a," is linear with W_f/P_{S3} demand. Therefore,

$$a = K_o \, (W_f/P_{S3}) \tag{1}$$

where "a" is positive in the direction that opens the flapper.

From a moment balance on the error bar, we get:

$$F(a) + R_4 \left[L_4 - \frac{1}{1.125}(h-h_o)\right] = R_{24}\left[L_{24} + \frac{0.5}{1.125}(h-h_o) + (y-y_o)\right](0.5) \tag{2}$$

From a force balance on the power piston, we get:

$$R_{45}\,(L_{45} + x) + (0.785)\,D_1^{\,2}\,(P_x - P_o) = (0.785)\,(D_2^{\,2} - D_1^{\,2})\,(P_y - P_x) \tag{3}$$

A pressure balance from rod-to-case gives:

$$(P_y - P_o) = (P_y - P_x) + (P_x - P_o) \tag{4}$$

From a flow balance on the head end of the power piston, we get:

$$\frac{146(0.785)D_o^{\,2}}{\sqrt{\rho}}\; C_o\sqrt{(P_s - P_x)} + (0.785)D_2^{\,2}\,\dot{x} = 146\,\frac{(C_N \pi D_N h)}{\sqrt{\rho}}\sqrt{(P_x - P_o)} \tag{5}$$

From a flow balance on the rod end of the piston, we get:

$$\frac{77}{200}\sqrt{(P_s - P_y)} = (0.785)(D_2^{\,2} - D_1^{\,2})\dot{x} + \frac{77}{250}\sqrt{(P_x - P_o)}$$

(in LOHM form) (6)

A LOHM is a unit of resistance to fluid flow where 1000 LOHMS will flow 50 pph of water at 25 psid.

More pressure balances give:

$$(P_s - P_o) = (P_s - P_y) + (P_y - P_o) \qquad (P_s - P_o = \text{Constant}) \tag{7}$$

$$(P_s - P_o) = (P_s - P_x) + (P_x - P_o) \tag{8}$$

The feedback spring cam motion gives:

$$y = 1.152\ x^2 \qquad (9)$$

In the above nine equations, there are ten variables, all of which, except for the input (W_f/P_{S3}), appear at least twice. It is therefore possible to find x as a function of W_f/P_{S3}.

Linearizing, transforming, and combining the above equations gives:

$$\Delta a = K_o\ \Delta(W_f/P_{S3}) \qquad (10)$$

$$F\ \Delta a - R_4\ \left(\frac{1}{1.125}\right)\ \Delta h = R_{24}\ \left(\frac{0.5}{1.125}\right)\ \Delta h(0.5)+R_{24}(0.5)\ \Delta y \qquad (11)$$

$$R_{45}\ \Delta x +(0.785)D_1^{\ 2}\ \Delta(P_x-P_o) = (0.785)(D_2^{\ 2}-D_1^{\ 2})\left[\Delta(P_y-P_o)-\Delta\ (P_x-P_o)\right] \qquad (12)$$

$$\frac{-146C_o(0.785)D_o^{\ 2}}{2\sqrt{\rho}\sqrt{(P_s-P_x)_o}}\ \Delta(P_x-P_o) + (0.785)D_2^{\ 2}\ S\ \Delta x =$$

$$\frac{146C_N\pi D_N h_o\Delta(P_x-P_o)}{2\sqrt{\rho}\sqrt{(P_x-P_o)_o}} + \frac{146C_N\pi D_N}{\sqrt{\rho}}\ \sqrt{(P_x-P_o)}\ \Delta h \qquad (13)$$

$$\frac{-77}{2(200)\sqrt{(P_s-P_y)_o}}\ \Delta(P_y-P_o) = 0.785(D_2^{\ 2}-D_1^{\ 2})S\Delta x +$$

$$\frac{77}{2(250)\sqrt{(P_y-P_o)_o}}\ \Delta(P_y-P_o) \qquad (14)$$

$$\Delta y = 2(1.152)\ x_o\Delta x \qquad (15)$$

Figure 39 shows the above equations in block diagram form.

Figure 40 is a repeat of Figure 39 using the following constants and steady-state conditions for 13,500 pph flow and P_s-P_o = 1050 psi:

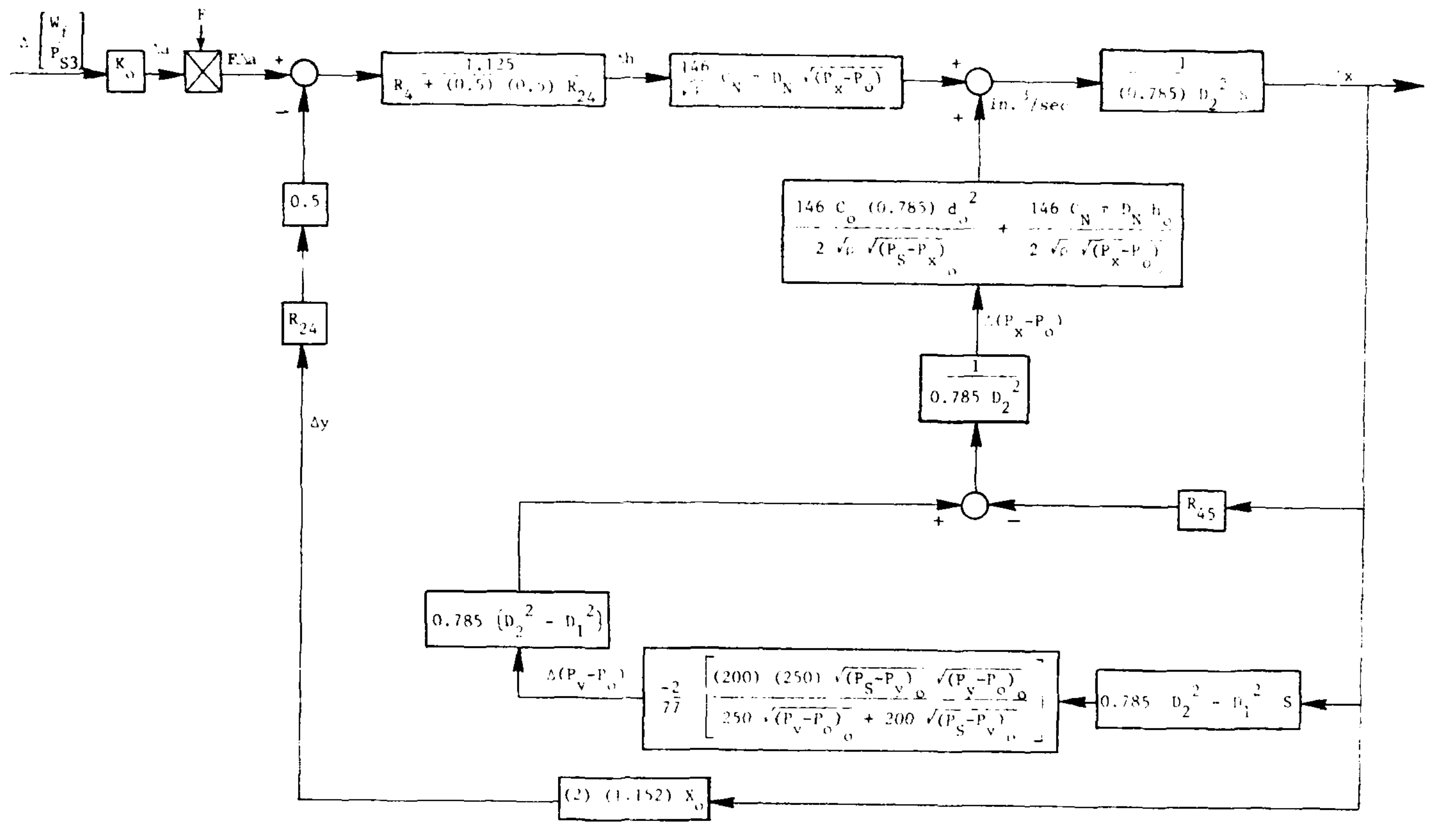

Figure 39. Linearized Block Diagram - Backup Control.

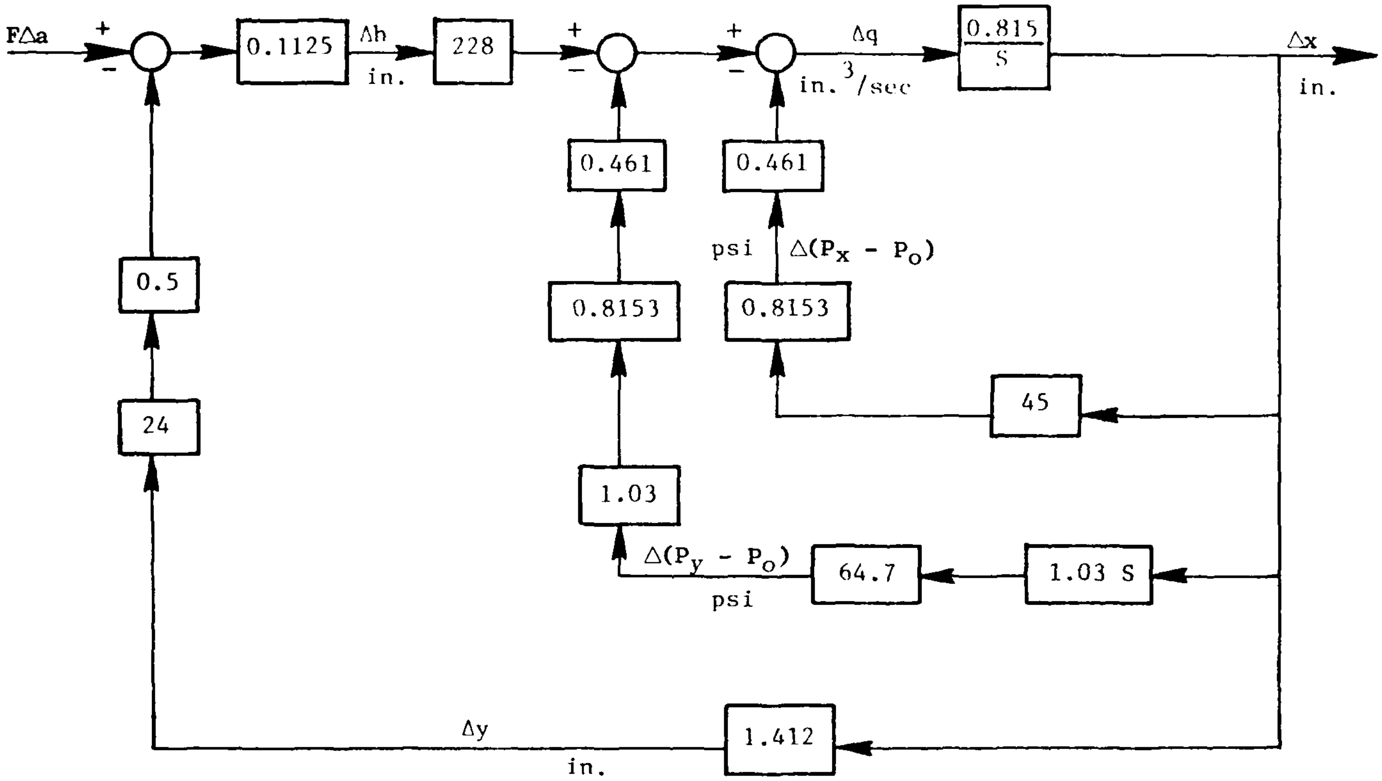

Figure 40. Linearized Block Diagram - Backup Control, Takeoff Conditions (P_S-P_o = 1050 psi).

$R_4 = 4$ lb/in.	$D_2 = 1.25$ in.
$R_{24} = 24$ lb/in.	$P_x - P_o = 496$ psi
$C_x = 0.7$	$P_s - P_x = 554$ psi
$C_o = 0.75$	$P_y - P_o = 620$ psi
$D_N = 0.028$ in.	$P_s - P_y = 430$ psi
$D_o = 0.021$ in.	$h_o = 0.0045$ in.
$R_{45} = 45$ lb/in.	$x_o = 0.613$ in.
$D_1 = 0.5$ in.	

The metering valve is contoured to give:

$$W_f = 41{,}500\ x^2$$

Thus, $$\Delta W_f = 83{,}000\ x_o\ \Delta x$$

Assuming that the throttling valve effect introduces a 0.03 second lag, and applying block diagram algebra to Figure 40, the overall system of interest can be shown to be:

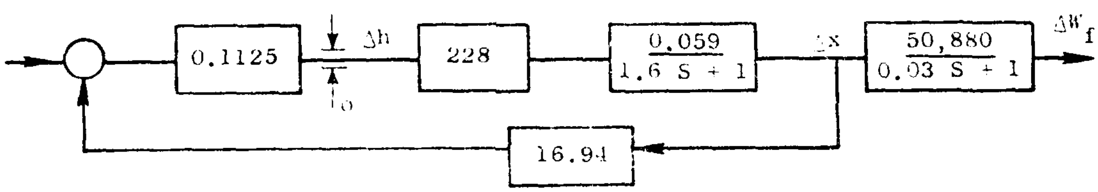

The speed servo loop was neglected since its time constant is less than 0.001 second. Second-order effects from component and fluid inertia were also neglected. An estimate of the governor frequency response was obtained by treating the control as a second-order system composed of two time constants, 0.062 second and 0.03 second. Using the expected 0.053 W_f/P_{S3} ratios per rpm, the calculated governor frequency response, with P_{S3} constant, is shown in Figure 41.

4. <u>EXPECTED TRANSFER CHARACTERISTICS</u>

An estimate of the fuel flow response following a transfer, assuming a large difference in primary and backup demands existed, was made previously and reported in AFAPL-TR-77-92 (Reference 1). The resulting W_f transient (Figure 42) showed no tendency to overshoot, even with a relatively large W_f difference (2540 pph, or about 17 percent) between

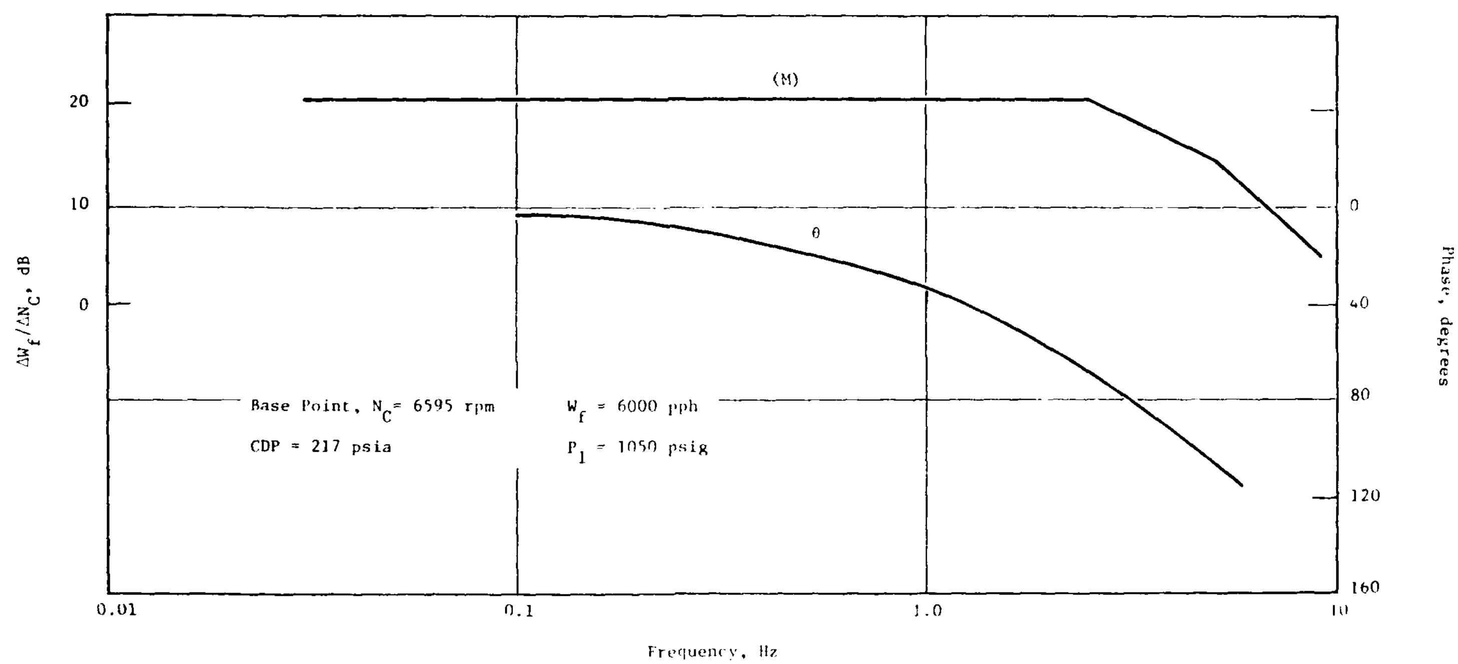

Figure 41. Backup Control Calculated Governor Frequency Response.

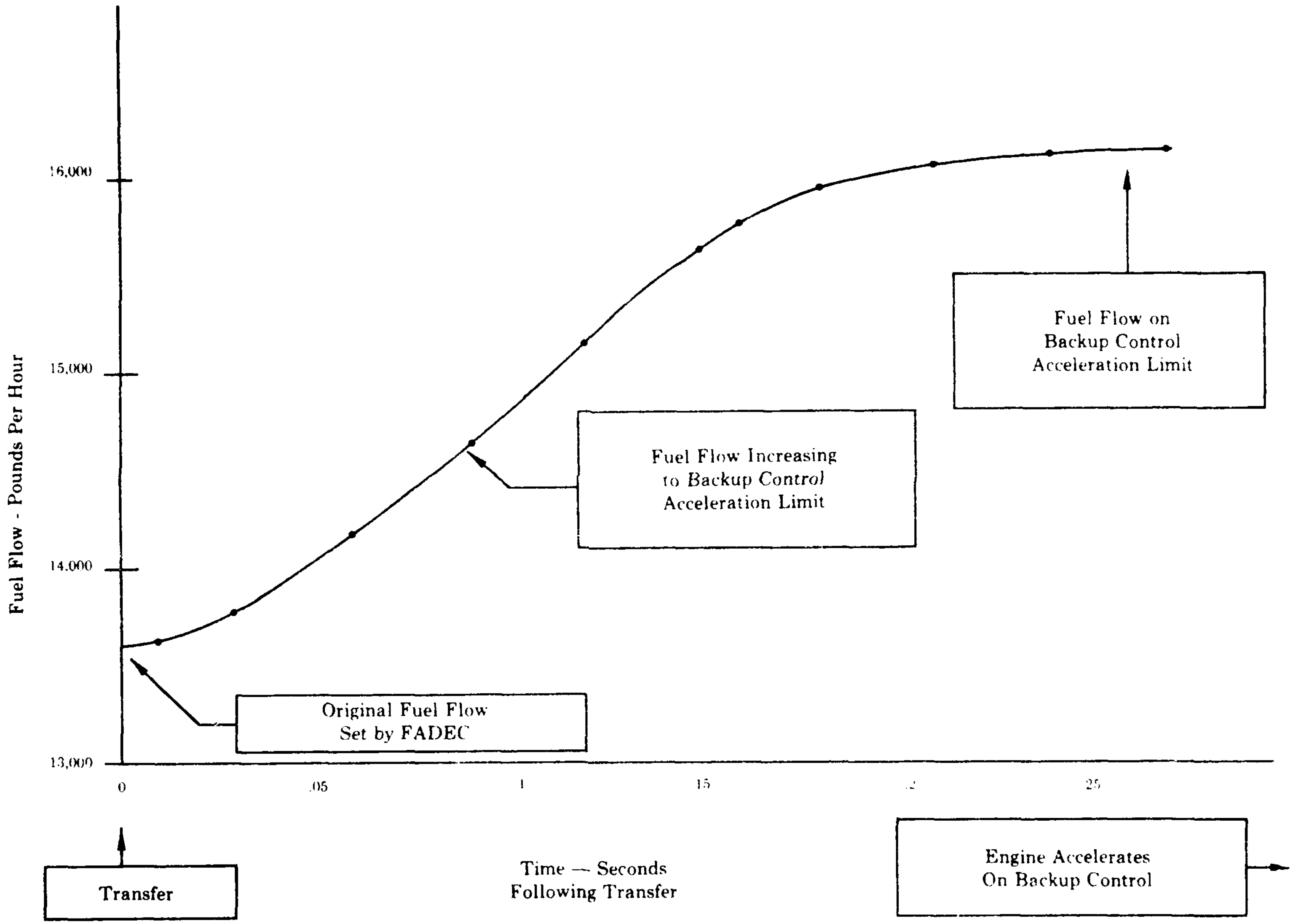

Figure 42. Fuel Flow Transient Upon Transfer.

the two controls.

The previous study made the simplifying assumption that the pressure on the rod side (see Figure 38) of the metering valve power piston was a constant 69 percent of the supply pressure. This resulted in an effective time constant for the metering valve of 0.0043 second. Referencing the schematic of Figure 38, and applying equations 3 through 8 of the basic system description of Section IV-3, it was shown that the slew velocity of the metering valve is limited by the sizes of the orifices on the rod side of the power piston. For a 0.036 inch diameter orifice on the return side, a 0.033 inch diameter orifice on the supply side, and a $P_S - P_o$ = 1050 psi, the slew velocity in the open-flapper direction is 0.34 inch per second. When the effect of the two orifices is considered in the transient analysis, as was done in Section IV-3, the effective time constant of the metering valve is found to be 0.062 second. The resulting change in the expected response following a transfer was small - about 0.15 second longer than the response previously calculated.

SECTION V

TEST RESULTS

1. PRELIMINARY CALIBRATION

A preliminary calibration of the backup control was conducted at the General Electric Company facilities at Lynn, Massachusetts. Because the J85-21 main fuel control is manufactured there, a test stand was available for calibrating the β_c schedule and for setting the PLA max and min stops, the overspeed switch, and the hydromechanical overspeed limit. The resulting calibration data are included in Appendix B.

The β_c schedule was initially calibrated using $T_{2.5}$ sensor simulator pressure. The results were very satisfactory, only one point being slightly out of limits.

The $T_{2.5}$ sensor is a modified J85-21-engine type. It was calibrated over the temperature range of 20° F to 200° F. Calibration results are shown by Table I where the "E" dimension is the distance from a reference to the sensor output servo piston position (see Figure 7). The $T_{2.5}$ sensor was installed and the β_c schedule was partially rechecked. A slight shift (about 0.004 inch) in the schedule is apparent when these data are compared to those taken with the $T_{2.5}$ sensor simulator. This was attributed to the accuracy of the sensor calibration (Table I).

A preliminary check on the acceleration and deceleration schedules was also conducted. The only fuel source readily available was one of small capacity. Therefore, instead of having the flow be measured through the fuel valve, the acceleration schedule plus other flow data were obtained by measuring the metering valve position at which "null" servo pressure occurred. The measurements were converted to fuel flow by using the equation:

$$W_f = 46,000\ x^2$$

where x is the metering valve position in inches. The constant 46,000 is based on the triangular port shape and a metering head of 53 psid. The minimum flow stop was set to a measured port opening of x = 0.0767 inch, which converts to a 270 pph flow. This value of x was used as the reference for the other metering valve position readings. The resulting acceleration schedule data indicated only minor deviations. The deceleration schedule was within limits.

The electrical overspeed switch and the hydromechanical overspeed limit were set within limits. The PLA max and min stops were also set within limits. The backup control was then shipped to the General Electric Company facility at Evendale, Ohio.

TABLE 1.

TEMPERATURE SENSOR CALIBRATION

Temperature $T_{2.5}$ °F	Desired Reference Dimension, "E" - In.	Measured Reference Dimension, "E" - In.
20	1.6004	1.6072
40	1.5849	1.5903
60	1.5696	1.5752
80	1.5546	1.5564
100	1.5398	1.5410
120	1.5253	1.5262
140	1.5110	1.5110
160	1.4970	1.4955
180	1.4832	1.482
200	1.4696	1.4685
220	1.4563	
240	1.4431	
260	1.4302	
280	1.4175	
300	1.4050	

The test setup used for the above testing at AEG Lynn is shown by Figures 43 and 44. Looking at Figure 43, the dial indicator at the upper left-hand corner was used to measure feedback cable travel (β_c). The dial indicator at the right center was used to measure the metering valve position. A β_c actuator is shown below the β_c calibration fixture. Figure 44 shows the other side of the backup control. The power lever shaft and the shutoff valve shaft are shown pointed toward the upper edge of this picture.

2. CALIBRATION

The remainder of the backup control calibration was conducted at Evendale, Ohio. The results are included in Appendix B. The data taken at Lynn, Massachusetts, for the throttle stop adjustments, the core stator schedule (β_c), the electrical overspeed signal, and the hydromechanical overspeed limit are also included.

The acceleration schedule limits used for the calibration log sheets were calculated based on an existing J85 main fuel control cam (2108). However, the most readily available hardware was selected to build the backup control. In this particular control this resulted in using a cam that is different (2103). Figure 45 shows a comparison of the two cams at $T_{2.5}$ = 224° F. At that time, the cam difference was considered to be the reason the first, thirteenth, and fourteenth points on the acceleration schedule were slightly out of limits. The acceleration schedule calibration required a high metering valve pressure drop. This was considered to be the cause for the "rich" deceleration schedule. The decel schedule is a fixed W_f/P_{S3} ratio and not a function of the 3-D cam. The resulting acceleration and deceleration schedules, however, allowed sufficient margins between themselves and the engine steady-state operating line. This was necessary for the subsequent transient response testing.

Early in the subsequent transient testing, when the loop was closed on the stators (β_c), it was found that the stators did not respond to $T_{2.5}$ changes. Investigation revealed that the temperature sensor had not been properly installed - that is, the feedback link did not engage the servo piston (see Figure 8). This caused the sensor to remain at a low $T_{2.5}$ position - about 20° F. The effect this was presumed to have had on the acceleration cam is shown in Figure 45. The wide difference in the expected schedules for 2108 ($T_{2.5}$ = 224° F) and 2103 ($T_{2.5}$ = 20° F) further explains why the acceleration schedule did not calibrate as expected and why the required metering valve pressure drop was 63 psid instead of the expected 53 psid.

The backup control was shipped from the AEG Lynn facility, where the $T_{2.5}$ sensor had been removed to reduce the risk of shipping damage to the capillary tube. The sensor was reinstalled at the AEG Evendale facility, and this is when the feedback link failed to get engaged with the servo piston. Once the sensor was reinstalled in the normal manner, the stators responded to $T_{2.5}$ changes.

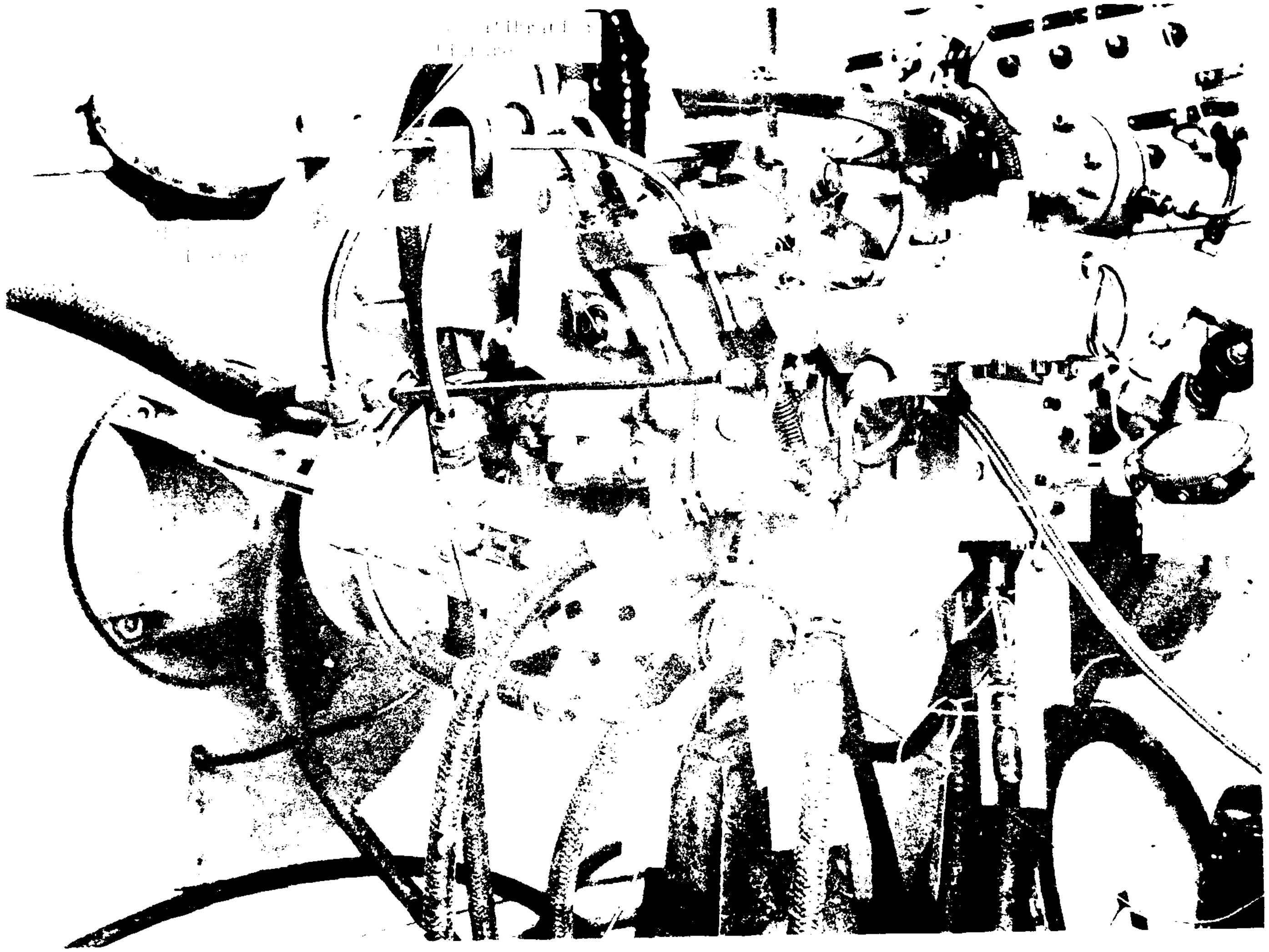

Figure 13. VCE Backup Control Preliminary Calibration Test Setup, Left Side View.

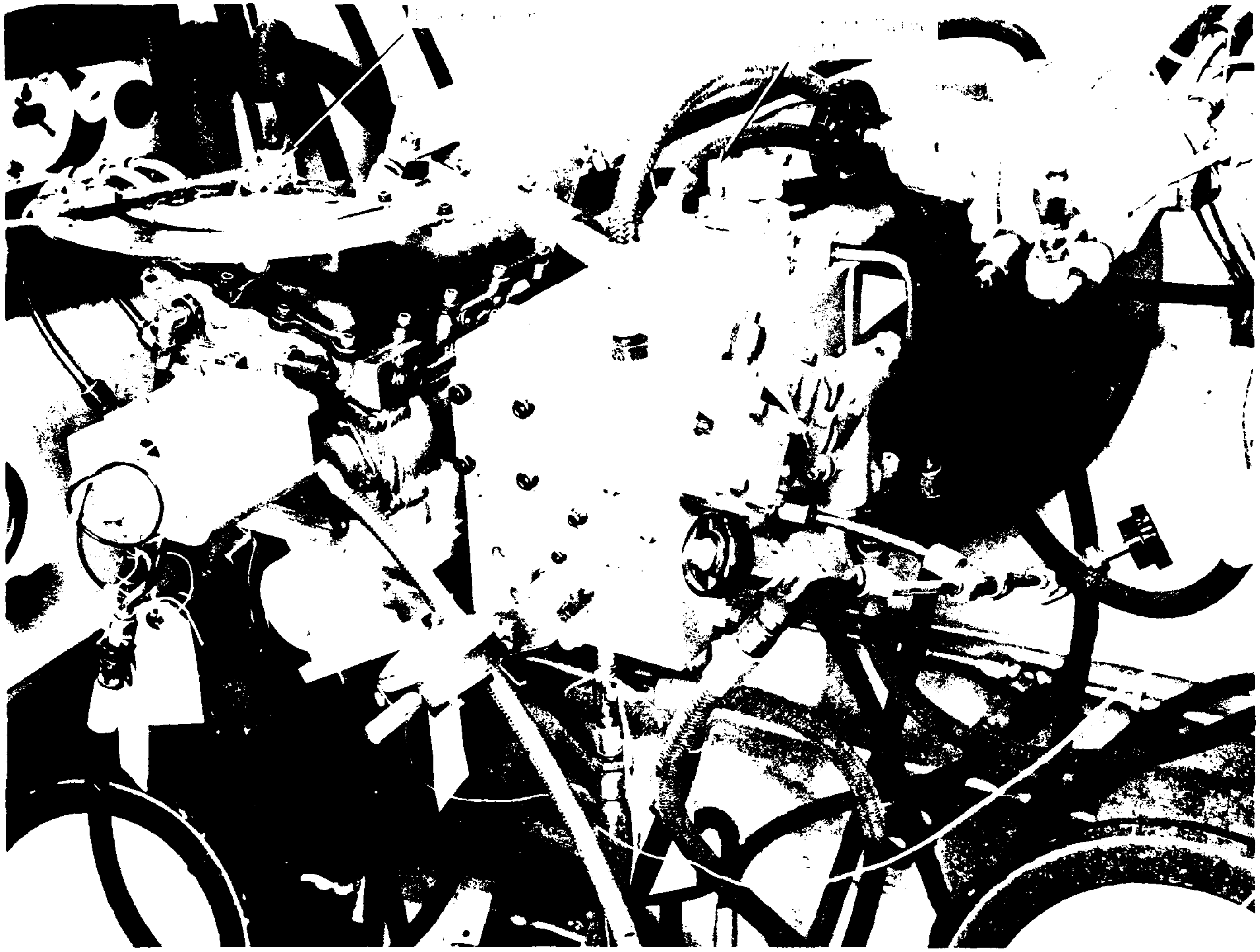

Figure 14. VCE Backup Control Preliminary Calibration Test Setup, Right Side View.

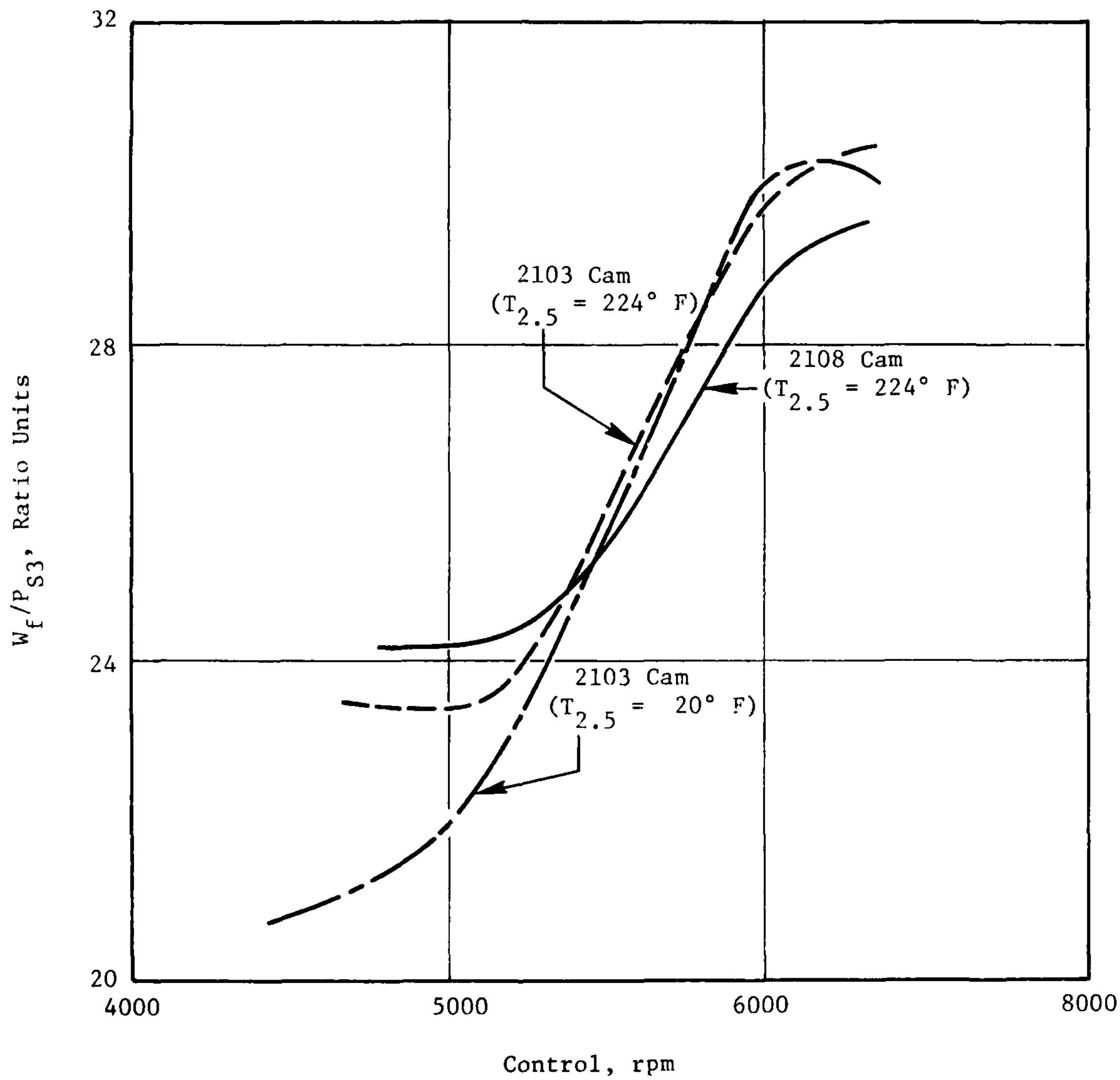

Figure 45. Comparison of Cam Schedules.

The shutoff valve leakage was out of limits. The leakage indicates that the mating parts require additional lapping, which will be done before the control is used on any engine test.

The test setup used for calibration and subsequent transient response testing is shown by the three photographs that constitute Figures 46, 47, and 48. Figure 46 shows the backup control on the test stand at the left and the F101 augmentor fuel pump on the test stand at the right. Figure 47 is a view of the backup control showing the hydromechanical computer. In contrast with the machined bodies for the other subassemblies, the computer is enclosed in a cast housing. The enclosure wrapped in white insulating material is the test fixture for the $T_{2.5}$ sensor. Figure 48 shows the F101 augmentor fuel pump. This type of pump is intended for the JTDE testing. An F101 augmentor fuel filter, mounted to the pump inlet, is also shown. This pump and filter were used as the fuel pressure source for all the testing.

3. BACKUP CONTROL TRANSIENT RESPONSE

When operating in the backup mode, hydromechanical components provide the normal engine control functions:

- rpm governing as a function of power lever position
- Scheduling of main fuel flow as a function of N_2, P_{S3}, and $T_{2.5}$ on accelerations, and as a function of P_{S3} on decelerations
- Scheduling of β_c as a function of N_2 and $T_{2.5}$

Steady-state and transient response characteristics, when in the backup mode, were of interest because of the adaptation of the larger flow metering valve to the J-85 computer mechanization. Testing to determine the performance of the backup control consisted of the following:

- Defining fuel flow (W_f) and variable stator vane (β_c) oscillations on accelerations and decelerations.
- Defining governor droop characteristics.
- Determining frequency responses of fuel flow and stators to N_2 and of fuel flow to P_{S3}.

Figure 49 shows the bench setup used for testing the backup control. Both open-loop and closed-loop testing were employed. Open-loop fuel flow and stator oscillations, obtained by operating the control at fixed values of N_2, P_{S3}, $T_{2.5}$, PLA, and control inlet fuel pressure, showed random drifts of ± 20 pounds per hour (fuel flow) and $\pm$ 0.001 inch (stator). Head regulator oscillations were typically $\pm$ 0.2 psi. Figure 50 is a typical steady-state trace.

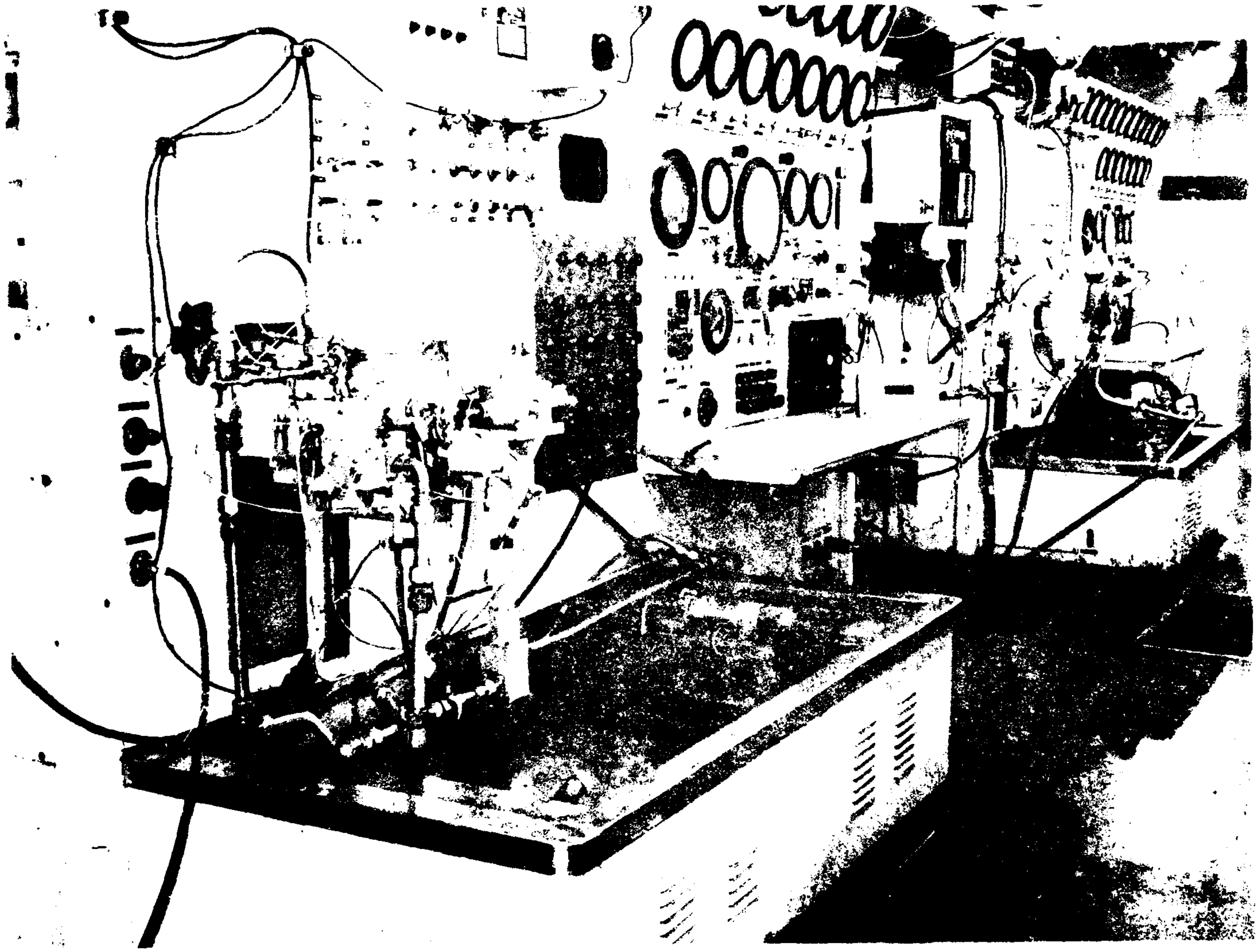

Figure 46. Setup Used for Testing the Backup Control.

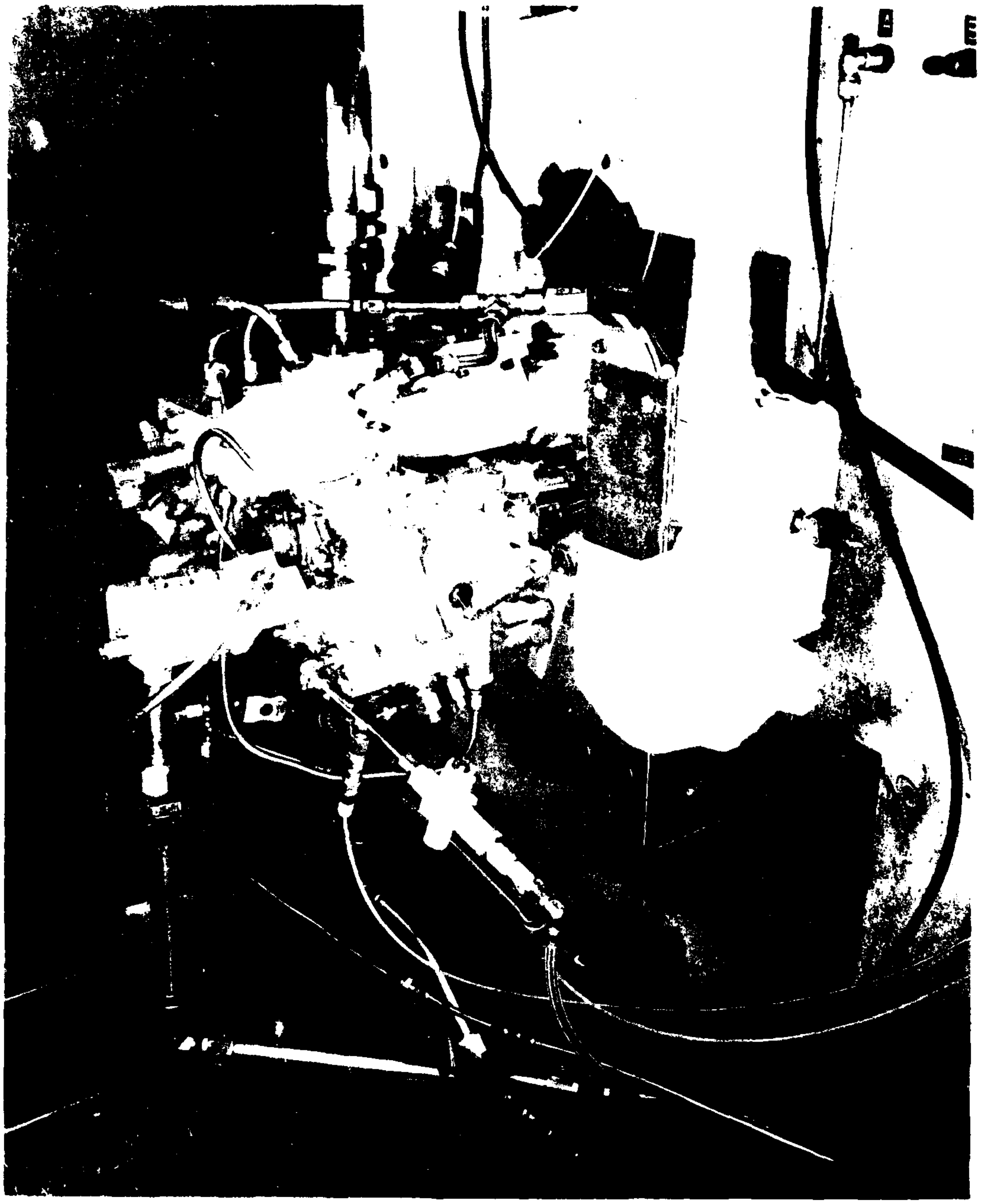

Figure 47. View Showing the Computer Section of the Backup Control.

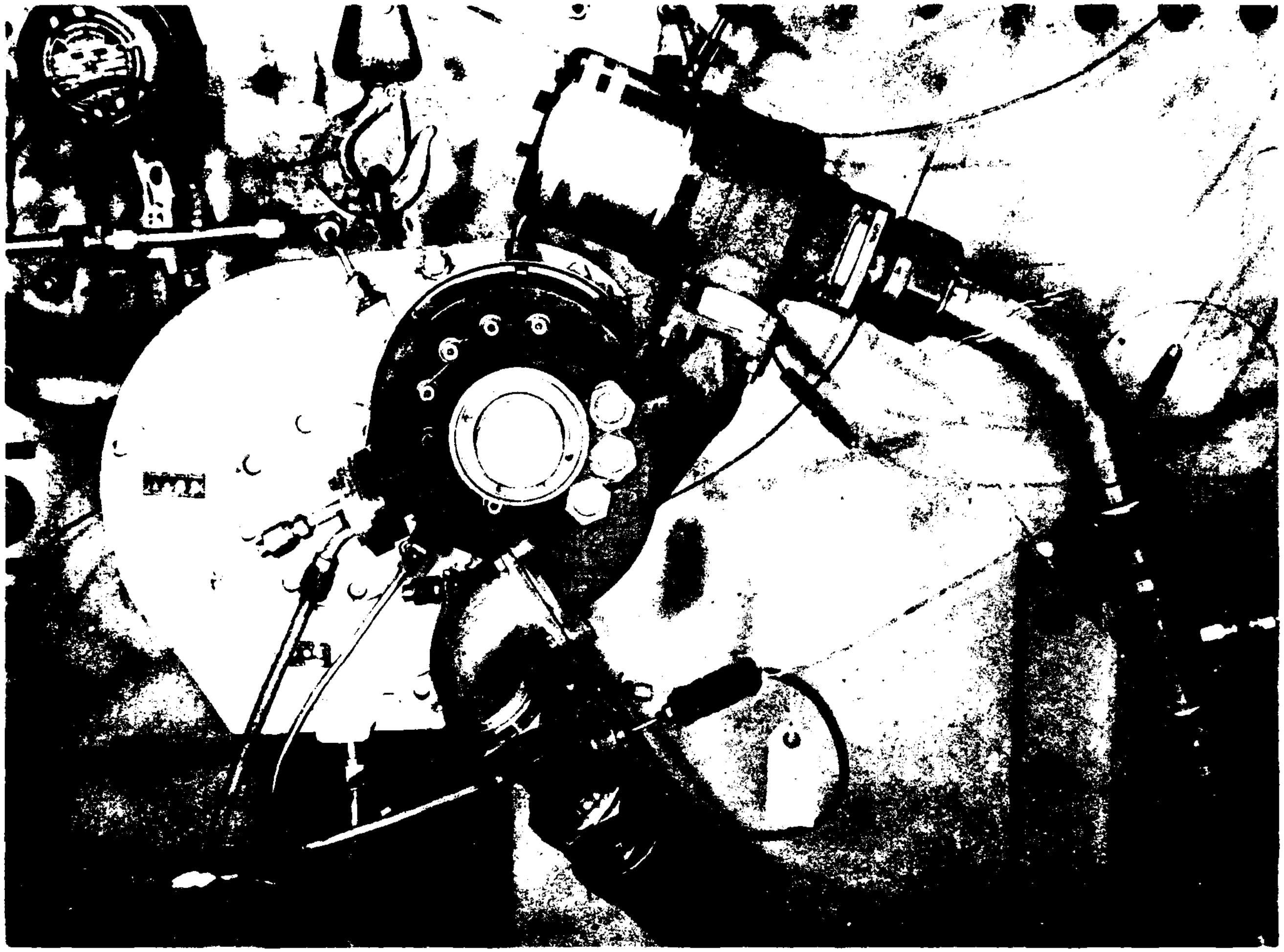

Figure 48. F101 Augmentor Fuel Pump and Filter Mounted to Test Stand.

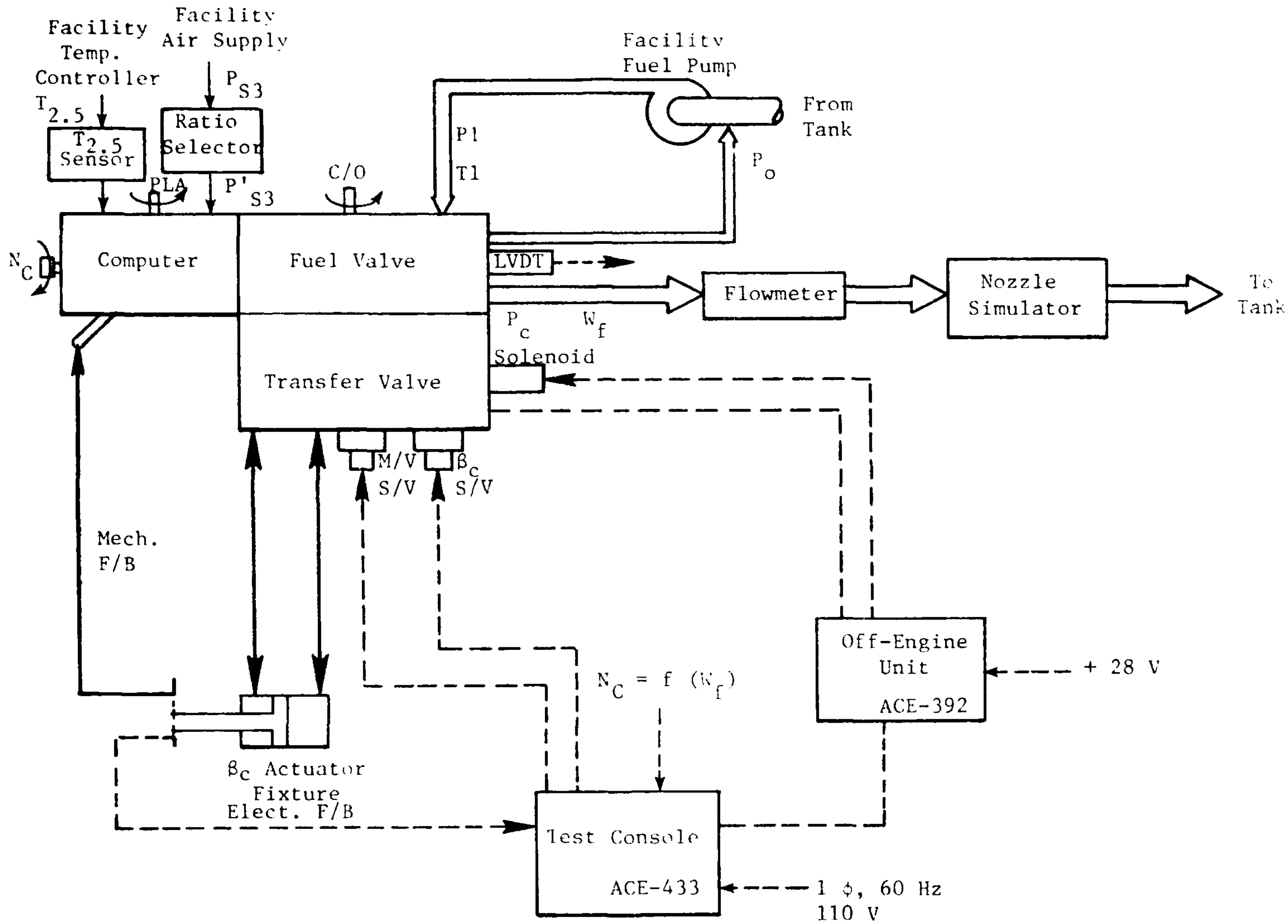

Figure 49. Setup for Transient Testing of Backup Control.

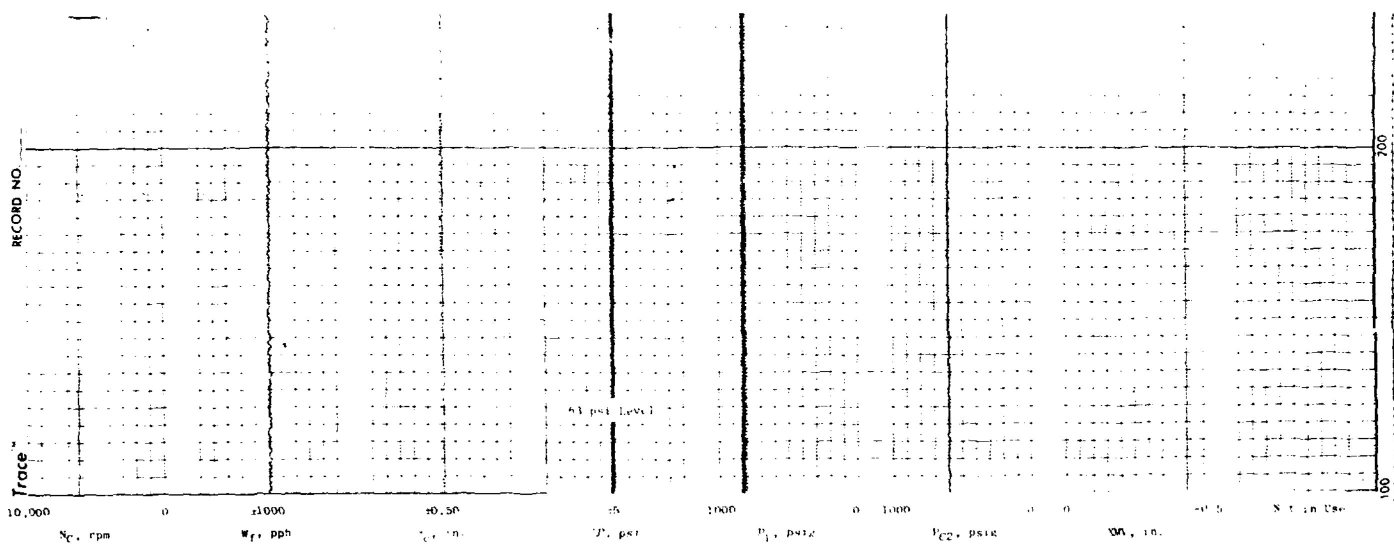

Figure 50. Trace of Backup Control at Steady State.

Figures 51 and 52 show fuel flow, variable stator position, and head oscillations on a speed ramp condition of ± 600 rpm per second, with P_{S3}, $T_{2.5}$, PLA, and control inlet fuel pressure fixed. Fuel flow can be seen to be stable, with little oscillation on the acceleration and deceleration and little overshoot during governor cut-in, when the governor takes over the control of fuel flow.

Figures 53 and 54 show typical throttle bursts and chops, operating closed-loop and using the dynamics of the GE23 engine in the closed-loop simulation. The control can be seen to ride the acceleration or deceleration until the governor modulates W_f to hold N_2 at the demanded power setting.

Figures 55, 56, and 57 show typical open-loop governor characteristics which define the governor droop and hysteresis. The droop characteristics are seen to vary with N_2 level, yielding higher gain at higher power settings. The displayed 0.053 W_f/P_{S3} ratios per rpm at the high speed points were expected with the J-85 computer. Speed hysteresis, which increased inversely with power setting, is observed to be constant at a given power setting regardless of speed swings.

In the J-85 main fuel control, the W_f feedback spring is attached directly to the metering valve. To allow using a larger metering valve with a triangular port for the backup control, a rack and pinion, a cam and a bellcrank were added between the metering valve and the feedback spring. This resulted in more friction, which increases hysteresis and reduces repeatability. Although the increased hysteresis is still acceptable for this backup control, the production version of the backup control would be mechanized similarly to the J-85 main fuel control. Its hysteresis would be less, comparable to that of the J-85 main fuel control.

Frequency response testing on the governor ($\Delta W_f/\Delta N_2$) and the stators ($\Delta \beta_c/\Delta N_2$), typical traces of which are shown in Figure 58, produced magnitude and phase characteristics shown in Figures 59 and 60. Flow response to P_{S3} ($\Delta P_{S3}/\Delta N_2$) was almost identical to flow response to N_2, since both speed and P_{S3} work through the nutcracker/flapper and fuel valve power piston system.

Fuel flow response was lower than anticipated, primarily because of governor hysteresis. As seen in Figure 59, correcting the calculated response of Figure 41 for magnitude and phase effect of 50 rpm hysteresis gives relatively close correlation to the test data.

4. TRANSFER TO BACKUP MODE

When operating in the primary mode, the transfer valve blocks the backup W_f and β_c servovalve outputs so that interference between the two controls is prevented. During this mode of operation the backup control

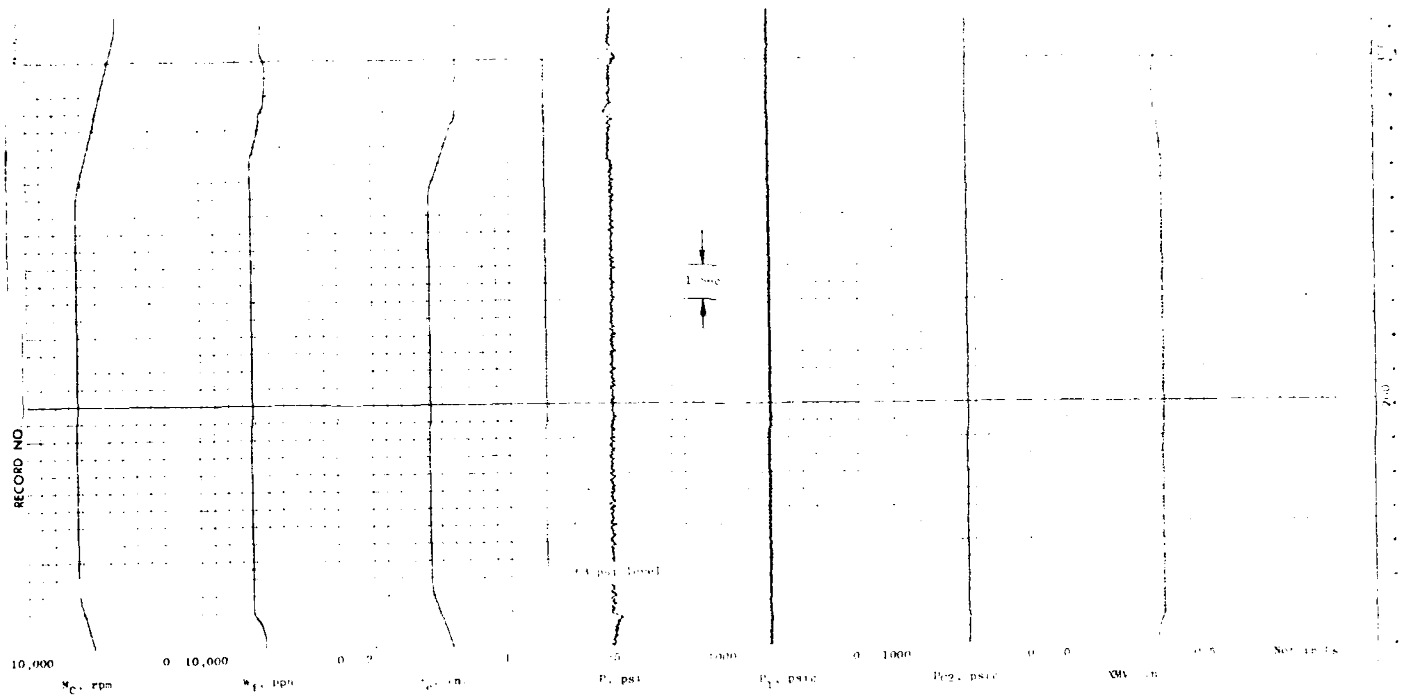

Figure 51. Open-Loop Trace of Backup Control Acceleration and Deceleration, 600 Control rpm/sec.

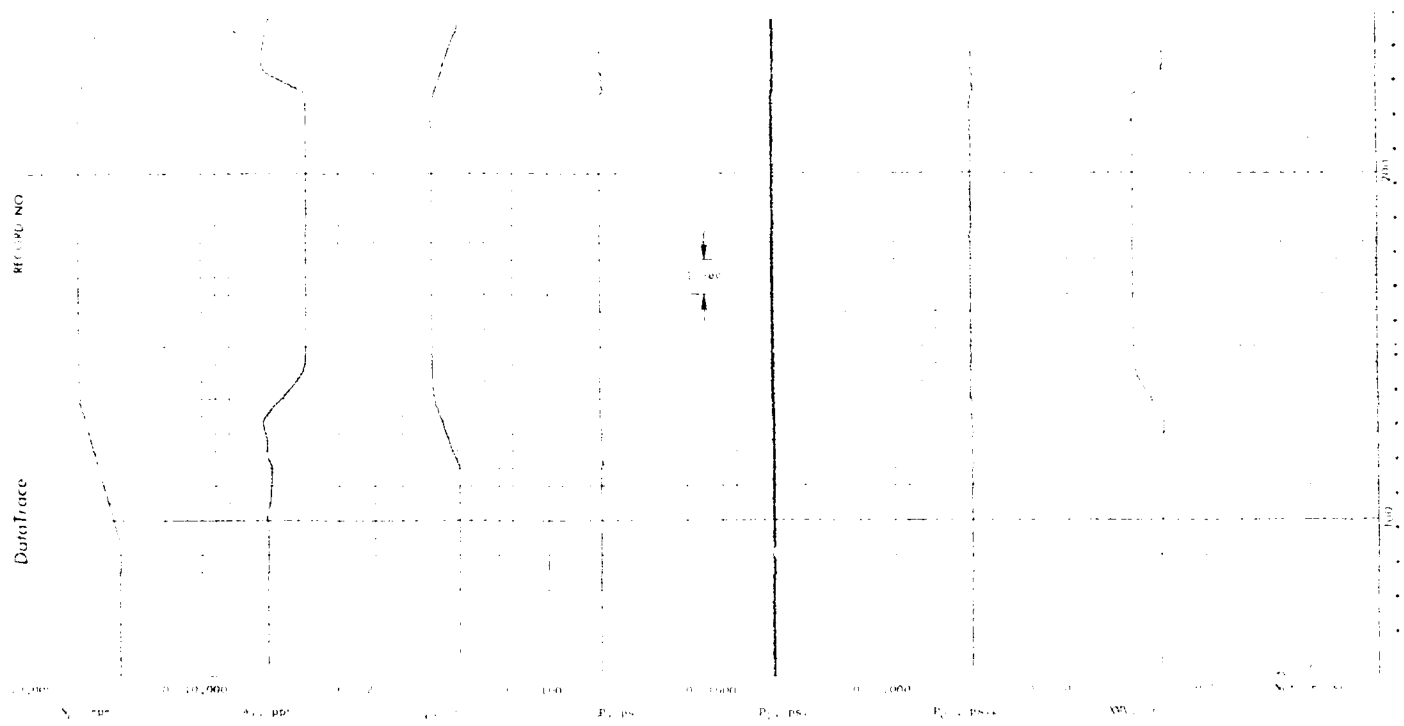

Figure 52. Open-Loop Trace of Backup Control Acceleration with Governor Cut-In, 600 Control rpm/sec.

AD-A094 730 GENERAL ELECTRIC CO CINCINNATI OH AIRCRAFT ENGINE GROUP F/G 21/5
BACKUP CONTROL FOR A VARIABLE CYCLE ENGINE.(U)
JUL 80 H B KAST F33615-76-C-2086
UNCLASSIFIED R80AEG450 AFAPL-TR-79-2069 NL

2 OF 2
AD
A094 730

END
DATE
FILMED
3-81
DTIC

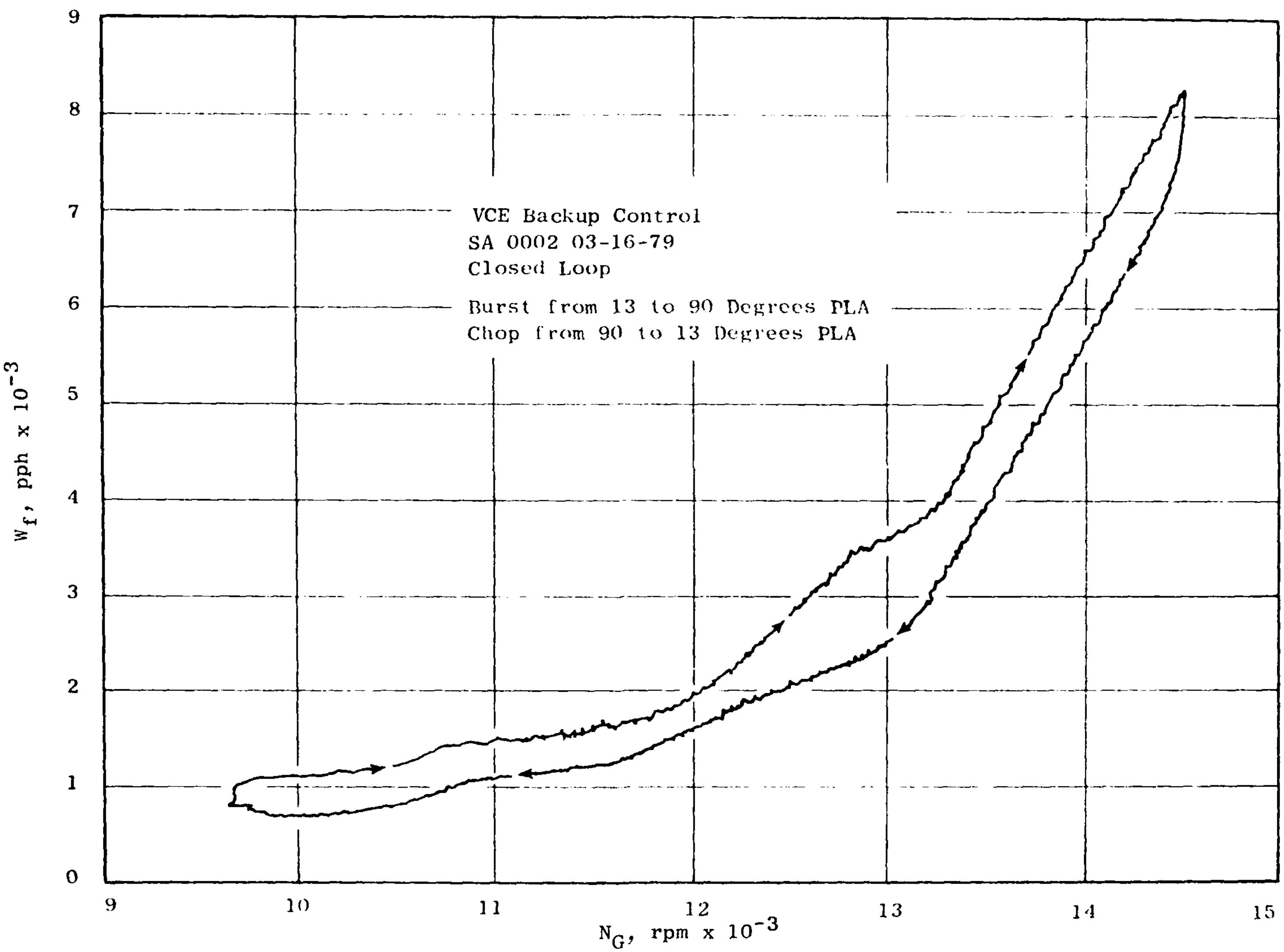

Figure 53. Closed-Loop Throttle Burst and Chop, Full Throttle Excursion.

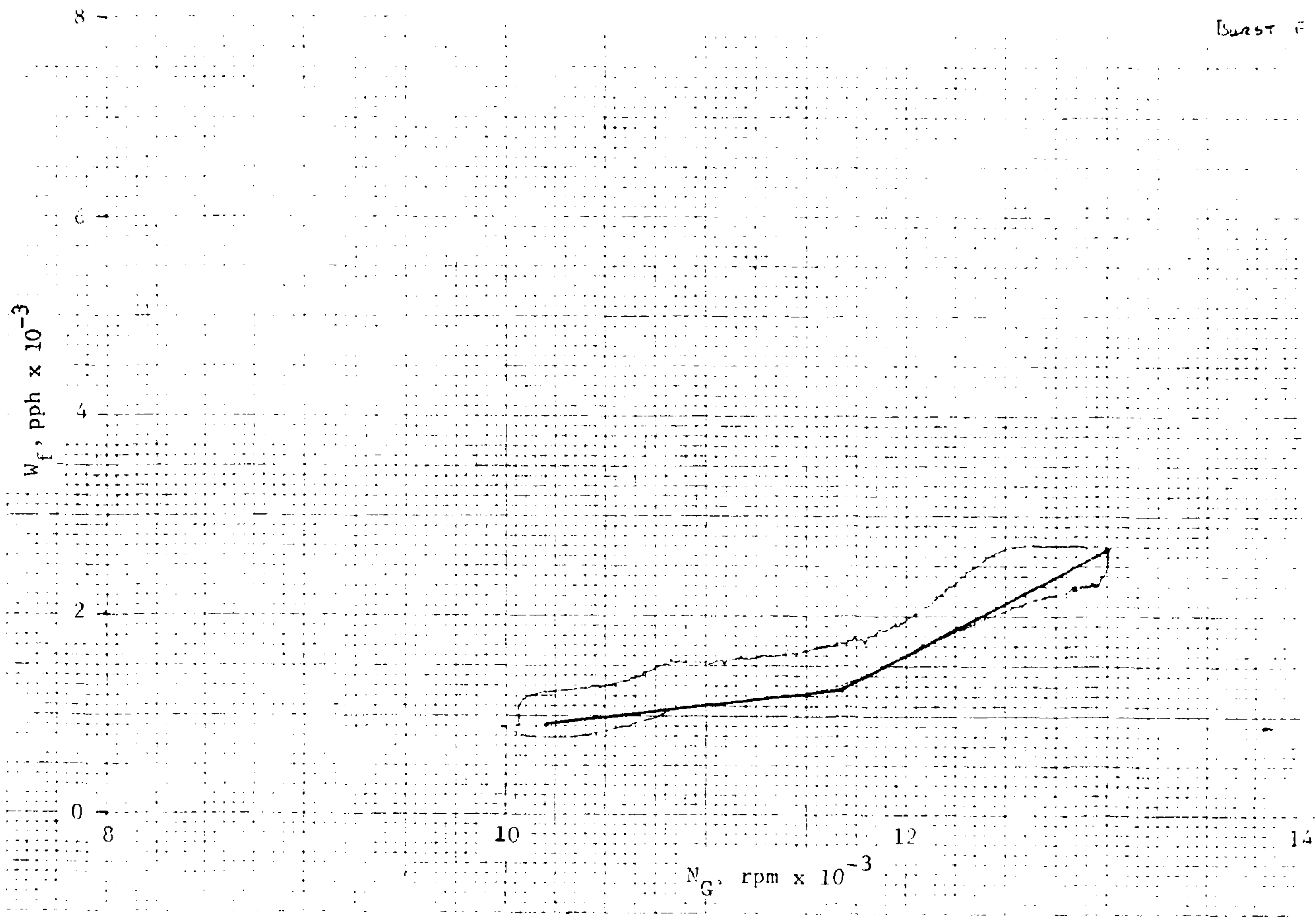

Figure 54. Closed-Loop Throttle Burst and Chop, Part Throttle Excursion.

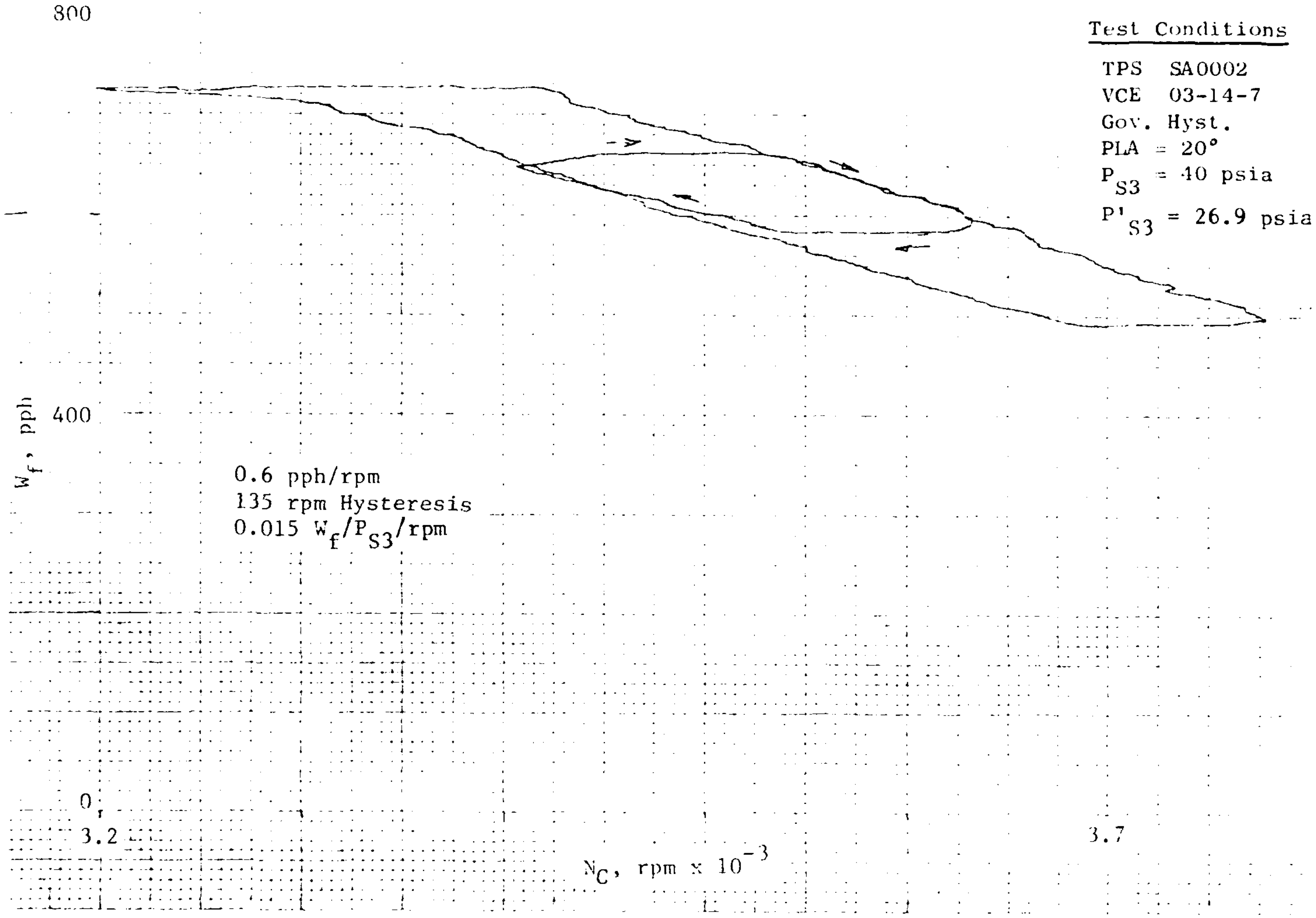

Figure 55. Open-Loop Governor Characteristics, Low Speeds, Showing the Governor Hysteresis.

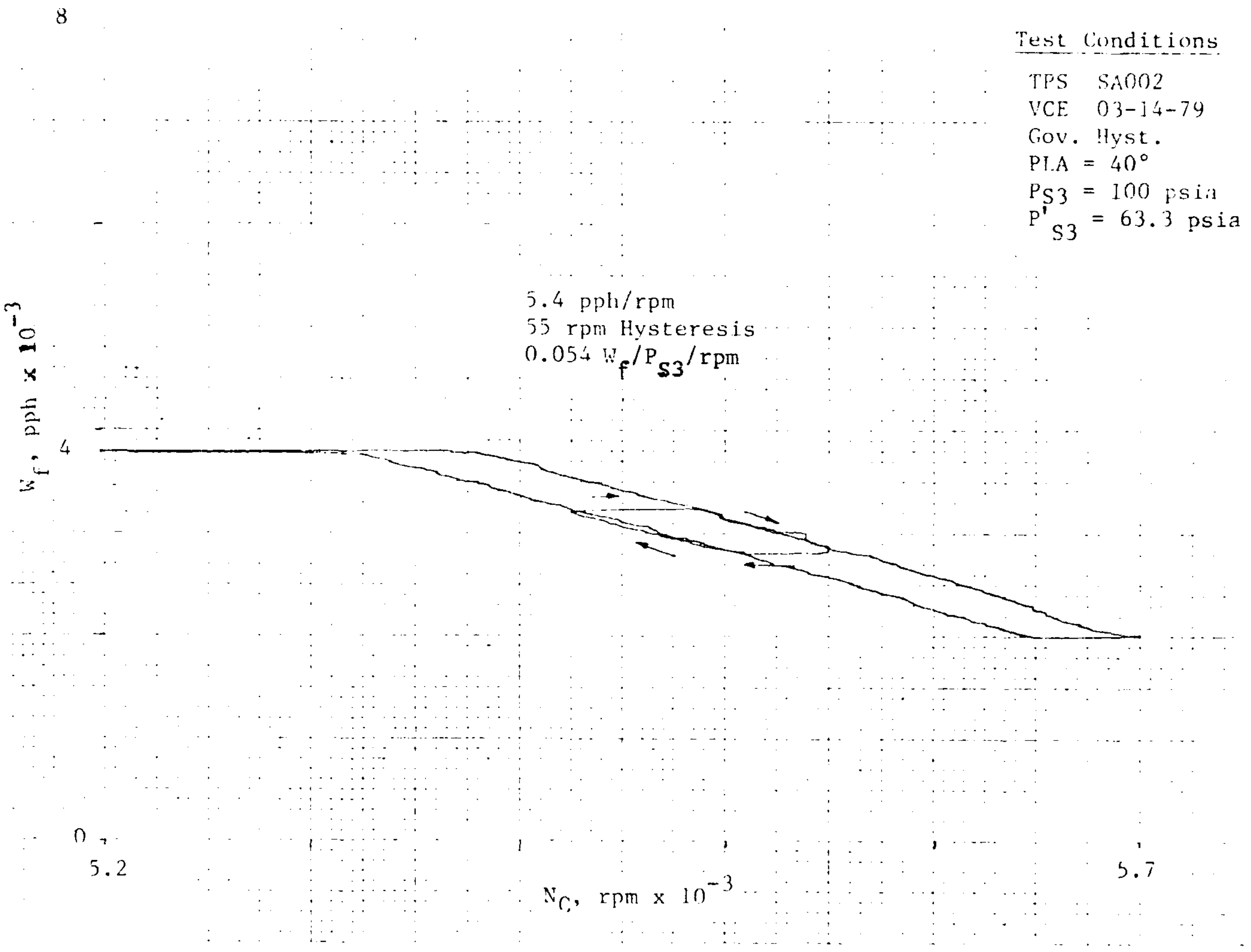

Figure 56. Open-Loop Governor Characteristics, Mid Speeds, Showing Governor Hysteresis.

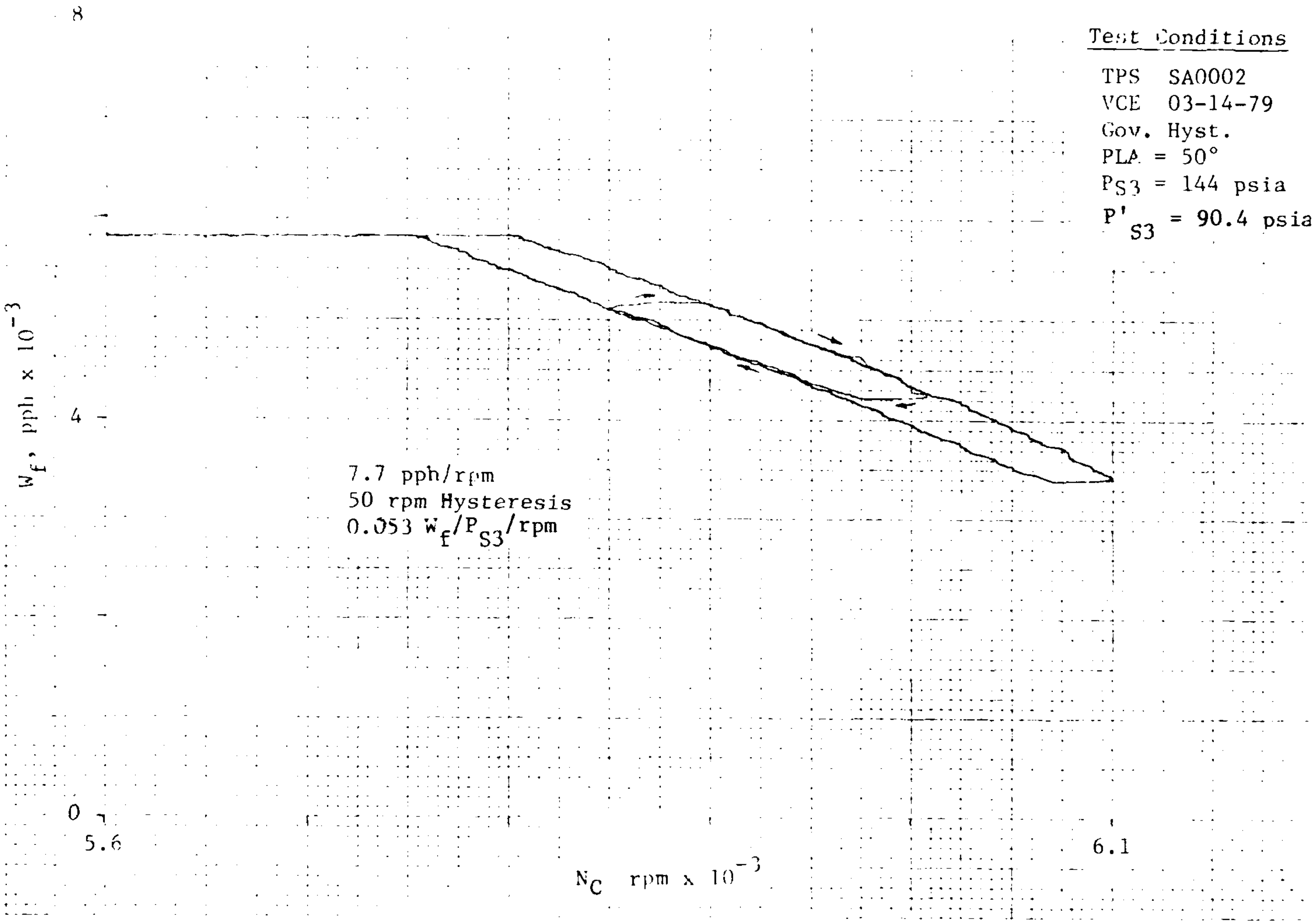

Figure 57. Open-Loop Governor Characteristics, High Speeds, Showing Governor Hysteresis.

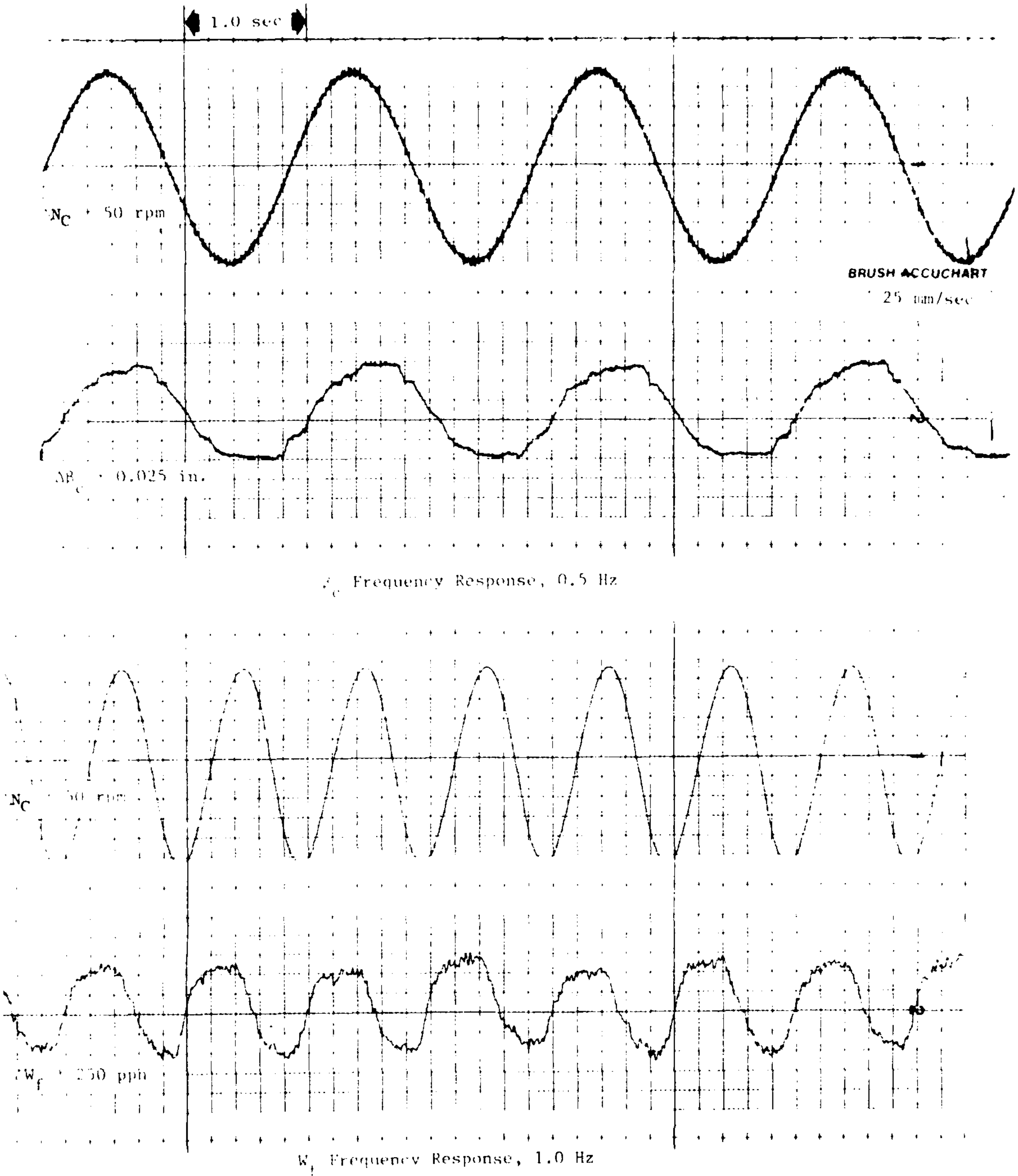

Figure 58. Typical Frequency Response Traces.

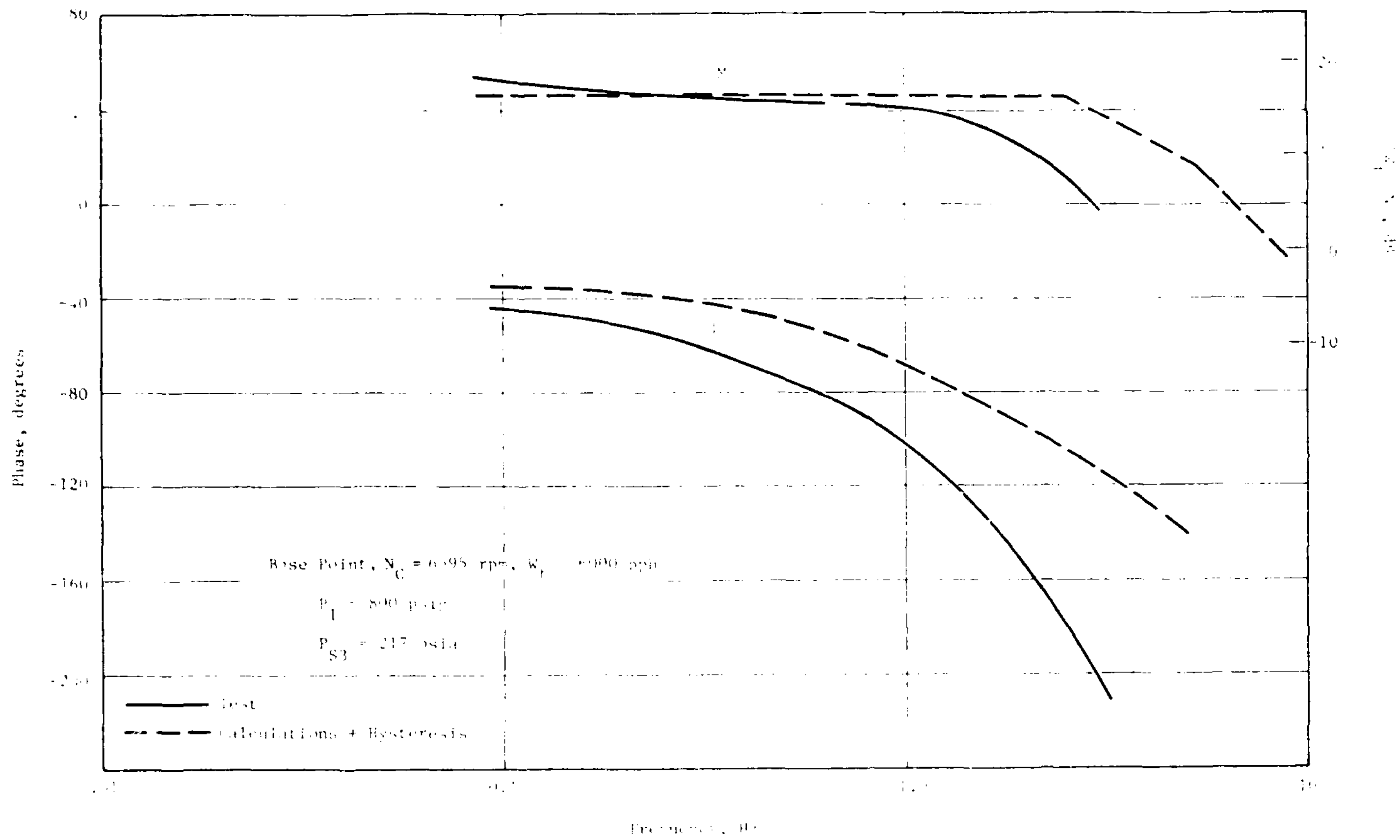

Figure 59. Backup Control Governor Frequency Response.

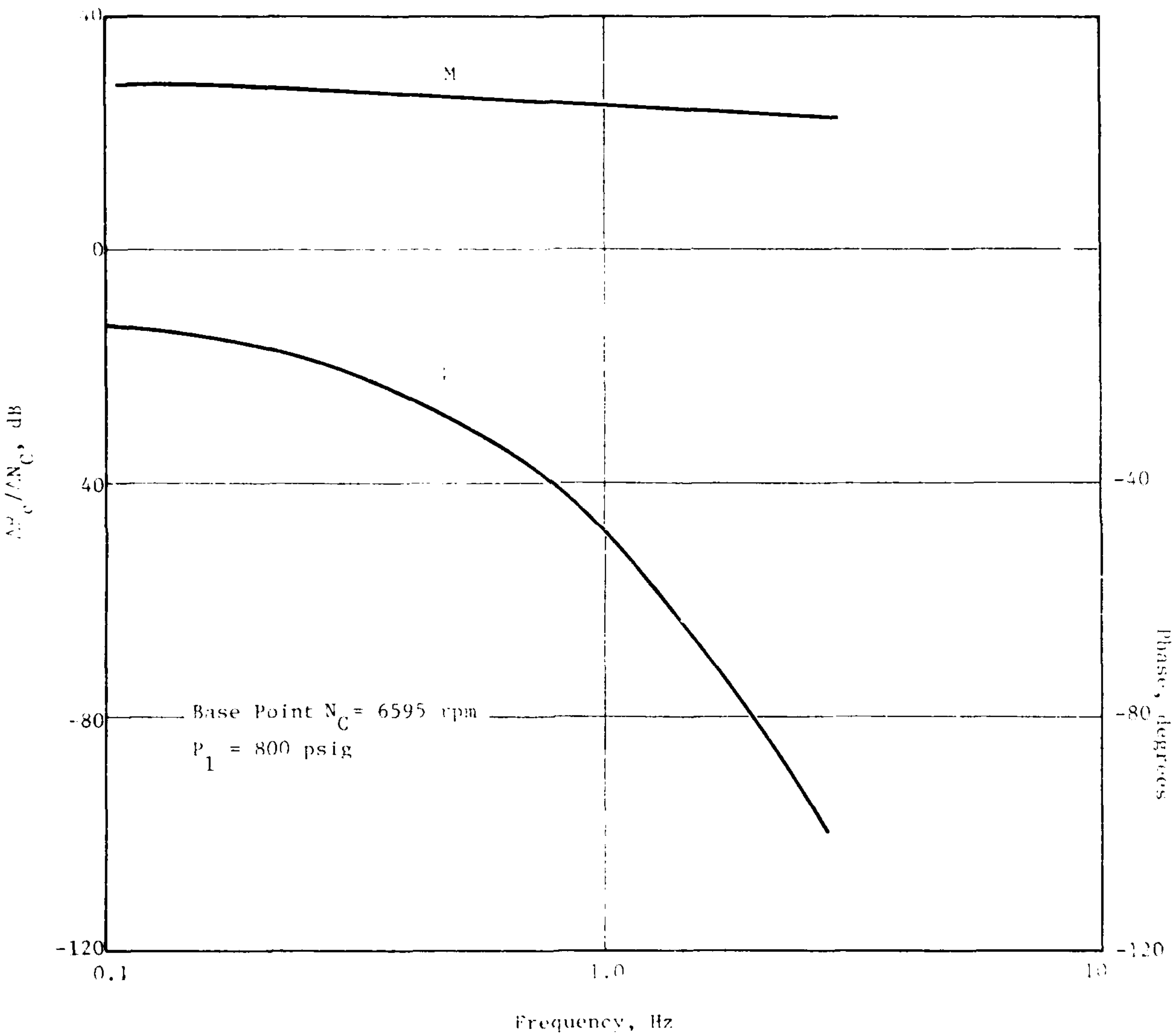

Figure 60. Backup Control Variable Stator Frequency Response.

is continuously tracking the engine. Because there are schedule differences between the two controls, backup control errors can exist which could position the hydraulic error amplifier (or servovalve) to a saturated condition at the instant of transfer. Thus transfer transients following a switch from primary operation were of primary concern. Testing to determine the transient performance of the backup control consisted of:

- Defining the responses obtained following a transfer to backup from various steady-state and transient conditions
- Defining transfer characteristics upon automatic switching to backup mode by the overspeed switch
- Defining governor action upon modulation of the throttling valve by the valve driven by the hydromechanical speed sensor upon extreme overspeed.

Transient behavior following transfer from the primary mode to the backup mode was obtained by establishing an error between the two controls while operating closed-loop. Both small and large errors were intentionally set. Transfers at both steady-state and ramp conditions were made. Typical transient behavior following transfer at steady-state conditions is shown in Figures 61 through 64. As seen on the traces, small errors between the two modes produced only slight momentary transients. Fuel flow peaked approximately 200 pounds per hour rich but recovered to the backup-demanded flow within 0.6 second. Stator transients showed a similar result. With intentional large errors existing at the instant of transfer, fuel flow merely went to the acceleration or deceleration schedule, causing the simulated engine to accelerate or decelerate normally until fuel flow was modulated to hold speed at the condition demanded by the backup control power lever setting. Stators followed speed with a slight overshoot and undershoot before stabilizing at their new requested position.

Automatic transfers to backup upon overspeed conditions were identical transients to those shown in Figure 64. The system transferred at the proper preset overspeed, and fuel flow responded to the level called for by the power lever.

Figure 65 shows the action of the hydromechanical governor, which acts to close the throttling valve to reduce flow in an extreme overspeed. Fuel flow was cut back at the proper overspeed condition. With the test bench operating closed loop, speed decreased when flow dropped, opening the throttling valve. Speed then increased until the overspeed point was reached and flow reduced. A limit cycle with a period of approximately 3.1 seconds was established, with control speed varying between 7000 and 7500 rpm.

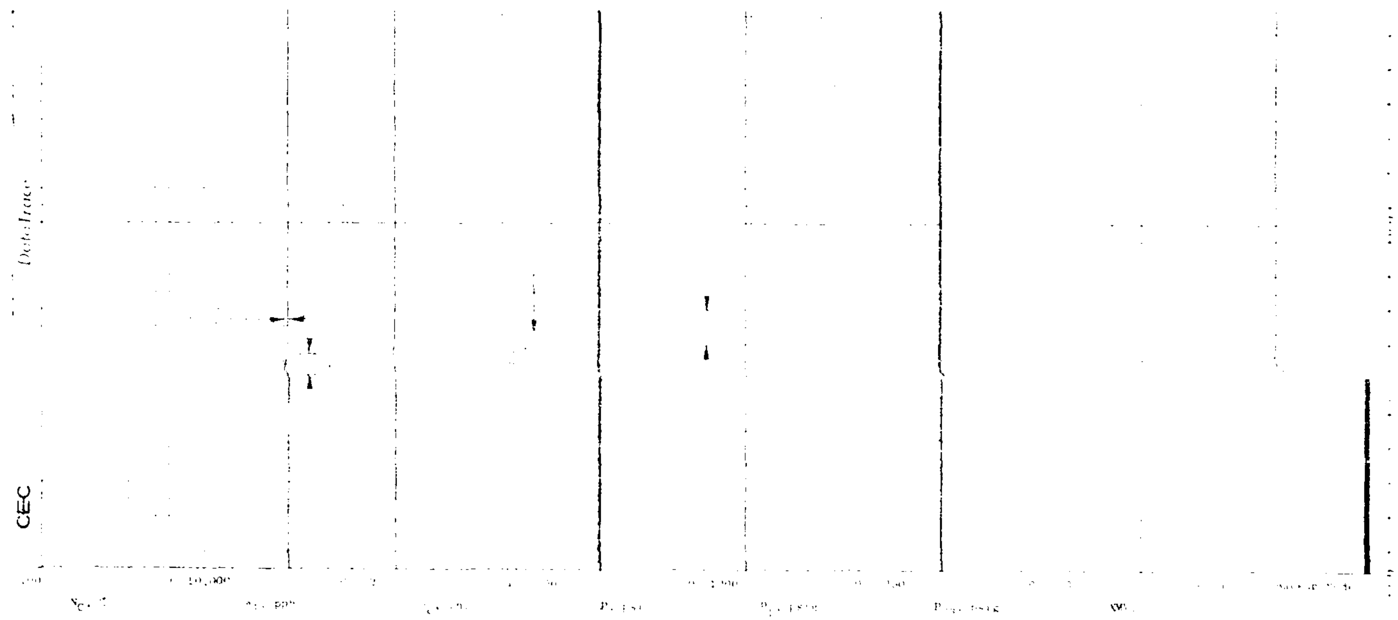

Figure 61. Primary-to-Backup Transfer During Accel, Small Transient Offset Error, ~ 70° PLA.

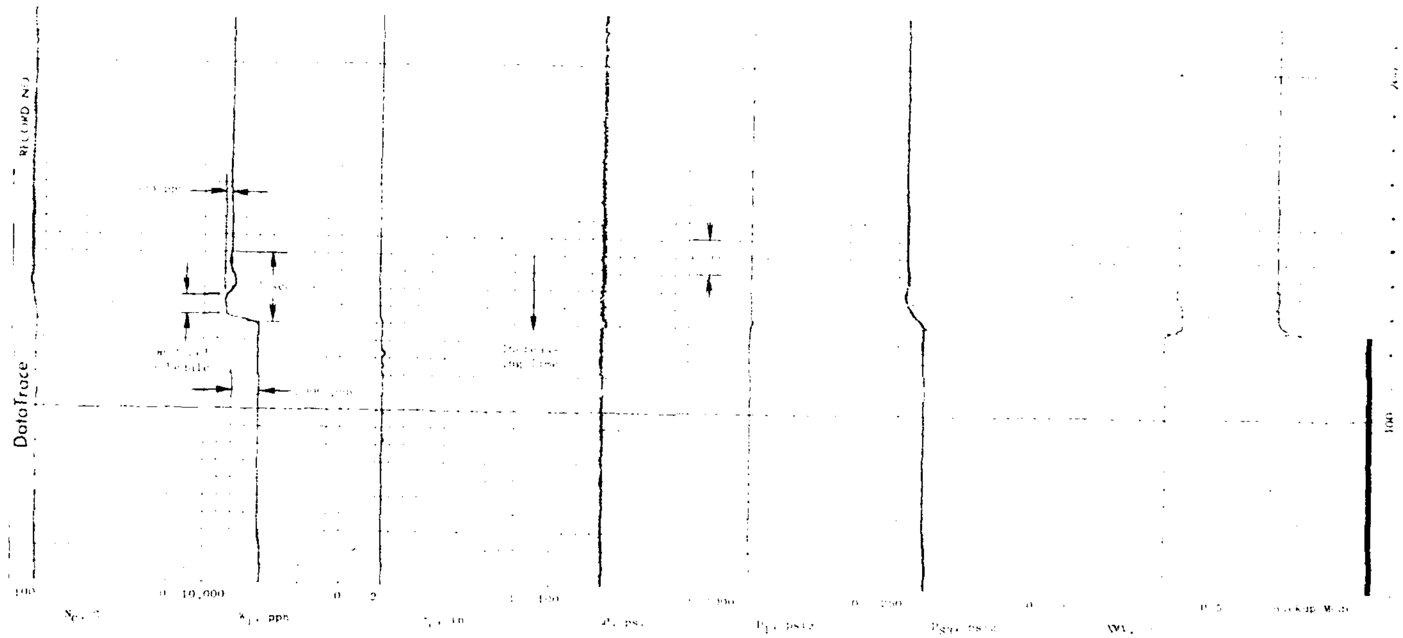

Figure 62. Primary-to-Backup Transfer During Accel, Large Transient Offset Error, ~ 70° PLA.

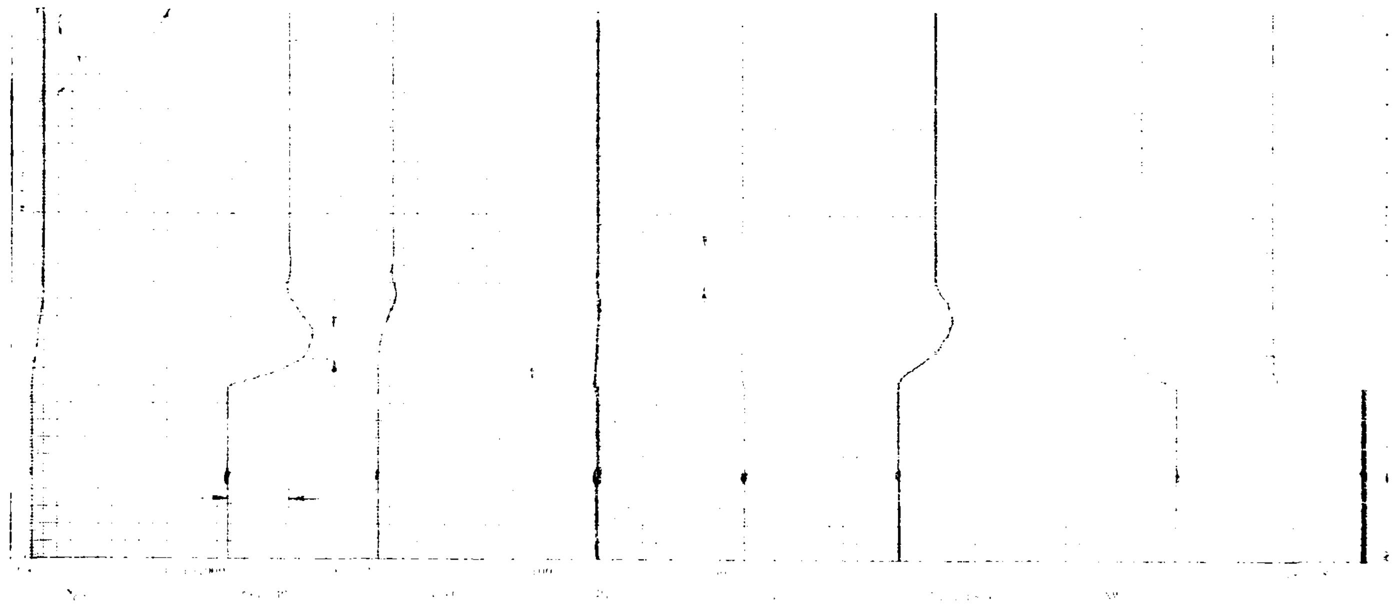

Figure 63. Primary-to-Backup Transfer During Accel, Large Transient Offset Error, $\sim 50^{\circ}$ PLA.

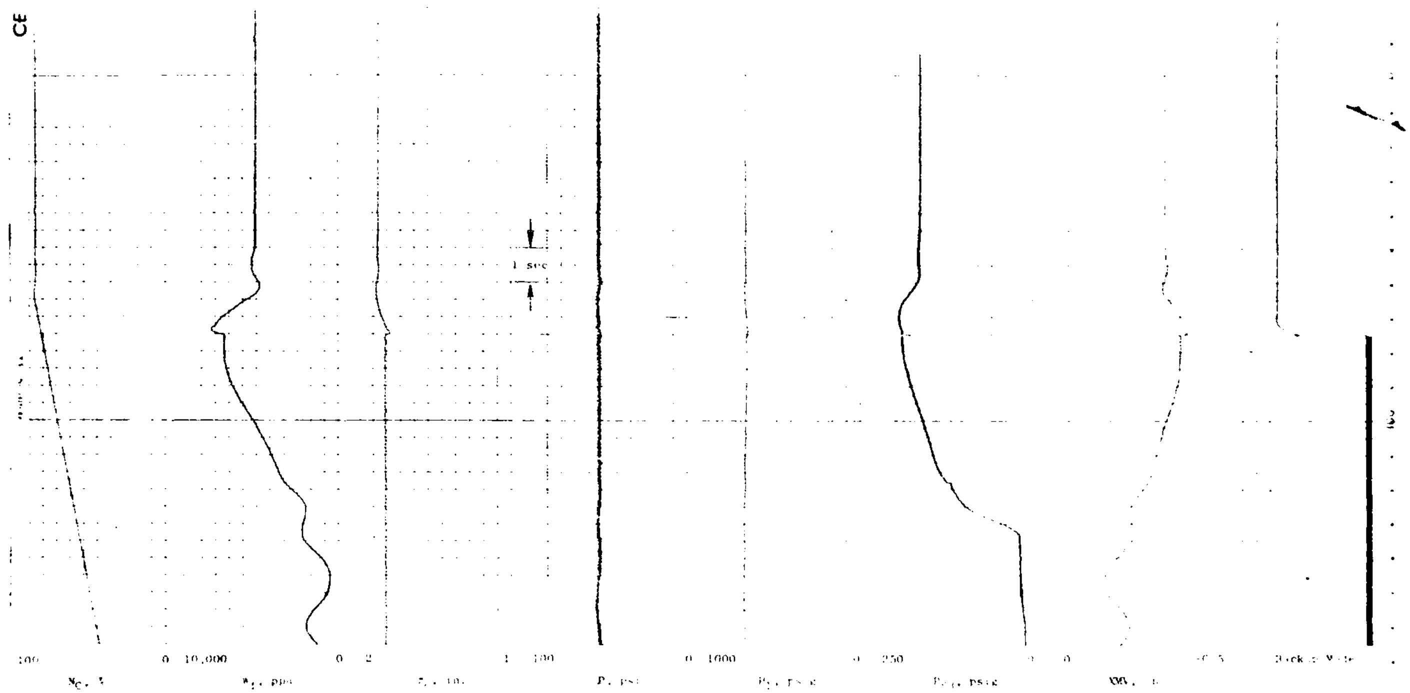

Figure 64. Primary-to-Backup Transfer During Accel, Ramp Transient of 5% Speed/sec, ~ 60° PLA.

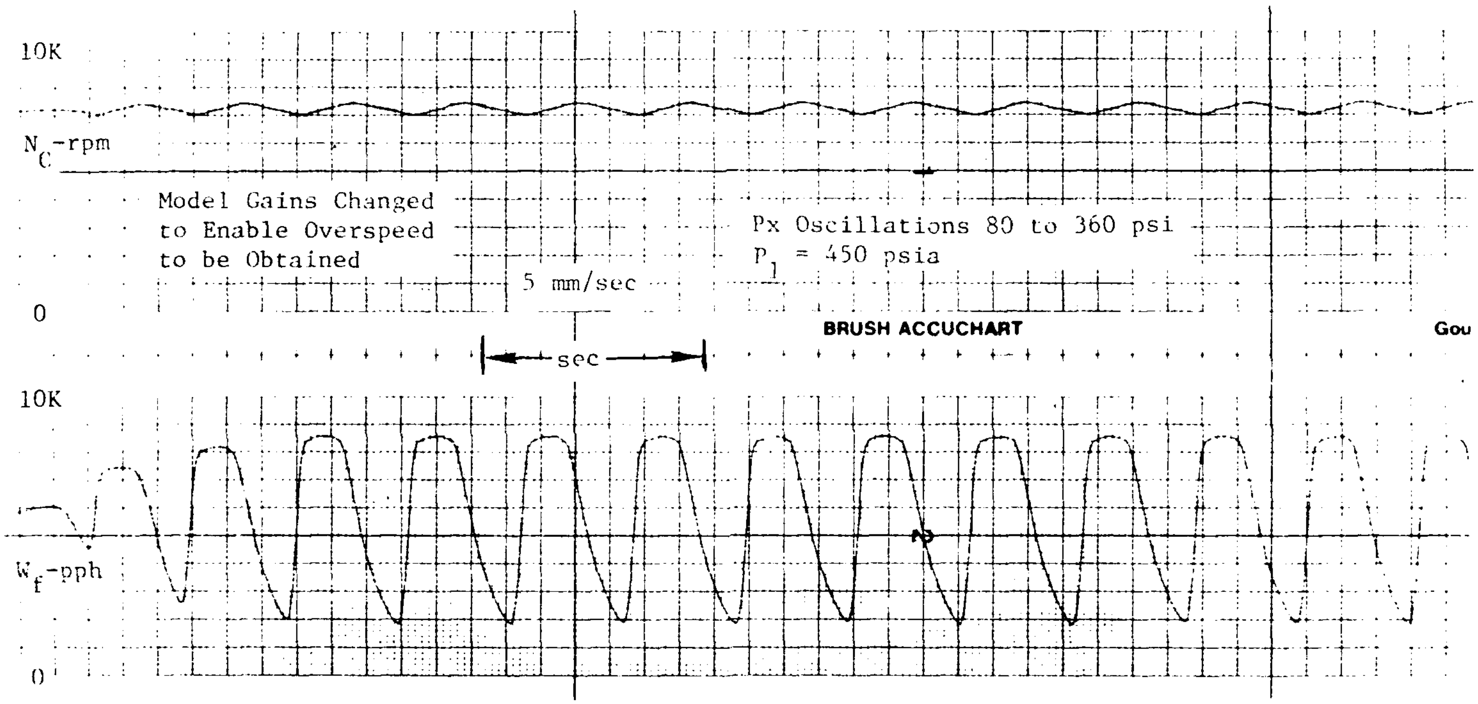

Figure 65. Hydromechanical Overspeed Trace.

5. CYCLIC ENDURANCE

The planned endurance test consisted of the following steps:

1. Check calibration

2. Run 40 hours of accel/decel cycles

3. Conduct 100 transfers to the backup mode by going overspeed

4. Conduct 10 overspeed transients during which the hydromechanical overspeed valve modulates the throttling valve

5. Recheck calibration

Step 2 of this test required operating closed-loop in the backup mode. The power lever was cycled from idle (70% rpm) to max (100% rpm) and the engine model plus the test setup caused the drive speed, fuel flow, and P_{S3} to cycle. Temperature ($T_{2.5}$) cycling was not planned.

The calibration check disclosed that accel schedule repeatability was not satisfactory. Experimentation indicated that applying current to the primary W_f servovalve would change fuel flow a small amount. It was suspected that transfer valve leakage caused a null shift in the flapper servo in the hydromechanical computer. The transfer valve was needed only for Step 3 of the planned endurance test. This portion of the test was conducted first. Speed was ramped successfully 100 times in the primary mode to the point where the overspeed switch tripped and automatic transfer to the backup mode occurred. The transfer valve was then removed.

The calibration check, with the transfer valve removed, indicated that the repeatability problem was still present. Temperature sensor performance was then checked and the performance was found to be very erratic. As discussed previously, the sensor was installed improperly upon arriving at AEG Evendale. It was now suspected that it had been damaged during that installation. A suspected cause for the observed action was that the jet pipe was bent, keeping receiver pressures too low to properly control the sensor servo piston.

The temperature sensor servo pistion was shimmed to the high temperature position. The accel schedule was run twice; the data are shown by Table 2. The repeatability was considered normal. (It should be noted that, for the J85 main fuel control, the fuel flow feedback spring is attached directly to the metering valve. The backup control has a rack and pinion, a shaft, a cam, and a bell crank between the metering valve and the feedback spring. It is expected that a J85 control would have even better repeatability.) The remainder of the endurance testing was

TABLE 2.

ACCEL SCHEDULE DATA TAKEN BEFORE
AND AFTER THE ENDURANCE TEST

Data Point	N_c, rpm	P_{S3}, psia	P_{S3}^{1}, psia	Before* W_f, pph	Before* W_f, pph	After W_f, pph
1	6360	30.5	21.0	1404	1456	1396
2	6360	54	34.7	2321	2348	2302
3	6360	67	42.7	2852	2892	2857
4	6360	90	57.1	3784	3827	3798
5	6360	104	65.9	4348	4387	4341
6	6360	114	72.2	4749	4778	4736
7	6360	144	91.2	5951	5990	5913
8	6360	176	111.3	7205	7249	7177
9	6360	222	140.8	8923	8981	8942
10	4770	54	34.7	1599	1602	1567
11	5175	67	42.7	2119	2131	2096
12	5565	90	57.2	3412	3445	3440
13	5710	104	66.0	4099	4112	3972
14	5840	114	72.3	4859	4831	4805
15	6120	144	91.2	5950	5971	5999

*Second set of calibration data to show repeatability.

then conducted. This included 1600 accel/decel cycles at 90 seconds per cycle (about 40 hours). The accel data taken after the endurance testing is also shown by Table 2.

6. SUMMARY

The overall performance of the backup control during the test phase was very satisfactory. A total of 173 bench test hours were accumulated. This testing is a big step in qualifying the backup control for on-engine use.

The test results indicated that some changes should be made to the latching solenoid valve and the transfer valve before the backup control is used on-engine. The latching solenoid valve coils should be replaced with ones capable of withstanding 28 volts continuous duty as originally intended. The vendor overlooked a note on the drawing and used coils sufficient for momentary power only. The proper coils would be about 1.5 inches in diameter versus the present 1.0 inch.

The transfer valve leakage affected the backup control W_f servo. A null shift became evident when current was applied momentarily to the primary W_f servovalve. The transfer valve leakage should be reduced by adding seals to the spool.

The $T_{2.5}$ sensor problem was attributed to damage caused by improper installation. This is a proven component so no changes are recommended. The hysteresis in the speed loop, although higher than desired, is expected to cause a random but acceptable "wander" during engine test. The expected wander amplitude will be about ± 55 engine rpm (or $\pm 0.35\%$) at rated engine speed.

SECTION VI

CONCLUSIONS

The concept of using gas generator speed demand combined with fuel flow scheduling has provided a practical basis for the variable cycle engine backup control development. Success has been achieved in adapting a control built with hydromechanical technology to interface with a primary digital electronic control, thus providing a backup that is free from environmentally induced common failure modes.

Testing of the resulting backup control indicates that satisfactory transient response has been achieved. This backup control has demonstrated the required type of transfer action. It was shown that stall-free transfer can be achieved by having the backup unit continuously compute the controlled variables and thus track the engine operation, in readiness for backup action. These developments have led to a practical and effective backup control.

This technology places the variable cycle engine one step closer to application reality - especially for the single-engine aircraft application. Finally, this accomplishment makes it reasonable to begin the introduction of full authority digital electronic controls at an earlier stage of weapon system development than would have been practical otherwise.

SECTION VII

RECOMMENDATIONS

Based on the results achieved by building, testing and evaluating this Backup Control for a variable cycle engine, it is recommended that the activity be continued toward practical engine applications. Certain design improvements identified during testing could simplify and enhance on-engine usage, and should therefore be incorporated next.

Using the hardware prepared here, the development should proceed directly to on-engine testing using the GE-JTDE, for which the control was designed. Such on-engine measurements should be directed toward obtaining data correlation against a FADEC as the primary control operating a variable cycle engine.

APPENDIX A - SUBSYSTEM SAFETY ANALYSIS

The subsystem safety (or hazard) analysis identifies the components within the subsystems whose performance degradation or functional failure could result in a hazardous condition. This analysis includes failure modes and the effects on safety when failures occur in the subsystem components.

A safety analysis has been completed on the backup control subsystem and the results are given in Table A-1. The hazard levels used herein are as defined in MIL-STD-882 (July 1969):

Category I - Negligible - will not result in personnel injury or system damage

Category II - Marginal - can be counteracted or controlled without injury to personnel or major system damage.

Category III - Critical - will cause personnel injury or major system damage, or will require immediate corrective action for personnel or system survival.

Category IV - Catastrophic - will cause death or severe injury to personnel, or system loss.

Table A-1. Backup Control Subsystem Safety Analysis

Potential Hazard	Safeguards and Design Considerations	Recommended Design Change	Hazard Level
1. Overspeed of the fan and compressor rotors may occur if the main engine control fails in a mode which results in an excess of fuel supply to the engine.	1. The primary/backup control combination contains the following redundant overspeed control features: a) The primary control acceleration fuel schedule is designed to rapidly reduce fuel flow if slight engine overspeed occurs beyond the normally scheduled core rotor speed. b) Further overspeed protection is provided by the primary control separate fan speed loops which provide normal engine limits at intermediate or greater power settings. c) If N_G overspeed occurs, the hydromechanical backup control speed sensor power piston trips an electrical switch which initiates transfer to the backup control. The switch allows current to a solenoid valve which ports pressures such as to stroke the transfer valve to the backup position. In this position, the transfer valve allows only the backup servovalve to control the fuel metering valve. d) If N_G overspeed occurs due to a stuck-open metering valve, a servovalve driven by the backup control speed sensor power piston modulates the throttling valve to control fuel flow. This provides overspeed protection at a slightly higher level than that which tripped the switch in Item c) above. e) The relationship between N_F and N_G is such that hazardous N_F overspeed is not expected within the engine operating envelope in the backup mode.	1. None	1. I (If some redundant speed control remains) III (If all redundant speed control is lost)

Table A-1. Backup Control Subsystem Safety Analysis (Continued)

Potential Hazard	Safeguards and Design Considerations	Recommended Design Change	Hazard Level
2. Overpressure of the compressor casing due to excess W_f at high M_o and low altitude.	2. The primary/backup control combination overspeed protection features described in Item 1 above also serve to guard against overpressure. In addition, the primary control contains a P_{S3} limit function which reduces W_f with increasing P_{S3} once the normal limit is reached. The maximum W_f stop on the fuel valve also provides some P_{S3} limiting.	2. None	2. I (If some redundant control protection remains) III (If all redundant control is lost)
3. Portions of the fuel valve and the hydromechanical backup computer are subjected to contamination and wear which could result in schedule shifts which may, in turn, cause thrust loss.	3. The primary control is electrical so 3-D cam wear is not applicable. The hydromechanical and electrohydraulic servovalves are protected by a wash filter in the fuel valve. A barrier fuel filter is provided between the main fuel pump and main engine control to filter out large contaminant particles ahead of the fuel valve.	3. None	3. I
4. Turbine overtemperature can occur if W_f is supplied in excess to the engine.	4. The turbine is protected against overtemperature by the same means which protect against overspeed (see Item 1 above). N_G limiting is a very satisfactory means for limiting T_{41} over the full flight envelope and this is provided in both the primary and backup mode. The primary control system includes a pyrometer which measures high pressure turbine blade temperature. This is used in the turbine temperature limiting circuit. If the pyrometer fails, FADEC has the capability of calculating T_4 and transferring to T_4 control.	4. None	4. I

Table A-1. Backup Control Subsystem Safety Analysis (Continued)

Potential Hazard	Safeguards and Design Considerations	Recommended Design Change	Hazard Level
5. A malfunctioning $T_{2.5}$ sensor can cause β_C schedule shifts which could result in stall.	5. The primary control includes a Failure Indication and Corrective Action (FICA) feature which accommodates $T_{2.5}$ sensor and related circuit failure. This feature allows operation of the engine with only a slight change in performance upon failure of the electrical $T_{2.5}$ sensor. In addition, the backup control provides a fully redundant $T_{2.5}$ sensor which would be used during operation in the backup mode.	5. None	5. I
6. A malfunction of the β_C feedback could cause stall or loss of thrust.	6. The electrical β_C position is an LVPT, which is very similar to an LVDT, and these have a low failure rate. In addition, the primary control has FICA, which accommodates sensor failure (see Item 5 above). The backup control has a fully redundant mechanical feedback cable.	6. None	6. I
7. An alternator failure could cause loss of power and the primary control.	7. Loss of power to the primary control causes automatic transfer to backup control. Aircraft power (28 vdc) is used to energize the solenoid valve on the transfer valve. The backup control is not dependent on the alternator. Loss of power to the primary control also causes a zero-current signal to the fail-fixed servovalves controlling the servos, not modulated in the backup mode, causing them to drift toward their desired stops.	7. None	7. I
8. Failure of the W_f or β_C servovalves can cause low W_f or stall, thus loss of thrust.	8. The servo fluid for these servovalves is filtered to 40 micron absolute to minimize the possibility of binding in the second stage. The first stage is a jetpipe which offers contamination insensitivity. The backup control provides fully redundant servovalves and the transfer valve blocks the output of the primary servovalves in the backup mode.	8. None	8. I

Table A-1. Backup Control Subsystem Safety Analysis (Concluded)

Potential Hazard	Safeguards and Design Considerations	Recommended Design Change	Hazard Level
9. If the FADEC fails to function, it may result in thrust loss.	9. FADEC is designed with high reliability as a major objective. An advanced hybrid packaging approach, which was specifically designed to withstand the cyclic thermal environment, was used. Other features include use of LSI and MSI to reduce the number of interconnections; alumina substrates with tungsten metalization and Kovar leads to reduce expansion differences; and short, conductive heat transfer paths. FADEC uses FICA to accommodate failures of sensors and related circuits. Redundant clocks and PLA inputs are used. FADEC also uses self-test which detects a high percentage of failures inside the electrical unit itself. If the self-test features indicate "lack of good health," transfer to backup control is automatically initiated. Means are also provided to allow the pilot to transfer to the backup control.	9. None	9. I
10. The backup control modulates W_f and β_C. Other servo loops, such as A8, could cause dry thrust loss.	10. Upon transfer to backup control, the servovalves on the remaining servo loops will receive a zero-current signal. The fail-fixed servovalves, combined with orifices, will cause these servos to drift toward the desired stop, reaching it in 10 to 90 seconds. With the variable geometry at the desired positions and A/B off, the engine will provide at least 90% of intermediate thrust.	10. None	10. I

APPENDIX B

CALIBRATION DATA

S/N GAT 06021

BACKUP CONTROL UNIT CALIBRATION LOG

CONTROL S/N GAT 06021

TESTER C. King

DATE 2/79

1. Throttle Stops

   a) Set pointer at PLA = 91.5 degrees with 0.0938-inch-diameter pin inserted in cover calibrating hole.

   b) Close PLA and check stop location applying 30 ± 5 in.-lb of torque. Read PLA = 0 degrees.
      Limit: 0 ± 0.5 degree

   c) Open PLA and check max stop location applying 30 ± 5 in.-lb of torque. Read PLA = 115 degrees.
      Limit: 115 ± 0.5 degree

2. Shutoff Valve

   a) Set P_1 = 350 ± 5 psig and shut off lever at 2 degrees.

   b) Disconnect outlet fitting and measure leakage.

      Leakage* = 275 cc/min.

      Limit: 5 cc/min.

*See Section V, paragraph 2 for an explanation of this observation.

3. Deceleration Schedule

a) Set PLA = 13 degrees

$T_{2.5}$ = 224 $\pm$ 5° F

N_C = 6130 (91%)

P_1 = 800 $\pm$ 20 psig

b) Set P_{S3} and P_c as follows and record W_f

Set P_{S3}	Set P_c	W_f	Limit
93	200	1290	960/1440
80	200	1190	840/1260
60	200	930	620/930
50	200	800**	500/740
*30	200	560**	300/450

* Check this point by applying 18.9 psia directly to the bellows. The P_{S3} ratio selector takes 63% of applied pressure accurately down to about 50 psia.

4. Minimum Fuel Flow

a) Set PLA = 13 degrees, P_{S3} = 15 $\pm$ 1 psia and $T_{2.5}$ at 75 $\pm$ 10° F

b) Adjust the minimum flow stop

Minimum Flow 280 pph

Limits - 260/280 pph

**See Section V, paragraph 2, for a discussion of these values.

5. Maximum and Idle Speed Adjustments

a) Set $T_{2.5}$ at 224° F $\pm$ 5° F

b) Set PLA, P_{S3} absolute, N_C, P_1, and P_c as follows and set idle and maximum speed adjustments to get W_f within limits. Record measured W_f.

PLA	P_{S3}	N_C	P_1	P_c	W_f	Instructions
13	30	3370	400	200	740	Set Idle Adjustment Limits: 600/750
92	217	6739	1000	500	8040	Set Max Adjustment Limits: 7700/8500

6. <u>Acceleration Schedule</u>

Set PLA, $T_{2.5}$, N_C, P_1, P_c and P_{S3} absolute as indicated and record resulting W_f. (Barometric Pressure: __________ psia)

Pt. No.	PLA Deg.	$T_{2.5}$ °F	N_C RPM	P_1 psig	P_c psig	P_{S3} psia	W_f pph	W_f Limits, pph
1	92	224	6360	1000	200	* 33	1260	1270/1430
2	92	224	6360	1000	250	54	2120	2080/2340
3	92	224	6360	1000	250	67	2610	2575/2900
4	92	224	6360	1000	300	90	3530	3460/3900
5	92	224	6360	1000	400	104	4060	4000/4500
6	92	224	6360	1000	400	114	4440	4380/4970
7	92	224	6360	1000	500	144	5630	5540/6240
8	92	224	6360	1000	500	176	6800	6770/7630
9	92	224	6360	1000	600	222	8540	8540/9625
10	92	224	4770	500	200	54	1740	1580/1780
11	92	224	5175	500	250	67	2210	2010/2270
12	92	224	5565	750	300	90	3290	2930/3300
13	92	224	5710	750	400	104	3950	3480/3920
14	92	224	5840	1000	700	114	4620	3990/4500
15	92	224	6120	1000	500	144	5620	5410/6100

*Apply 21.0 psia directly to bellows chamber for this test point.

7. Core Stator Schedule, β_C

a) Set PLA = 92 degrees

P_{S3} = 30 psia

P_C = 200 psi

P_1 = 500 psi

b) Set $T_{2.5}$ and N_C as indicated and measure arm position.

$T_{2.5}$ Sensor
S/N RPA - 04660

Ret. Arm Pos. = 0.847

Limits: 0.827/0.867

F/B Cable Pos. ____

Point No.	$T_{2.5}$	N_C	Test	Limits
1	56	6053	0.720	.680/.720
2	84	6220	0.722	.680/.720
3	120	6448	0.723	.680/.720
4	157	6668	0.720	.680/.720
5	224	6847	0.670	.625/.672
6	335	6809		.465/.523
7	157	6668	0.707	.680/.720
8	84	6448	0.724	.680/.720
9	56	6220	0.722	.580/.720
10	157	6739		.698/.743
11	157	6303		.563/.616
12	157	5634		.362/.422
13	157	4468		0/.080
14	157	4125		0 (max)
15	157	6303		.563/.616

Hysteresis	7-4 =	+0.013	Limit-
	8-2 =	+0.002	±.015
	9-1 =	+0.002	
	15-11=		

7. Core Stator Schedule, β_C

a) Set PLA = 92 degrees

P_{S3} = 30 psia

P_c = 200 psi

P_1 = 250 psig

b) Set $T_{2.5}$ and N_C as indicated and measure arm position.

$T_{2.5}$ Sensor Simulator

S/N 11 - 3A

Ret. Arm Pos. = 0.847

Limits: 0.827/0.867

F/B Cable Pos. 0.847

Point No.	$T_{2.5}$	psi	N_C	Test	Limits
1	56	119	6053	0.715	.680/.720
2	84	125	6220	0.718	
3	120	132	6448	0.720	
4	157	139	6668	0.717	
5	224	152	6847	0.667	.625/.672
6	335	175	6809	0.488	.465/.523
7	157	139	6668	.0703	.680/.720
8	84	125	6448	0.720	.680/.720
9	56	119	6220	0.718	.580/.720
10	157	139	6739	0.720	.698/.743
11	157	139	6303	0.622	.563/.616
12	157	139	5634	0.402	.362/.422
13	157	139	4468	0.026	0/.080
14	157	139	4125	-0.075	0 (max)
15	157	139	6303	0.614	.563/.616

Hysteresis	7-4 =	-0.014	Limit-
	8-2 =	+0.002	±.015
	9-1 =	+0.003	
	15-11=	-0.008	

8. Droop Lines

a) Set $T_{2.5} = 75 \pm 10° F$

b) Set PLA, P_{S3}, N_C, and P_c as indicated and record W_f.

PLA	P_{S3}	P_c	N_C	W_f	W_f Limits
13	30	200	3170	860	
13	30	200	3270	780	
13	30	200	3370	690	600/750
13	30	200	3470	610	
13	30	200	3370	610	600/750
92	217	500	6540	8280	
92	217	500	6640	8290	
92	217	500	6739	8150	7700/8500
92	217	500	6840	7720	
92	217	500	6739	8000	7700/8500

9. <u>Electrical Overspeed Signal</u>

a) Attach a continuity checker across pins one and two at the overspeed switch connector.

b) Increase N_C until continuity occurs.

Indicated N_C 7020 rpm

Limits - 6975/7040

10. <u>Hydromechanical Overspeed Limit</u>

a) Set P_1 = 1000 psig
P_c = 500 psig
P_{S3} = 217 psia
$T_{2.5}$ = $75 \pm 10^\circ$ F

b) Increase N_C until W_f is 500 ± 100 pph.

Indicated N_C 7196 rpm

Limits- 7175/7245

REFERENCES

1. Kast, Howard B., Hurtle, James E., and Poppel, Gary L., "Backup Control for a Variable Cycle Engine," Phase I Interim Technical Report, Air Force Aero Propulsion Laboratory, AFAPL-TR-77-92, December 1977.

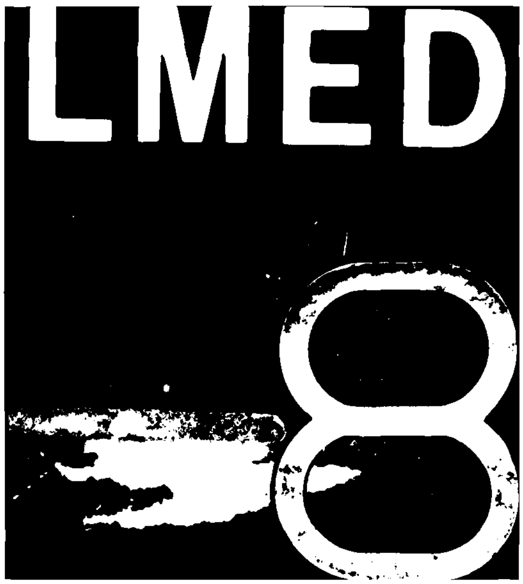
LMED
8